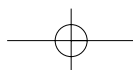
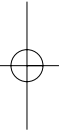




The rabbit Vx2 auricle carcinoma  
An animal model for development of new  
locoregional treatment strategies against squamous  
cell carcinoma of the head and neck





Robert J.J. van Es  
Department of Oral and Maxillofacial Surgery  
University Medical Center Utrecht  
Heidelberglaan 100  
3584 CX Utrecht  
the Netherlands

This publication was financially supported by contributions from:  
The Prof.dr. P. Egyedi Stichting; Rhône-Poulenc Rhorer; Knoll b.v; van Straten  
orale implantologie; IsoTis n.v; Martin nederland b.v; Robouw medische techniek  
b.v; B. Braun Medical b.v. divisie Aesculaap.

© R.J.J. van Es, Utrecht 2001

All rights reserved. No part of this publication may reproduced or transmitted in any form or by any means, electronic or mechanical, including photocopy, recording, or any information storage and retrieval system, without permission in writing from the copyright owner.

Internet: <http://pablo.ubr.ruu.nl/~proefsch/gnk>  
[www.library.uu.nl](http://www.library.uu.nl)

Design/lay-out: Audiovisuele Dienst UMC Utrecht

Printing: Drukkerij Zuidam & Uithof

ISBN: 90-393-2640-1





The rabbit Vx2 auricle carcinoma  
An animal model for development of new  
locoregional treatment strategies against squamous  
cell carcinoma of the head and neck

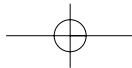
Het Vx2 oorschelp-carcinoom bij het konijn  
Een diemodel voor evaluatie van nieuwe behandelmethoden  
van het hoofd-hals carcinoom  
(met een samenvatting in het nederlands)

Proefschrift

Ter verkrijging van de graad van doctor aan de Universiteit Utrecht  
op gezag van de Rector Magnificus, Prof. Dr. H.O.Voorma,  
ingevolge het besluit van het College voor Promoties  
in het openbaar te verdedigen op  
dinsdag 20 maart des middags te 16.15 uur

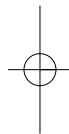
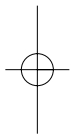
door

**Robert Jelle Johan van Es**  
Geboren op 8 november 1962, te Amersfoort

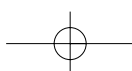


Promotores: : Prof. Dr. R. Koole  
: Prof. Dr. P.J. Slootweg

Co-promotor : Dr. H.F.J. Dullens



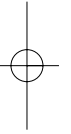
The studies described in this thesis were performed at the Department of Oral and Maxillofacial Surgery (Head: Prof.dr. R. Koole), the Department of Pathology (Head: prof.dr. J.G. van den Tweel), University Medical Center Utrecht and the Division of Cell biology and histology (Head: Prof.dr. W. den Otter) of the Faculty of Veterinary Medicine, University of Utrecht, the Netherlands.



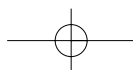


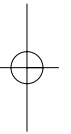
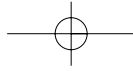
‘One never knows, do one!’

‘Fats’ Waller



Voor mijn patiënten



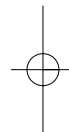
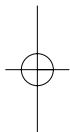


## List of abbreviations:

ANOVA	= Analysis of variance
AA	= Arterio-arteriolar
AV	= Arterio-venous
BCG	= Bacillus Calmette-Guèrin
Dex	= Dextran hydrogel
EBV	= Epstein-Barr virus
EORTC	= European Organisation for research and treatment of cancer
HNSCC	= Squamous cell carcinomas of the head and neck
HE	= Haematoxylin and Eosin
<sup>166</sup> Ho	= Holmium-166
<sup>166</sup> HoPLA	= Holmium-166 poly(L-lactic acid)
HPV	= Human papilloma virus
IL-2	= Interleukin-2
i.a.	= intra-arterial
i.v.	= intra-venous
NZW	= New Zealand White
Num.	= Number weighted mean diameter
PAS	= Periodic Acid Schiff
PCC	= Plaveiselcel carcinoom
PCCHH	= Plaveiselcel carcinoom in het hoofd-hals gebied
PDT	= Photodynamic therapy
s.c.	= subcutaneous
SCC	= Squamous Cell Carcinoma
IU	= International Units
<sup>99m</sup> Tc	= Technetium-99m
VEGF	= Vascular Endothelial Growth Factor
Vol.	= Volume weighted mean diameter



## Contents





## Contents

<b>Chapter 1</b>	<b>General introduction and aim</b>	<b>1</b>
	1.1 Squamous cell carcinoma of the mouth and oropharynx	3
	1.2 Alternative treatment modalities	6
	1.3 Animal models for novel therapies against head and neck cancer	12
	1.4 The Vx2 squamous cell carcinoma in rabbits	13
	1.5 Aims of the investigation	15
<b>Chapter 2</b>	<b>Evaluation of the rabbit Vx2 auricle carcinoma as a model for head and neck cancer in humans</b>	<b>17</b>
<b>Chapter 3</b>	<b>Peri-tumoural IL-2 treatment of the rabbit Vx2 head and neck cancer model induces a systemic anti-tumour activity</b>	<b>33</b>
<b>Chapter 4</b>	<b>Intra-arterial embolisation therapy</b>	<b>47</b>
	4.1 Intra-arterial therapy	49
	4.2 Embolisation particles for tumour treatment	51
	4.3 Current applications of i.a. embolisation therapy	55
	4.4 Possible strategies for embolisation therapy of head and neck cancer	57



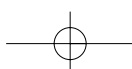
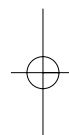


---

Contents

<b>Chapter 5</b>	<b>The Vx2 carcinoma in the rabbit auricle as an experimental model for intra-arterial embolisation of head and neck squamous cell carcinoma</b>	<b>59</b>
<b>Chapter 6</b>	<b>Establishment of an optimal size of microspheres for embolisation of the rabbit Vx2 head and neck cancer model</b>	<b>73</b>
<b>Chapter 7</b>	<b>Effects of intra-arterial embolisation of the rabbit Vx2 head and neck cancer model with radioactive holmium-166 poly(L-lactic acid) microspheres</b>	<b>89</b>
<b>Chapter 8</b>	<b>Summary, discussion and conclusions</b>	<b>105</b>
	8.1 Summary and general discussion	107
	8.2 Final conclusions	111
	8.3 Suggestions for further research	112
<b>Chapter 9</b>	<b>Samenvatting (Summary in Dutch)</b>	<b>113</b>
<b>References</b>		<b>119</b>
<b>Dankwoord</b>		<b>135</b>
<b>Curriculum vitae</b>		<b>138</b>





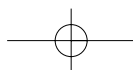
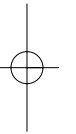
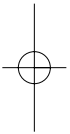
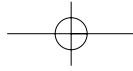


chapter

**1**

General introduction and aim





## 1.1 Squamous cell carcinoma of the mouth and oropharynx

### 1.1.1 Epidemiology

Cancer is a chronic disease with a relatively low incidence but high mortality rate that represents the second most common cause of death world-wide. Squamous Cell Carcinoma (SCC) is the most common malignant neoplasm of the upper aero-digestive tract. Cancers of the lip, oral cavity and oropharynx comprise about half of all squamous cell carcinomas in the head and neck area and around 2% of all new cancer cases [Davis and Zitsch, 1999].

In the Netherlands the average number of new cases over the period 1989-1995 was around 1,000 per annum. The incidence is rising with an annual increase of 4-6% in absolute patient numbers, primarily attributed to demographic changes. European Standardised incidence Rates (ESR) for the Netherlands are shown in Table 1.1.

**Table 1.1.** SCC of the lip, mouth and oropharynx. ESR per 100,000 persons (Visser et al., 1998)

	Male	Female
<b>Lip</b>	<b>2.2</b>	<b>0.4</b>
<b>Oral cavity</b>	<b>5.4</b>	<b>2.8</b>
<b>Oropharynx</b>	<b>2.0</b>	<b>0.7</b>
<b>Total</b>	<b>9.6</b>	<b>3.9</b>

Of all oral cavity cancers, 34 % is situated in the tongue, 30% in the floor of the mouth, 16% in the buccal mucosa and 11% on the gums. Of all oropharyngeal cancers, 28% is situated at the base of the tongue, 42% in the lateral wall, including the tonsils and 13% in the soft palate. Of the oral cancers, about 30% of the patients, and of the oropharyngeal cancers already 50% present with advanced (Stage IV) disease [Visser et al., 1998].

There is a wide geographical variation in occurrence of SCC's at various sites of the upper aero-digestive tract. The incidence figures in the Netherlands are roughly comparable with statistics from the USA [Davis and Zitsch, 1999], but are considerably lower than in France, India or Hong Kong, possibly due to variations in predisposing factors involved [Batsakis, 1999].

### 1.1.2 Aetiology

Predisposing factors for oral and oropharyngeal SCC that have been identified include low socio-economic status, poor oral hygiene with poor dentition and dietary deficiencies, particularly iron and avitaminosis of A and C [Batsakis, 1999]. The most important and independent environmental factors are cigarette smoking and alcohol consumption. Although nicotine and alcohol abuse have an independent carcinogenic potential, its combined use is synergistic and leads to a 7-fold increase of relative risk. Chewing betel quid and the use of smokeless tobacco or snuff, probably induce a 4-fold increase of risk [Thomas and Wilson, 1993; Wray and McGuirt, 1993; Batsakis, 1999].

There is increasing evidence that viruses are involved in the development of at least a subset of Head and Neck Squamous Cell Carcinomas (HNSCC) [Scully, 1992; Gillison et al., 1999]. The Epstein-Barr virus (EBV) is considered a direct causative agent in development of nasopharyngeal carcinoma [Vasef et al., 1977; Scully, 1992]. Several studies support an etiologic role for human papilloma virus (HPV), particularly for poorly differentiated tumours arising from Waldeyer's tonsillar ring [Gillison et al., 1999]. However, the association between HPV and oral SCC is controversial and the actual mechanism by which it initiates malignant transformation remains ill-defined [Bradford and Carey, 1999]. Variations observed in the presence of HPV DNA may be related to detection methods, source of tumour tissue and geographical variations [Miguel et al., 1998]. The HPV subtypes 16 and 18 are typically classified as 'high risk' with an odds ratio of about 4.3, but also types 6 and 11 are considered potentially carcinogenic [Nishioka et al., 1999; Bradford and Carey, 1999]. Two possible mechanisms of HPV tumour induction exist: HPV infections can increase the susceptibility for tobacco carcinogens and HPV onco-proteins block the activity of tumour suppressor genes like p53 and the retinoblastoma gene [Li et al., 1992; Bradford and Carey, 1999].

Familial susceptibility to HNSCC is well known, with increased relative risks varying from 3.8 to 7.9 if a first degree relative had cancer of the head and neck [Foulkes et al., 1996]. The application of molecular biology can reveal specific genetic alterations or hereditary factors involved [Sikora, 1994; Bradford and Carey, 1999]. The clinical importance to assess individual intrinsic cancer susceptibility to HNSCC was demonstrated by Cloos et al. [1996].

### 1.1.3 Prevention

Involvement in smoking prevention and cessation is a valuable contribution that doctors can make to present and future health. Health education strategies, motivating both the healthy population and patients to quit smoking should be encouraged. However, excessive alcohol and tobacco consumption apparently are habits not easily broken [Bolman and De Vries, 1998]. Moreover, after abstinence from smoking 15 to 30 years seem required to approximate the risk of non-smokers [Million, 1994]. Patients cured of their first HNSCC have about a 3-4% per year risk of developing a second primary cancer [Day and Blot, 1992; Haughey et al., 1992; Jovanovic et al., 1994; Van Es et al., 1996]. Prevention could also play a role in reducing this risk. Initially it was hoped that retinoids could suppress the risk of a second cancer [Hong et al., 1990]. Unfortunately, the extensive EORTC chemoprevention study has proven otherwise: The 2-year supplementation of retinyl palmitate and/or N-acetylcysteine yielded no benefit in terms of survival, event-free survival or second primary tumours [Van Zandwijk et al., 2000]. Because no effective prevention measures are available, our attention has to be mainly focussed on treatment of already developed malignancies.

### 1.1.4 Conventional treatment and treatment failure

The management of SCC of the mouth and oropharynx requires a comprehensive treatment plan that addresses all aspects of the disease process and the patient rehabilitation [O'Brien et al., 1992]. Conventional treatment with curative intent depends on tumour site and tumour stage [Vokes et al., 1993]. It usually consists of surgery, radiotherapy or a combination of both modalities for resectable lesions and a combination of chemotherapy and radiotherapy for advanced tumours [Taylor et al., 1997].

Ionising radiation can be delivered either by an external beam or by interstitial implantation of radioactive sources [Almond, 1999]. Interstitial radiotherapy has the advantage that it allows delivery of a high local dose of radiation to the tumour without destroying local anatomy or inducing xerostomia [Close et al., 1993; Podd et al., 1994].

Chemotherapy is usually delivered intravenously either concurrent with radiotherapy or as induction therapy followed by radiotherapy [Stupp and Vokes, 1999]. Though regularly applied, the role of intra-arterial (i.a.) chemotherapy for HNSCC remains controversial [Stupp and Vokes, 1999]. Reason why this therapy is discussed under 'alternative treatment modalities' (see paragraph 1.2).

Today, it is still the classical triad of surgery, radiotherapy and chemotherapy that dominates our therapeutic arsenal. However, during the past two decades survival

rates of patients with advanced stage HNSCC have shown minimal improvement [Heys et al., 1993]. Substantial numbers of patients are still dying from both loco-regional recurrence and distant metastases despite continuing advances in surgical and radiotherapeutic management, in spite of more radical operations and new computer assisted irradiation techniques. To date, still about 25% of the patients with oral cancer and 50% of the patients with oropharyngeal cancer eventually die from their disease [Woolgar et al., 1999]. Relative survival rates of advanced oral and oropharyngeal carcinomas are even as low as 20-30% [Visser et al., 1998]. HNSCC can spread to distant sites. Available data strongly suggest that a significant percentage of distant metastases occur as a result of loco-regional treatment failure [Slootweg et al., 1996; Million, 1999]. At present there is no clear evidence from controlled studies that systemic chemotherapy has any benefit in long-term control of oral SCC [Kovács et al., 1999]. Therefore, SCC of the mouth and oropharynx must be considered primarily a loco-regional disease. Improving the disappointing low cure rates of large head and neck cancers is a major challenge. This requires alternative treatment modalities.

## 1.2 Alternative treatment modalities

Several therapeutic options may be considered as adjuvant or alternative treatment modalities for HNSCC.

### 1.2.1 Intra-arterial chemotherapy

The pharmacokinetic rationale for i.a. or regional drug delivery is based on mathematical models that link drug concentration of the target site with response [Collins, 1984]. As such, selective i.a. infusion can offer a therapeutic advantage over systemic drug administration. The goal of regional administration of chemotherapy is to add anatomic selectivity to the inherent physiologic selectivity of antineoplastic agents [August, 1996].

Nowadays, i.a. chemotherapy is routinely applied in treatment of malignancies of the liver [Aigner, 1998] and extremities [Nijhuis et al., 1999]. For HNSCC, i.a. mono-chemotherapy was initially given with palliative intent [Sullivan and Daly, 1961]. Later, various treatment schedules based on the combination of multi-drug chemotherapy regimens and radiotherapy have been developed and used with curative intent [Noorman van der Dussen, 1986]. Unfortunately, a high complication rate prevented its more general use. Recent advances made in interventional radiology

allowed i.a. chemotherapy to make its comeback as alternative option in the management of HNSCC [Robbins et al., 1996; Kovács et al., 1999].

### 1.2.2 Immune-stimulation

The application of biological response modifiers to manipulate the anti-cancer host defence is one of the alternative therapeutic approaches to both regional and disseminated disease.

#### 1.2.2.1 The Ribivaccine

At the end of the 1960s the group of Ribin [Ribi et al., 1973] demonstrated that mycobacterial cell wall components were able to suppress tumour growth and to induce regression of solid tumours. The compound consisted of certain fractions of *Bacillus Calmette-Guèrin* (BCG) attached to minute oil droplets and became known as 'Ribivaccine'. It was one of the first biological response modifiers and heralded the beginning of immunotherapy against cancer. Retarded tumour growth, complete regressions and prolonged survival were obtained in guinea pig hepato-cellular carcinoma and rabbit squamous cell carcinoma models [Ribi et al., 1975; Edwards et al., 1975; Jeglum et al., 1985]. The Ribivaccine immunotherapy has been applied to patients with HNSCC [Donaldson, 1972; Perlin, 1979]. Despite the encouraging results in the animal studies and the induction of significant changes in the peri-tumoural infiltrate of human oral cancers, the value of adjuvant BCG-immunotherapy in terms of tumour free survival has never been demonstrated [Schlesinger et al., 1980]. The BCG vaccine is still used incidentally together with other biological response modifiers as 'adjuvant multi-modality immunotherapy' and claimed to be effective in treatment of oral cancer [Fukazawa et al., 1994].

#### 1.2.2.2 The cytokine Interleukin-2

With increasing knowledge of the intercellular regulatory molecules that play an important role in our immune system, attention soon focussed on more specific stimulation of the immune system with cytokines. Cytokines are soluble proteins secreted by a.o. lymphocytes and macrophages and act as intercellular regulatory molecules in a paracrine manner. Since the second half of the 1980s, interest was directed on the cytokine interleukin-2 (IL-2). IL-2 is a 14-17 kD glycoprotein secreted by T-helper lymphocytes and is encoded by a single gene on chromosome 4 in humans [Reichert et al., 2000]. It was one of the first cytokines produced in large quantities by means of recombinant DNA technology. IL-2, a major autocrine growth factor for T lymphocytes, stimulates the growth of natural killer

cells and enhances their cytolytic functions. It also acts as a growth factor for human B cells and stimulates their antibody synthesis [Heys et al., 1993; Reichert et al., 2000].

Intra- or peri-tumoural application of low dose IL-2 in various experimental animal models proved very effective in inducing regressions of both local and metastatic tumours [Franzke et al., 1994, Den Otter et al., 1996]. In the mid-1990s IL-2 became an integral element in the treatment of patients with advanced renal cell carcinoma, bladder cancer and metastatic malignant melanoma [Heys et al., 1993]. Conflicting data have been published on the treatment of an expanding range of advanced other malignancies in humans. Until now, the treatment of HNSCC patients with IL-2 regimens has shown little benefit [Matthijsen et al., 1994; Vlock et al., 1994] which may in part be due to suboptimal regimens of IL-2 application [Den Otter et al., 1996].

Current methods of cytokine immunotherapy consist of systemic bolus administration, repeated local injections or local delivery of cytokine gene-engineered cells [Lang et al., 1999]. Systemic administration of IL-2 is associated with prohibitive toxicity and proved of limited benefit for patients. Repeated multiple painful peritumoural injections of free IL-2 are clinically not feasible due to discomfort for HNSCC patients and the short half-life of the cytokines in vivo. Local sustained delivery of cytokines using gene-modified tumour cells is difficult to implement in clinical practice. The continuous local delivery of IL-2 via the intra-arterial route [Tubaro et al., 1991; Gore et al., 1992; Lygidakis et al., 1995] seemed an ideal solution to circumvent these obstacles. Unfortunately, considerable problems maintaining the patency of arterial lines and local complications due to line-infections were reported [Gore et al., 1992].

### 1.2.3 Interventional genetics

Gene therapy technology covers the field of getting foreign genes into cells so that their DNA can be transcribed into mRNA and the encoded protein product synthesised to produce a therapeutic effect. The therapeutic gene is transferred into tumour cells using a vector. The mode of gene transfer can be classified into chemical, physical and viral. The most important method of transfer of DNA currently being used is viral vectors [Robbins et al., 1998].

To date, four main types of genes can be introduced in tumour cells [Ganly et al., 2000]:

---

**General introduction**

1. Anti-oncogenes, which suppress the expression of an oncogene. As yet, no applications for HNSCC are reported.
2. Replacement-genes which restore a defective suppressor gene. The p53 suppressor gene is mutated in almost 100% of the HNSCCs [Kropveld et al., 1999]. Inactivation of p16 is reported in 80-90% of the HNSCCs. Recently, phase I and II trials reintroducing p53 or p16 were carried out in patients with advanced and recurrent HNSCC. Complete remissions were observed in 7-11%. [Clayman et al., 1998; Rocco et al., 1998; Lamont et al., 2000].
3. Genes which enhance immune surveillance. Increasing the immunogenicity of the tumour by transfecting MHC class I and II genes alone proved insufficient for immune induction. Co-stimulatory molecules are also required [Lin et al., 1993; Lang et al., 1999]. Alternatively, tumour cells can be transfected with cytokine receptor genes such as IL-2 to improve the effectiveness of tumour infiltrating lymphocytes.
4. Genes coding for an enzyme capable of activating an inert pro-drug into an active cytotoxic agent. The most common gene used is the herpes simplex virus thymidine kinase gene, which renders cells sensitive to the nucleoside analogue ganciclovir, by converting ganciclovir into an active phosphorylated compound that terminates DNA synthesis. This therapy caused reduced growth of tumours in nude mouse models [Ganly et al., 2000; Morris et al., 2000].

Because the main obstacle of current gene therapy is the poor tumour transduction, the use of a replication-competent virus, which selectively replicates in tumour but not in normal tissue, is advantageous. Deleted adenoviruses are currently used for this purpose, either by delivering a therapeutic gene into the tumour [Morris et al., 2000] or by replicating themselves and so causing lysis of tumour cells infected. The E1B 55kDa deleted adenovirus, Onyx-015, selectively replicates in and lyses tumours with non-functional p53. In phase II trials 22% complete remissions were obtained by combining Onyx-015 with i.v. cisplatin and 5-fluorouracil for patients with recurrent HNSCC [Ganly et al., 2000].

Still, many hurdles in gene therapy technology have yet to be overcome, before we will witness a reduction in the number of patients dying from cancer [Sikora, 1994; Morris et al., 2000].

**1.2.4 Inhibition of angiogenesis and Vascular targeting**

Neo-vascularisation or angiogenesis involves the formation of new blood vessels. This process can convert a small cluster of mutated cells or 'in-situ cancer', into a large tumour mass capable of spreading to other organs. If angiogenesis of a tumour is blocked, its growth is restricted up to a size of 1-2 mm, because of lack of

readily available nutrients and oxygen [Folkman, 1996]. Tumours make two types of proteins: One kind stimulates angiogenesis and the other inhibits it. The balance between them determines whether the tumour can turn on angiogenesis and can expand its growth. The ability to switch on angiogenesis depends mainly on a decrease in the production of the inhibiting proteins [Folkman, 1996].

#### **1.2.4.1 Anti-angiogenic therapy**

Anti-angiogenic therapy is based on the application of drugs that interfere with neo-vascularisation of the tumour. The treatment does not aim to destroy the tumour itself, but prevents it from growing by limiting its blood supply. It keeps tumours in a dormant state within their diffusion-restricted size as long as the drug is administered. As such, it is a long-term treatment turning cancer into a chronic disease with a low mortality rate, however without curing it [Folkman, 1996].

Among the many angiogenesis inhibiting compounds available, worth mentioning are Endostatin, a 20kDa fragment of collagen XVIII, Angiostatin, a 38kDa fragment of plasminogen and TNP-470, a synthetic fumagilline analogue. These agents have proven to inhibit tumour angiogenesis and metastatic growth in animal models. The TNP-470 has recently been tested in clinical trials for various tumours [Bloemendal et al., 1999]. With respect to oral SCC, intra-tumoural injection of TNP-470 induces significant tumour regression in a rabbit tongue carcinoma model [Masumoto et al., 1999]. However, growth of human oral SCC-lines in nude mice were unaffected by TNP-470 treatment [Gleich et al., 1998].

A very potent and specific compound stimulating angiogenesis, is the Vascular Endothelial Growth Factor (VEGF). It is produced by virtually all tumours [Folkman, 1996]. Monoclonal antibodies against VEGF have been reported to block the growth of experimental tumours and to augment the effect of irradiation [Gorski et al., 1999]. Recently, angiogenesis inhibition and gene therapy were combined by transfection of antisense VEGF into HNSCC cell lines but no effect on tumour growth was observed [Nakashima et al., 2000].

#### **1.2.4.2 Vascular targeting with monoclonal antibodies**

There are other means of compromising the vascularisation of tumours. Tumours may be treated by starvation as a result of destruction, blockage or thrombosis of their vessels. This can be achieved mechanically by super-selective embolisation of the feeding arterioles with microspheres [Kato et al., 1994]. As tumour endothelial cells are different from their counterparts in normal tissues, it can also be done on a molecular level by using antibodies directed at unique or highly upregulated antigens on tumour endothelial cells, ideally without cross-reactivity with cells outside

---

**General introduction**

the tumour [Bloemendal et al., 1999]. The phage display technology recently allowed the generation of large quantities of human monoclonal antibodies [Rossenu et al., 1997]. Specific antibodies against tumour endothelium-associated surface antigens can be applied as selective carries to direct cytotoxic drugs, radionuclides or immuno-modulating agents [Bloemendal et al., 1999].

Radiolabelled, tumour-selective monoclonal antibodies against tumour cell surface antigens instead of tumour endothelium have also been tested. Until now only modest results have been obtained in the application of these antibodies for the treatment of patients with solid cancers [Bruland, 1995; De Nardo et al., 1999].

**1.2.5 Photodynamic therapy**

Photodynamic therapy (PDT) is a treatment modality that utilises a hematoporphyrin derivative compound also called 'photo-sensitising drug', which is inert until activated by laser-generated light. After i.v. injection, the photosensitising agent is preferentially retained in malignant cells. At a fixed time interval after injection, the photo-sensitiser molecules are activated by red light of a specific wavelength (630 or 652 nm). The activated agent interacts with oxygen to produce reactive oxygen species (e.g. free radicals), which are involved in the mediation of photodynamic cytotoxicity and tissue destruction [Hsi et al., 1999]. PDT is currently used in patients with early and advanced stage cancer of the lung, the digestive- and genitourinary tract [Dougherty et al., 1998].

In treatment of HNSCC, PDT is effective for small cancers but it is not yet clear in which cases such treatment is more effective than other currently acceptable approaches. To date, PDT is mainly indicated for superficially spreading early cancers because the penetration of the light in the tissues is limited to 5-10 mm [Biel, 1995; Nauta et al., 1996]. For large tumours, PDT might have a clinical benefit in palliation [Ell and Glossner, 2000]. Its advantage is that it can be repeated and does not interfere with conventional treatment modalities.

Many issues regarding pharmacokinetic data of photosensitizers, newer technology involved in light sources, optimal treatment regimens that take advantage of the pharmacophysiology of photoablation, and light dosimetry still require solution. As technologic advances occur, especially interstitial PDT may have significant application [Webber et al., 1999].

### 1.3 Animal models for novel therapies against head and neck cancer

To evaluate the feasibility of novel treatment strategies against HNSCC, animal cancer models are necessary. For HNSCC basically three types of animal tumour models exist:

1. Spontaneously occurring tumours, such as the sheep ear SCC [Harker and Stephens, 1992] and the bovine ocular SCC [Den Otter et al., 1993]. However, these tumours are rare in the Netherlands and it is difficult to create standardised experimental conditions for these models.
2. Tumours induced by topical application of carcinogens such as the 4-Nitroquinoline-1-oxide (4NQO) mouse and rat SCC [Steidler and Reade, 1984; Nauta et al., 1995] and the 9,10-dimethyl-1,2-benzanthracene (DMBA) hamster cheek pouch carcinoma [Shklar, 1972]. Unfortunately, tumour induction is rather time-consuming. Dysplastic lesions occur after 3 to 4 months of application of the carcinogen and there is a latency period (which appears to be in inverse proportion to the application period) of another 14-26 weeks before carcinomas develop. Unlike the human SCC, these lesions not always lead to infiltrating carcinomas and cervical lymph node metastases are rarely seen. Also chromosomal alterations appear to be different from the SCC as seen in the human situation [Lin et al., 1994]. Moreover there is an additional mortality of the animals because of cumulative toxicity of the cancer inducing agents [Hawkins et al., 1994].
3. Tumours induced by inoculation with a transplantable cell line, such as the prostate derived SCC in the Fischer rat [Karanfilian et al., 1982] and the skin SCC in the Wag-Rij rat [Schouwenburg et al., 1980].

Because of the small calibre of the external carotid artery branches, all HNSCC models in rodents are inevitably dependent on microsurgical techniques if used for studies on i.a. delivery of drugs [Schouwenburg et al., 1980]. To study the effects of i.a. chemotherapy, Davidson et al. [1986], developed a macroscopic hind limb SCC model in the rabbit. Harima et al. [1996] used the uterus and Päufer et al. [1996] used the liver of the rabbit as tumour implantation site to study the effects of chemo-embolisation. However, extrapolation to the head and neck area is debatable because of site-specific differences in the organ microenvironment, such as vascularity, nature of tumour vessels and variations in lymphatics and draining lymph nodes, as well as differences in local immune response and tissue specific

paracrine factors [Fidler, 1995; Müller et al., 1998]. Rabbits possess large, translucent ears. Tumour growth and tumour angiogenesis can be studied in detail at this site [Tromberg et al., 1990]. A Vx2 auricle carcinoma model would couple the ease of transplantability to a rather large laboratory animal with a sufficient calibre of the external carotid artery branches, suitable to study i.a. delivery of drugs to the head and neck area.

## 1.4 The Vx2 squamous cell carcinoma in rabbits

### 1.4.1 History

Naturally occurring cutaneous papillomas of domestic rabbits are induced by a virus discovered by Shope and Hurst in 1933. Due to malignant transformation, these papillomas give rise to squamous cell carcinomas. Inoculation of Shope-papilloma virus containing extracts at scarified skin spots induces carcinomas after about 10 months [Kidd et al., 1936]. Kidd et al. reported the first successful transplantation of such a carcinoma called 'V1' in 1936, but growth was lost on a second transfer. In the experiment that led to the development of the 'V2' carcinoma cell line, transplantation was successful in only 5% of the inoculated Dutch belted rabbits initially. In the third tumour generation carcinomas already successfully grew in 21% of the inoculated animals. Transplantation is reported until the fourteenth generation. By then the V2 SCC was growing rapidly in most animals, into which it was transplanted [Kidd and Rous, 1940]. During the course of serial transfers, the V2 tumour became increasingly anaplastic in histologic appearance. In the 1950s, transplantation of the V2 carcinoma appeared successful not only in other rabbit species, but also at several sites in guinea pigs, mice, hamsters and rats [Greene, 1953]. Because of the now existing different stocks of cell lines world wide with different transplant generations, the carcinoma became addressed as 'Vx2' tumour. Stewart et al. (1959) gave a detailed description of the histology of the Vx2 tumour in the New Zealand White (NZW) rabbit.

Since the 1960s, the Vx2 tumour is used in a large variety of experimental studies (see paragraph 1.4.3):

1. To get insight into the various mechanisms of carcinogenesis, such as angiogenesis, dissemination and host immuno-competence.
2. To test various new treatment modalities against cancer, such as anti-angiogenic and intra-arterial therapies.

#### 1.4.2 In vitro growth of the Vx2 cell line

From the mid-1960s on, reports on the development of in-vitro cell lines from the Vx2 carcinoma have appeared in the literature. Osato and Ito [1967] developed an in-vitro Vx2 and less anaplastic Vx7 cell-line, but the Vx2 culture was lost and has never been re-established. Later, others have reported about established in-vitro Vx2 lines for various studies mainly on tumour prostaglandin E2 synthesis and calcium metabolism [Voelkel et al., 1975; Yoneda et al., 1985]. However, these cell-lines were not meant for re-implantation into the rabbit.

Galasko and Haynes [1976] demonstrated that a culture medium containing 10% DMSO, an anti-freeze component to maintain sufficient cell viability after thawing, is essential for successful storage of the Vx2 cells at  $-196^{\circ}\text{C}$  in liquid Nitrogen.

Shah and Dickson [1978b] further reported on the preservation of the Vx2 tumour in-vitro, but observed that the ability of their Vx2 cell line to re-grow in-vivo was lost in due time: The Vx2 tumour cells grown in culture for over 3 weeks failed to produce tumours when inoculated into rabbits. In 1982, Easty and Easty have developed a Vx2 cell line that was successfully re-implanted after several months of continuous culture and have described the culture conditions in detail.

The ability to maintain the Vx2 tumour in culture makes a variety of in-vitro studies possible and avoids the necessity for serial transplantation in rabbits, thus reducing the number of animals used for research. However, in practice most investigators prefer the propagation of the Vx2 line in-vivo by intra-muscular passage in the hind paw [Muckle and Dickson, 1971; Herman et al., 1976; Tromberg et al., 1990; Conlon et al., 1992; Wagner, 1994; Harima et al., 1996; Matsumoto et al., 1999].

#### 1.4.3 In-vivo Vx2 models and tumour transplantation

The Vx2 carcinoma cell line in the rabbit has been used in several studies:

1. To evaluate i.a. chemotherapy schedules in e.g. the liver [Wagner, 1994; Päufer et al., 1996], the uterus [Harima et al., 1996], the kidney [Gadeholt-Göthlin and Göthlin, 1995] and the bladder [Hoshi et al., 1997].
2. To study tumour angiogenesis [Brem and Folkman, 1975; Tamargo et al., 1991; Matsumoto et al., 1999].
3. To evaluate host immuno-competence against tumours [Muckle and Dickson, 1971; Jeglum et al., 1985; Carroll et al., 1995].

The transplantation of the Vx2 cells can be achieved either by injecting tumour cell suspensions [Herman et al., 1976; Wagner, 1994; Harima et al., 1996; Matsumoto et al., 1999] or by implanting solid tumour pieces [Brem and Folkman, 1975; Tamargo et al., 1991]. The use of cell suspensions is technically

easy. It has the advantage of allowing to establish the percentage of vital cells injected by Trypan blue exclusion, and makes it possible to inject approximately equal amounts of vital cells in each transplantation subsequently, yielding equally sized tumours. However, the injection pressure can cause accidental infusion of tumour cells into vessels resulting in early lung metastases, a phenomenon known as 'seeding at implantation' as well as early lymph node metastases [Gadeholt-Göthlin and Göthlin, 1995]. When assessing the effects of loco-regional i.a. anti-tumour therapy, these artificially created lungmetastases are disadvantageous as they diminish the survival of the rabbits considerably. When assessing the effects of immunotherapy however, metastases are beneficial for determining systemic anti-tumour activity [Muckle and Dickson, 1971].

## 1.5 Aims of the investigation

The primary aim of this study is to develop an animal model that can be used for evaluation of new loco-regional treatment strategies against HNSCC. The second aim is to evaluate the possibilities of new intra-arterial embolisation therapies, either with dextran hydrogel microspheres that can slowly release anti-tumour drugs or with radioactive poly(L-lactic acid) microspheres that contain the beta-emitting isotope holmium-166 ( $^{166}\text{HoPLA}$ ).

More specifically:

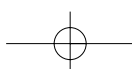
- The study will evaluate, if the Vx2 carcinoma cell line transplanted into the rabbit auricle renders a suitable head and neck cancer model with respect to the success rate of tumour transplantation, the tumour growth speed and the occurrence of lymph node and lung metastases. The effects of transplantation with tumour suspensions either fresh or cryopreserved or with tumour pieces are analysed (Chapters 2 and 5).
- This Vx2 head and neck cancer model is used to study the histologic effects of peri-tumoural IL-2 and to establish whether IL-2 therapy can induce complete remissions and a systemic immune response (Chapter 3).

For non-resectable head and neck cancers, theoretic considerations concerning the application of intra-arterial embolisation therapies are presented (Chapter 4).

The Vx2 head and neck cancer model is subsequently used:



- To develop a technique for i.a. perfusion that is easy to handle and not dependent on microsurgery (Chapter 5).
- To assess the possible use of dextran hydrogel microspheres for i.a. tumour embolisation (Chapter 5).
- To evaluate the distribution of embolisation particles of a variable size in the primary tumour, the lungs and the brain, both in-vivo and histologically after sacrifice (Chapter 6).
- To analyse the effects of i.a. radio-embolisation with holmium-166 on Vx2 tumour growth. The efficiency of i.a. infusion of  $^{166}\text{HoPLA}$  microsphere suspensions, the efficacy of retention of  $^{166}\text{HoPLA}$  microspheres within the primary tumour and the leaching of free holmium-166 into urine and faeces will be assessed (Chapter 7).





chapter

2

Evaluation of the rabbit Vx2 auricle  
carcinoma as a model for head and neck  
cancer in humans



---

R.J.J. van Es, H.F.J. Dullens, A. van der Bilt, R. Koole, P.J. Slootweg

Journal of Cranio-Maxillofacial Surgery 2000;28:300-307



## Abstract

**Introduction:** This study investigates whether the Vx2 carcinoma cell line, transplanted into the rabbit auricle, can be used as a head and neck cancer model. The biologic behaviour of this model is evaluated, comparing tumour transplantation with either tissue pieces or cell suspensions.

**Materials and methods:** 36 Adult NZW rabbits received s.c. injections of Vx2 Suspensions (Group S) and 11 rabbits received solid Vx2 Pieces (Group P) into both auricles. In Group S, 16 rabbits were sacrificed at various days before (S1) and 15 after (S2) the 28th day following transplantation. In the other 5 rabbits transplantation failed. Animals in Group P were sacrificed every 2 weeks after the 28th day. At autopsy the size of the primary tumours and of lymph node, lung and other metastases were assessed. If transplantation failed, the maximal tumour size and the time at which regression took place were recorded. Exponential trend lines were used to create growth curves of metastases. Differences between groups were evaluated with the Chi-square test, correlations between parameters with Kendall's tau.

**Results:** The tumour take-rate in Group S and P was 78% and 59% respectively. The maximal size and time at which regression occurred was significantly different, amounting  $83 \pm 7 \text{ mm}^2$  at  $10.4 \pm 1.6$  days (Group S) and  $243 \pm 30 \text{ mm}^2$  at  $20.9 \pm 2.0$  days (Group P), respectively. Development of lymph node metastases was not different. In Groups P and S2, over 90% of the necks contained lymph node metastases. There was a trend for a higher incidence of lung metastases in Group S2 compared to Group P (47% vs. 14%). A significant correlation ( $p < 0.05$ ) between weight loss and the size of lung metastases was found.

**Conclusion:** Transplantation of the Vx2 tumour with cell suspensions produces a useful head and neck cancer model for loco-regional disease in which anti-tumour regimens against both the primary tumour and lymph node metastases can be tested. Transplantation with tumour pieces is not advised as the take-rate is low and spontaneous remissions occur at a late stage.

We thank W. den Otter for putting laboratory support at our disposal, A. Versluis and H. Boere for taking care of the rabbits, P. Rothengatter for the photography and R. Broekhuizen for his efforts in helping to establish an in-vitro Vx2 cell line.

## 2.1 Introduction

Improving the disappointing cure rates of large head and neck cancers is a major challenge, as relative survival rates of stage IV oral or pharyngeal carcinomas are still as low as 20-30% [Visser et al., 1998]. Animal cancer models can be of use in the development of new treatment strategies. For this purpose, the Vx2 carcinoma cell line in the rabbit has been used in several studies (see also 1.4.3):

1. To evaluate intra-arterial (i.a.) chemotherapy schedules.
2. To study tumour angiogenesis.
3. To evaluate host immuno-competence against tumours.

The transplantation of the Vx2 cells can be achieved either by injecting tumour cell suspensions or by implanting solid tumour pieces. Cell suspensions have the advantage of allowing to establish the percentage of vital cells injected by Trypan blue exclusion, and make it possible to inject approximately equal amounts of vital cells in each transplantation subsequently, yielding equally sized tumours. However, the injection pressure can cause accidental infusion of tumour cells into vessels resulting in early lung metastases, a phenomenon known as 'seeding at implantation' [Gadeholt-Göthlin and Göthlin, 1995], as well as early lymph node metastases. When assessing the effects of loco-regional i.a. anti-tumour therapy, these artificially created lung metastases are disadvantageous as they diminish the survival of the rabbits considerably [Gadeholt-Göthlin and Göthlin, 1995]. When assessing the effects of immunotherapy however, metastases are beneficial for determining systemic anti-tumour activity [Muckle and Dickson, 1971; chapter 3].

The present study investigates whether the Vx2 carcinoma transplanted into the rabbit auricle can be used as a head and neck cancer model. The success rate of tumour transplantation and the occurrence of lymph node and lung metastases of this rabbit Vx2 auricle carcinoma model is evaluated following transplantation with either tumour suspensions or tumour pieces.

## 2.2 Materials and methods

All animal experiments in this and the following chapters were performed in agreement with 'The Netherlands Experiments on Animals Act' (1977) and 'The European Convention for the Protection of Vertebrate Animals used for Experimental Purposes' (Strasbourg, 18.III.1986). Approval was obtained from 'The Utrecht University Animal Experiments Committee' (FDC/DEC-GNK numbers 96005, 98024 and 99053).

### 2.2.1 Animals

Adult female, specific pathogen free, Iffa Credo: New Zealand White (ICO:NZW) outbred rabbits weighing 2.5-3.5 kg were purchased from the Broekman Institute, Someren, the Netherlands. They were allowed to acclimatise for at least 5 days before use and kept in a closed system without isolator. Housing was in accordance with the guidelines of the Central Laboratory Animal Institute (CLAI, Utrecht, the Netherlands) in individual steel cages, 75x47x40 cm (type HD.1., UNO, Zevenaar, the Netherlands). Rabbits were fed with approximately 100 grams 'complete diet' pellets for rabbits (Type LKK 20, Hope Farms Ltd., Woerden, the Netherlands) per day, and acidified (hydrochloric acid, pH 2.7) tap water ad libitum. Environmental temperature was regulated between 18° and 20°C and non-regulated relative air humidity was approximately 60%. Air was refreshed at a rate of seven times per hour. Day/night cycle was 12/12h in artificial lighting with white lights on at 7:00h during summer time and at 6:00h during wintertime. All experiments were performed during daytime hours.

### 2.2.2 Tumour cells

#### 2.2.2.1 Origin and propagation

From the German Cancer Research Institute (Deutsches Krebs Forschungszentrum, DKFZ) an in-vitro Vx2 cell line [Kidd and Rous, 1940] was obtained, which originally was derived from a Vx2 tumour growing in Yellow-Silver rabbits. This line was successfully propagated in-vitro several times. However, re-plantation of this established line into ICO:NZW rabbits failed.

Subsequently, an in-vivo Vx2 cell line growing in NZW rabbits was obtained as a gift from the department of Radiology, Benjamin Franklin Medical Centre, Free University of Berlin in Germany. This cell line was successfully propagated in-vivo in ICO: NZW rabbits but failed to grow in III/VO and AX rabbits.

### The Vx2 auricle carcinoma model

Despite several attempts, by using different tumour fragments from the primary site, the lymph node and lung metastasis or by adding extra calcium to the culture medium [Yoneda et al., 1985], we failed to establish an in-vitro culture of this now well in-vivo growing Vx2 strain from Berlin.

The Heidelberg Vx2 strain might have failed to re-grow in the NZW rabbit in-vivo, because the cell line originated from a Yellow-Silver breed and was propagated in-vitro for too many cycles [Shah and Dickson, 1978b]. Therefore, tumour cells had to be propagated by intramuscular passage in the upper hind limb.

#### 2.2.2.2 Preparation

Dissected tumour tissue was fragmented and cautiously pressed through a nylon sieve (mesh size 200  $\mu\text{m}$ ) and collected in ice-cold RPMI 1640 medium (Gibco, Grand Island, New York, USA). After 2 centrifugation cycles and re-suspension, the Vx2 cell suspension was standardised at a density between 15 and 30x10<sup>7</sup> cells/ml. The number of cells in suspension was counted using a haemocytometer. Viability of cells was estimated by Trypan blue exclusion. To induce tumours, a 0.10-0.15 ml suspension containing 15 to 45x10<sup>6</sup> vital cells was injected with a 0.5 mm needle s.c.

Tumour pieces were obtained from non-necrotic, well vascularised portions of an aseptically excised hind paw tumour, as described earlier [Tamargo et al., 1991]. Portions were cut into 3x3 mm pieces in ice-cold RPMI 1640 medium and implanted in a small subcutaneous pocket. Both suspensions and pieces were used within 2 hours.

#### 2.2.3 Tumour transplantation

All hair was removed from the auricle by shaving the skin with a pair of clippers. Tumours were transplanted into the area between the central auricular artery and caudal margin, at the dorsal middle-third of both auricles (Fig. 2.1).



**Figure 2.1.**

Vx2 twin tumour model.  
Example of rabbit in Group S,  
2 weeks after transplantation.  
Tumours are located at the  
dorsal lateral side of both  
auricles (arrows).

Rabbits were excluded from further analysis if tumour transplantation failed in both auricles, i.e. if tumours did not grow progressively and regressed.

Group P consisted of 11 animals, i.e. 22 auricle implantations with solid pieces.

Rabbits from Group P were sacrificed every 2 weeks from day 28 after transplantation on, i.e. on days 28, 42, 56 and 70 respectively.

Group S consisted of 36 animals, i.e. 72 auricle transplantations with tumour suspensions. Time of sacrifice in Group S varied from day 3 to 67. Group S included 5 rabbits sacrificed at days 3, 7, 10, 14 and 21 after transplantation and 20 rabbits sacrificed at various times after transplantation within 1 day after a tumour embolisation experiment.

To compare Groups P and S, a Group S1 was composed of animals sacrificed before day 28: sixteen rabbits, of which four were killed in weeks 1-2 and twelve in weeks 3-4. Group S2 consisted of 15 rabbits sacrificed after day 28: Four rabbits in weeks 5-6, six rabbits in weeks 7-8 and five rabbits in weeks 9-10. The other 5 rabbits were excluded because transplantation failed in both auricles.

#### **2.2.4 Analgesia, sedation and euthanasia**

Analgesia and sedation during interventions were achieved with fentanyl/fluanisone, 0.1 ml/kg i.m. (Hypnorm<sup>®</sup>, containing fentanyl 0.315 mg/ml and fluanisone 10 mg/ml, Janssen-Cilag Ltd., Saunderton, UK). Rabbits were sacrificed with pentobarbital 0.3 ml/kg i.v. (Euthesate<sup>®</sup>, containing pentobarbital 200 mg/ml, Apharmo b.v., Arnhem, the Netherlands). Signs of pain or distress as indicated by the 'Guidelines on choosing an appropriate endpoint in animal experiments' (Canadian Council on Animal Care, 1998) were an indication for sacrifice.

#### **2.2.5 Clinical measurements, histopathological investigations and statistics**

Success of transplantation was characterised by the tumour take-rate. Body weight was recorded biweekly. Weight loss at sacrifice was defined as  $100\% \times (\text{maximum weight} - \text{weight at death}) / \text{maximum weight}$ . At autopsy, the tumour size was measured with callipers in two dimensions and recorded as surface area ( $A$ , mm<sup>2</sup>). Enlarged parotid (=first echelon), retromandibular (=second echelon) and cervical (=third echelon) lymph nodes were collected bilaterally. Both sides of the neck were scored independently for lymph node metastases. The largest diameter of each lymph node was measured with callipers and recorded. Inflated and fixed lung specimens were prepared as described by Kim et al. [1993] from all rabbits of Group P and 12 rabbits of Group S. A slice of each lung lobe was removed. The diameter of the largest visible metastatic nodule was measured with callipers and recorded. The abdominal organs were inspected for the presence of metastases. All

tissues were placed in 10% buffered formalin and paraffin sections ( $5 \mu\text{m}$ ) were prepared. Sections were stained with haematoxylin and eosin and studied by an experienced pathologist to confirm the presence of tumour cells.

If tumour transplantation failed, i.e. if there was no progressive growth or if spontaneous regression occurred, the Maximum Size ( $A_{\text{max}}$ , in  $\text{mm}^2$ ) of the primary tumour and the time at which this size was reached ( $T_{\text{max}}$ , in days) were noted. Differences between  $A_{\text{max}}$  and  $T_{\text{max}}$  of Groups S and P were assessed.

The size of lymph node and lung metastases was correlated with (1) time after transplantation, (2) size of the primary tumour and (3) loss of body weight. Kendall's tau was used to test for bivariate correlations. The growth of lymph node and lung metastases was assessed with exponential regression curves. Trend lines to correlate the diameter of the metastases ( $D(t)$ , in cm) with time ( $t$ ) were presented as :

$$D(t) = D_0 \cdot 2^{t/T}$$

where  $D_0$  is the size in cm at  $t=0$ , and  $T$  represents the 'tumour-size doubling time' (see chapter 5). The Chi-square test was used to assess differences between the two Groups in tumour take-rate and the number of animals with metastases in lymph nodes or lungs. P-values  $< 0.05$  were considered significant.

## 2.3 Results

### 2.3.1 Success of transplantation and spontaneous regressions

In Group S, 56 of the 72 transplantations succeeded (take-rate 78%). In Group P only 13 of the 22 implantations were successful (take-rate 59%). The Chi-square test showed a strong trend for a better take-rate in Group S ( $p < 0.1$ ).

Between Group P and S, differences in  $A_{\text{max}}$  and  $T_{\text{max}}$  of the tumours that did not grow progressively and subsequently regressed, were highly significant (Table 2.1): In Group P regressing tumours grew larger and went into remission later.

### 2.3.2 Lymph node metastases

Group P: In 12/13 (92%) of the necks that drained the primary tumour, a first echelon parotid metastasis was present (Fig. 2.2). The only negative neck contained an enlarged parotid lymph node, but no vital tumour cells were found. In 1/12 (8%) of the positive necks also a second echelon (i.e. retromandibular) metastasis was present. Group S: In 19/30 (63%) necks of the 16 rabbits of Group S1, a parotid metastasis was present. Of the 15 rabbits of Group S2, in 25/26 (96%) necks a parotid metas-

**Table 2.1.** Success of transplantation and mode of inoculation (Chi-square test)

	Group S	Group P	p-value
<b>Transplanted tumours</b>	<b>n=72</b>	<b>n=22</b>	
<b>Take-rate</b>	<b>78%</b>	<b>59%</b>	<b>.083</b>
<b>Amax (mm<sup>2</sup>)*</b>	<b>82.9 ± 7.1</b>	<b>243.2 ± 30.3</b>	<b>&lt;.001</b>
<b>Tmax (days)*</b>	<b>10.4 ± 1.6</b>	<b>20.9 ± 2.0</b>	<b>&lt;.001</b>

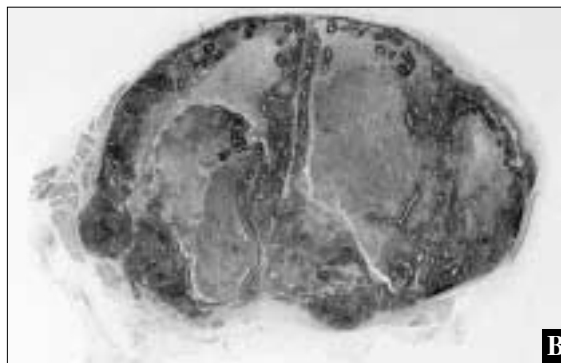
\*Amax = maximum tumour size before regression; Tmax = time at which Amax was reached.

**Figure 2.2.**

Typical image of first echelon lymph node metastasis.

A: Lymph node metastasis (arrow) in the left parotid. a = angle of the mandible.

B: Microscopy of lymph node on section (HE-staining, x10).



The Vx2 auricle carcinoma model

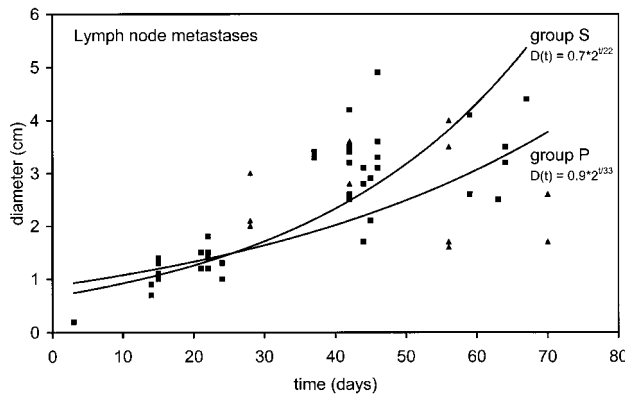


**Figure 2.3.**  
Exponential trend lines correlating the size of lymph node metastases and time after transplantation in Group S (■) and Group P (▲).

tasis was present and 7/26 (27%) necks had second echelon metastases. No third echelon metastases were found in either group. Differences in development of second echelon lymph node metastases between Group S2 and P were not significant. There was also no significant difference in growth of lymph node metastases between Groups S and P, with lymph node-size doubling-times of 22 and 33 days respectively (Fig. 2.3).

**2.3.3 Lung metastases**

Group P: One of the 7 rabbits (14%), sacrificed at day 42, had lung metastases.

Group S: Five of the 16 rabbits (31%) in S1 and 7 of the 15 rabbits (47%) in S2 had lung metastases (Fig. 2.4). Three rabbits that were sacrificed because of symptoms of tachypnoe and cyanosis on days 37, 44 and 59 respectively, had lung metastases larger than 14 mm in diameter. Differences in development of lung metastases between Group S2 and P were not significant.

When relating the size of the largest lung metastasis with the time after transplantation, an exponential trend-line was found (according to  $D(t) = 2.0 \times 2^{t/26}$ ) corresponding to a lung tumour-size doubling-time T of 26 days (Fig. 2.5). The size of the only metastasis in Group P did not differ from the sizes found in Group S. This trend line reaches a size of 14 mm at week 10 after transplantation.

No significant correlation was found between the size of the primary tumour and the development of lung metastases (Table 2.2). Only one rabbit (Group S1, sacrificed at day 10) had a 1 mm lung metastasis without evidence of tumour in the lymph nodes.

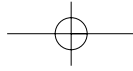


**Figure 2.4.**

Typical image of lung metastases in Group S, 6 weeks after transplantation.

- A: Heart-lung specimen with metastases (arrows).
- B: Microscopy of lung metastasis (m) on section (HE-staining, x10).

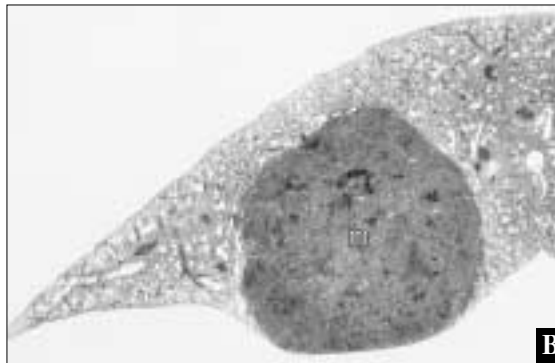
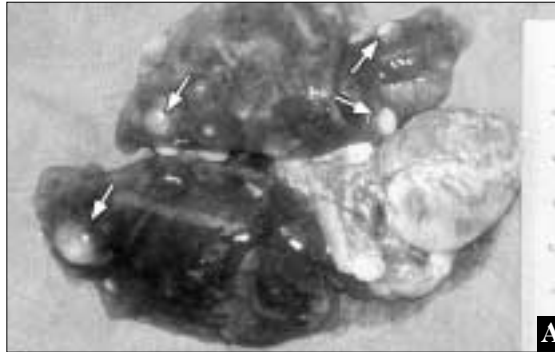
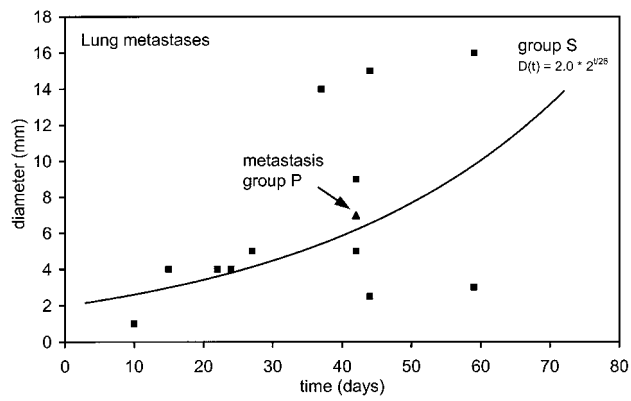


**Figure 2.5.**

Exponential trend line correlating size of lung metastases in Group S (■) with time. The only metastasis in Group P is depicted with a ▲.



The Vx2 auricle carcinoma model

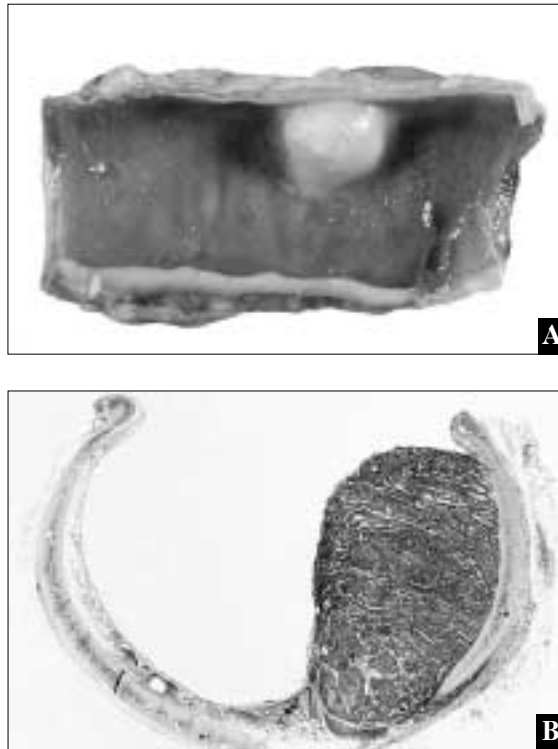


**Figure 2.6.**

Endo-tracheal metastasis,  
Group S, 27 days after  
transplantation.

A: Trachea cut open at dorsal  
side.

B: Microscopy of cross section  
through metastasis  
(HE staining, x10).

**2.3.4 Other metastases**

A 5 mm large endotracheal metastasis was found in one animal (3%) of Group S (Fig. 2.6). This rabbit died 27 days after transplantation, during the night. It was autopsied the next morning, revealing also multiple pulmonary metastases up to 5 mm in diameter. No metastases were found at other sites in this animal and any of the other rabbits.

**2.3.5 Weight loss**

A significant correlation was found between weight loss and primary tumour-size and between weight loss and size of lung metastases (Table 2.2). Weight loss of the 3 rabbits that had to be sacrificed because of massive pulmonary metastases ranged from 11.7 to 22.2% (average 17.2%).

**Table 2.2.** Correlation of tumour parameters in Group S (Kendall's tau)

	Time	Primary	Lymph node	Lung
<b>Time<sup>a</sup></b>	–			
<b>Primary<sup>b</sup></b>	<b>&lt;0.001</b>	–		
<b>Lymph node<sup>c</sup></b>	<b>&lt;0.001</b>	<b>&lt;0.001</b>	–	
<b>Lung<sup>c</sup></b>	<b>0.096</b>	<b>ns*</b>	<b>ns*</b>	–
<b>Weight loss</b>	<b>ns*</b>	<b>0.015</b>	<b>ns*</b>	<b>0.020</b>

<sup>a</sup>: time (days) after transplantation

<sup>b</sup>: size (cm<sup>2</sup>) of the primary tumour

<sup>c</sup>: diameter (mm) of the largest lymph node or lung metastasis

\* ns: not significant.

## 2.4 Discussion

### 2.4.1 Success of transplantation

In this study, successful transplantation of the Vx2 carcinoma was better using tumour cell suspensions than tumour pieces, yielding a take-rate of 78%. Many authors do not report their response rates explicitly [Muckle and Dickson, 1971; Tromberg et al., 1990; Gadeholt-Göthlin and Göthlin, 1995; Päuser et al., 1996; Harima et al., 1996; Hoshi et al., 1997; Matsumoto et al., 1999;]. Of those who do mention their success, take-rates of Vx2 suspensions injected intramuscularly in the hind limb vary from 95% to 100% [Herman et al., 1976; Wagner, 1994]. Take-rates of the implantation of tumour pieces in corneas has also not been stated explicitly [Brem and Folkman, 1975; Tamargo et al., 1991] although Brem and Folkman [1975] claim that spontaneous regressions did not occur.

'Non-takes' and spontaneous regressions are not easy to distinguish, because in the first week after transplantation always a reactive swelling occurs. It is an important issue however, because spontaneous regressions make statements on the efficacy of anti-tumour treatment unreliable. The regressed tumours in Group S can be addressed as 'non-takes', because the transplanted tumour mass subsided after 10 days with a maximum size of only 0.8 cm<sup>2</sup>. However the regressed tumours in Group P are true remissions: A substantial tumour mass (2.4 cm<sup>2</sup> on average) developed up till 21 days after transplantation before growth ceased.

---

**The Vx2 auricle carcinoma model**

The poor take-rate of 59% in Group P can be explained by the presence of a significant number of dead Vx2 cells, despite the fact that we took care to obtain well-vascularised tumour pieces. This may have had an immunisation effect stimulating an effective immune response and preventing outgrowth of tumour. This phenomenon is comparable with the transplantation failures seen when injecting cryopreserved tumour cell suspensions (chapter 5), or the tumour regression induced by local heating [Muckle and Dickson, 1971]. Furthermore the use of neonatal rabbits with an immature immune system [Brem and Folkman, 1975; Tamargo et al., 1991] can explain better take-rates. Also the site of transplantation of the primary tumour might influence the tumour take-rate: Kidd and Rous [1940] observed that 'as a rule the Vx2 cancer does badly in the subcutaneous tissue'. The fact that our model is based on subcutaneous growth in the auricle explains a less favourable take-rate when compared to models based on growth in muscle of the hind limb [Herman et al., 1976; Wagner, 1994] or tongue [Matsumoto et al., 1999]. This is why the transplantation of at least  $20 \cdot 10^6$  vital cells into the auricle is advised (chapter 5). The late spontaneous remissions in this study are a reason to advice against transplantation of tumour pieces in the Vx2 auricle model.

**2.4.2 Lymph node metastases**

Injecting tumour suspensions can force tumour cells into lymph vessels resulting in lymph node seeding at implantation. Nevertheless, in our model development of lymph node metastases appears to be independent from the technique of transplantation. The trend-lines correlating the size of lymph node metastases with time after transplantation as well as the incidence of first echelon metastases did not differ between the two groups. Though we found a trend for a higher incidence of second echelon (retromandibular) metastases in Group S (26% vs 8%), it was not statistically significant.

By day 28 after transplantation, more than 90% of the necks in both groups contained lymph node metastases. Matsumoto et al. [1999] even found 100% lymph node metastases after injecting Vx2 suspensions in the tongue. It is convenient to have an animal model in which both the primary tumour and the development of lymph node metastases can be linked to effects of an anti-tumour regimen [Matsumoto et al., 1999; chapter 3]. The easy accessibility of the first echelon parotidial metastases for measurements in-vivo makes this model useful for experimental studies on the effects of treatment regimens on regional lymph node metastases as well.

### 2.4.3 Lung metastases

Although a trend for a higher incidence of lung metastases was noted in Group S when compared to Group P, pulmonary seeding at implantation does not play a significant role in this model. The earliest sacrifice because of advanced pulmonary disease was noted at day 37 after transplantation. A size of 14 to 16 mm seems to be critical for pulmonary metastases in this model. At that point tachypnoe and cyanosis demand sacrifice of the animal. The trend line correlating the size of lung metastasis with time crosses this critical limit at 10 weeks after transplantation (Fig. 2.5). The development of lung metastases does seem to be a problem when injecting Vx2 suspensions into well vascularised parenchymatous tissues such as the kidney, the bladder, the uterus and also the tongue. Matsomoto et al. [1999], inducing tongue tumours, found already 80% lung metastases at day 22. Hoshi et al. [1997], inducing Vx2 bladder tumours, found 100% lung metastases at day 35. Gadeholt-Göthlin and Göthlin [1995], inducing Vx2 renal tumours, noted that 'all the control rabbits had to be killed because of advanced pulmonary disease after 32-38 days'. Harima et al. [1996], inducing Vx2 uterus tumours, noted that in the 5th week 'metastases to the lungs resulted in death of more than 80% of the animals'. These findings almost parallel the development of lung metastases when a Vx2 suspension is injected directly intravenously as seen in the pulmonary metastases model by Kim et al. [1993]. In contrast, Vx2 suspensions injected in skeletal muscle do not seed at implantation: In a cachexia model [Conlon et al., 1993], lungs were macroscopically free of tumour at 30-45 days and death from lung metastases only occurred at week 10 after intramuscular Vx2 tumour-injection [Muckle and Dickson, 1971]. This corresponds well with the findings in the present study and probably demonstrates the natural tendency of dissemination of Vx2 cells to the lung. Unfortunately, investigators that used Vx2 pieces as transplants do not report whether lung metastases occurred [Brem and Folkman, 1975; Tamargo et al., 1991]. From the data on the pulmonary metastases model by Kim et al. [1993] a tumour-size doubling-time (T) of 9.8 days can be deduced for lung metastases. This corresponds well with the T of the Vx2 at the auricle (chapter 5), varying from 4.5 to 9.9 days, but not with the T of the secondary lymph node and lung metastases in this model varying between 22 and 33 days. A theoretical existence of two different lung metastases growth curves, one related to the seeding at implantation and one related to the natural dissemination tendency of the Vx2 tumour itself, could not be discerned in this study.

#### 2.4.4 Other metastases

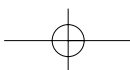
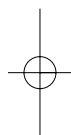
The endotracheal metastasis found in this study was either haematogenic or originated from Vx2 cells entrapped in the submucosal lymph sinuses. Like other investigators [Kidd and Rous, 1940; Muckle and Dickson, 1971; Gadeholt-Göthlin and Göthlin, 1995; Hoshi et al., 1997], haematogenic metastases at sites other than the lungs were not found in any of the animals. Also direct i.v. injection of Vx2 suspensions does not induce metastases outside the thorax [Kim et al., 1993]. Because the event is rare, it is not necessary to consider metastases at other sites in practice when using this Vx2 auricle carcinoma model.

#### 2.4.5 Weight loss

Weight loss appears to be strongly associated with the presence of lung metastases, a phenomenon also observed in humans. When weight loss exceeds 10%, sacrifice should be considered in the interest of the animal's well fare. Also Gadeholt-Göthlin and Göthlin [1995] report the sacrifice of 'sick-looking rabbits' with weight loss exceeding 10-15%. Additional important signs are tachypnoe and cyanosis. Because immature rabbits in study show weight gain, Conlon et al. [1993] define cachexia as '>15% deviation from previously determined normal growth'. In practice it is easier to use the definition of weight loss applied in this study, because determination of 'normal growth' needs an extra control group of non-tumour bearing rabbits. The weight loss seems related to loss of appetite [Conlon et al., 1993], which was not quantified in this study.

## 2.5 Conclusions

The biological behaviour of this Vx2 head and neck tumour model closely mimics head and neck cancer in humans. Tumour transplantation with solid pieces is not advised because of spontaneous regressions. Transplantation with tumour suspensions does not significantly raise the incidence of metastases to the lymph nodes or lungs. Thus, the phenomenon of artificially created metastatic deposits due to seeding at implantation does not play a significant role in this model. Also the occurrence of metastases at other sites is very rare. Lymph node metastases develop in more than 90% of the necks after the 4th week following transplantation. Therefore, this model can be used for experimental studies on the effects of treatment regimens targeting both the primary tumour and the metastases in draining lymph nodes.





chapter

3

Peri-tumoural IL-2 treatment of the rabbit  
Vx2 head and neck cancer model induces a  
systemic anti-tumour activity



---

R.J.J van Es, A.H.C. Baselmans, J.W. Koten, J.E. van Dijk, W. den Otter, R. Koole

Anticancer Research 2000;20:4163-4170 (modified version)



## Abstract

**Introduction:** Head and neck cancer is associated with impaired cell-mediated immune reactivity. A rabbit model with Vx2 Squamous cell carcinoma transplanted into both auricles was used to test the effects of a regimen for local IL-2 therapy, optimal in murine tumour models.

**Materials and Methods:** Peri-tumoural IL-2 treatment started when one of the tumours exceeded 2 cm<sup>2</sup> and consisted of 100,000 or 300,000 Chiron Units IL-2 or only solvent during 5 consecutive days.

**Results:** In 4/12 (33%) rabbits the treated primary tumours regressed completely, simultaneously with the non-treated contra-lateral tumours. Also metastases in draining lymph nodes of both treated and untreated primary tumours regressed in three of these animals. Three (25%) of all 12 treated animals were cured. Tumour cells injected in the cured animals were rejected. Histology of regressing tumours in cured cases showed an active granulomatous reaction with a histiocytic response, splitting up of tumour islands, and obstruction of blood vessels with fibrin thrombi.

**Conclusion:** These findings show local and systemic therapeutic effects of this peri-tumoural IL-2 regimen in a Vx2 head and neck cancer model.

We thank C.H.P. Pellicaan for preparing the IL-2 solutions, A. van der Bilt for his mathematical advice, A. Versluis and H. Boere for taking care of the rabbits, P. Rothengatter for the photography and J. Klaversteijn for preparing the histological sections.

## 3.1 Introduction

Immune-stimulation with IL-2 is considered a valuable adjuvant therapy for various human tumours such as advanced renal cell carcinoma, bladder cancer and metastatic malignant melanoma [Heys et al., 1993]. Squamous cell carcinoma of the head and neck (HNSCC) has been associated with impaired cell-mediated immune reactivity [Wolf et al., 1987]. Therefore, stimulation of immune reactivity with immune modulating agents such as Interleukin-2 (IL-2) may be therapeutically important. Animal models can assist in determining appropriate doses, time intervals, and location of injections for clinical trials with IL-2. Carroll et al. [1995] prevented progressive growth of the Vx2 Squamous cell carcinoma (SCC) implanted into the rabbit hind paw by biweekly peri-lesional injections of 10,000 U IL-2 (Hoffman-La Roche). However, complete tumor remissions did not occur. Moreover, the Vx2 hind paw model does not mimic the situation of a HNSCC in humans. Until now, variable results but no cures have been reported with peri-lesional injections or local infusions of IL-2 in humans with HNSCC [Gore et al., 1992; Vlock et al., 1994]. This may in part be due to different regimens of IL-2 application. Variable results have also been reported on peri-tumoural injections of IL-2 in animals with transplanted carcinoma cells, such as adenocarcinomas in rats [Hendriksson et al., 1992; Liu et al., 1996] and mice [Liu et al., 1994], hepatocellular carcinomas in guinea pigs [Claessen et al., 1992; Balemans et al., 1993] and alveolar carcinomas in mice [Dubinett et al., 1993]. Results in these studies varied from growth retardation up to 24% complete remission of the carcinomas.

The aim of the following study is to establish whether a regimen for local IL-2 therapy that is optimal in murine tumor models [Den Otter et al., 1996], is capable of inducing complete remissions in this new Vx2 head and neck cancer model.

## 3.2 Materials and methods

### 3.2.1 Rabbits

Fourteen adult female NZW rabbits were used under conditions as described in chapter 2.2.1.

### 3.2.2 Tumour cells

Vx2 tumour cell suspensions were prepared as described in chapter 2.2.2. The number of cells in suspension was counted using a haemocytometer. Viability of cells was estimated by Trypan blue exclusion.

### 3.2.3 Tumour induction and tumour challenge of animals with tumour remission

Hair was removed from the auricles. To induce tumours, 0.10 - 0.15 ml of a suspension containing  $15$  to  $35 \times 10^6$  vital tumour cells was injected with a 0.5 mm needle s.c. into both auricles. The injection site was the area between the central auricular artery and caudal margin, at the dorsal middle-third of each auricle.

In case of remission of the primary tumour, tumour resistance was tested by injecting  $30 \times 10^7$  vital Vx2 cells intramuscularly in the thigh of the hind paw.

### 3.2.4 IL-2 Injections

Human recombinant IL-2 was kindly provided by Chiron, Amsterdam, the Netherlands. IL-2 was suspended in a solvent containing water, glucose 5% and Haemacel 10% [Hoechst Marion Roussel, Hoevelaken, the Netherlands]. The IL-2 solutions were frozen in 2 ml polypropylene cryo vials (Greiner BV, Alphen aan den Rijn, the Netherlands) at  $-80^\circ\text{C}$  by flash point freezing. The vials contained 100,000 or 300,000 Chiron U IL-2/0.2 ml or 0.2 ml solvent only. The treatment groups were:  
Group A (n=6), treated with 100,000 U IL-2/0.2 ml/day  
Group B (n=6), treated with 300,000 U IL-2/0.2 ml/day  
Group C (n=2), treated with 0.2 ml solvent/day

IL-2 injections were started when the size of one of the auricle tumours exceeded  $2 \text{ cm}^2$ . IL-2 was administered daily on 5 consecutive days. Each day, the total volume of 0.2 ml was delivered in 4 portions of 0.05 ml in 4 quadrants immediately adjacent to only one tumour (the one that exceeded  $2 \text{ cm}^2$ ). The tumour in the other auricle was left untreated. The animals were treated blindly and the code was broken after evaluation of tumour regression.

### 3.2.5 Biopsies and sacrifice

Three days after completion of the 5-day IL-2 treatment, that is on day 8, an incisional biopsy was taken from the caudal quadrant of all treated tumours (n=14). Of animals A3,4,5 and B2,3,4 also a biopsy from the non-treated contra-lateral tumour was available. In case of progressive tumour growth, rabbits were sacrificed in the 8th week after transplantation or earlier in case of excessive tumour burden as indicated by loss of appetite, over 10% weight loss, tachypnoea, scratch infection of the auricle, or other indications as observed by the animal tenders.

### 3.2.6 Analgesia, sedation and euthanasia

For details on analgesia, sedation and euthanasia is referred to chapter 2.2.4. Biopsies were taken under additional local anaesthesia with lidocaine 2%.

### 3.2.7 Evaluation of tumour growth

The tumour size was measured with callipers biweekly in two dimensions and recorded as surface area ( $A$ ,  $\text{cm}^2$ ). Enlargement of lymph nodes in the neck was recorded biweekly by palpation and measured with a calliper. To calculate the time point at which tumours went into regression, i.e. the interval between the start of the IL-2 therapy and the first sign of remission, a mathematical model was used assuming the tumour to grow and regress exponentially with a fixed rate [Hasenclever et al., 1996]. Growth and regression are characterised by the relaxation times  $\tau_1$  and  $\tau_2$ , respectively i.e. the time the tumour surface has increased or decreased, respectively with a factor  $e$  ( $=2.72$ ). Relaxation times were estimated by the best fitting curve that applied to the following functions of  $A$ :

$$\begin{aligned} [1] \text{ increase } & A(t) = A_0 \cdot e^{t/\tau_1} \\ [2] \text{ decrease } & A(t) = A \cdot e^{-(t-t_1)/\tau_2} \end{aligned}$$

in which  $t_1$  is the time the tumour size is back at the level of  $A_0$ . The resulting tumour size is the composite of these two processes. This can be written as:

$$[3] A(t) = \{A_1(t) \cdot A_2(t)\} / \{A_1(t) + A_2(t)\}$$

Tumour regression is then assumed to commence at the time point at which the derivative of the function [3] equals zero, i.e. at the top of the curve as shown in Figure 3.2. In other words, the time at which tumours went into regression is the interval between the start of the IL-2 therapy and the first sign of remission.

### 3.2.8 Histopathology

At autopsy, the primary tumours were excised. Parotid and retromandibular lymph nodes were collected bilaterally. The thoracic and abdominal organs were inspected and location, number, and size of the metastases were recorded.

Biopsy and autopsy tissues were placed in 10% buffered formalin. Paraffin sections ( $5 \mu\text{m}$ ) were prepared and stained with haematoxylin and eosin. All sections were studied by a panel of 3 experienced pathologists. In later sessions consensus was obtained during a panel discussion.

## 3.3 Results

### 3.3.1 Clinical observations

The clinical observations are summarised in Tables 3.1 and 3.2. After transplantation, auricular tumours developed in 11/14 rabbits on both sides (i.e. twin tumours) and 3 rabbits had only single tumours (rabbits A2, A6, and B1). Eleven to 21 days were needed to reach the size of 2 cm<sup>2</sup> of the quickest growing tumour ( $\Delta T$ , Table 3.1). Thereafter, IL-2 treatment started.

Complete regression of treated primary tumours occurred in 4 out of 12(33%) IL-2 treated animals. Of these 4 rabbits, three (A1, B2, B3) had twin tumours. In each case the non-treated contra-lateral tumour regressed simultaneously with the perilesionally injected tumour (Figs. 3.1 and 3.2). So, there were 7 regressing tumours. The time point at which the tumours went into regression varied from 5 to 15 days (mean  $8.7 \pm 4.2$  days) after start of IL-2 therapy.

In rabbits with remission of their primary tumours, tumour resistance was tested by an intra-muscular injection with Vx2 tumour cells in the hind paw. No tumours developed within 2 weeks.

In 3 out of the 4 rabbits with complete regression of their primary tumours, enlarged neck nodes suggestive of metastases were present at the start of IL-2 treatment. In 2 of these 3 rabbits, the enlarged nodes disappeared simultaneously with their primaries. In the third rabbit however, the lymph node contra-lateral to the IL-2 injected primary, grew despite complete remission of both primaries (rabbit B3, Table 3.1).

Tumours grew progressively in the auricles of the 2 controls and all 8 non-regressor rabbits. This was accompanied by enlargement of the draining parotid lymph nodes (Figs. 3.3 and 3.4). Progressive growth of the primary tumour coincided with hyperaemia of the auricle and a purple discoloration of the skin adjacent to the tumour. The disappearance of these vascular signs was an important first clinical indication of tumour remission.

Start of the IL-2 injections in the non-responders varied from day 11-21 after transplantation.

### 3.3.2 Autopsy findings

#### 3.3.2.1 Rabbits with progressive tumour growth

Primary tumour growth progressed in the 2 controls and in 8 IL-2 treated animals, comprising a total of 18 progressing primary tumours. Two rabbits developed pul-

Peri-tumoural IL-2 treatment

Table 3.1. Data of treated animals

		$\Delta T$ day	Tumour size (cm <sup>2</sup> ) at day					$T \ddagger$ day	Metastases*	
			0	7	14	21	$\ddagger$		neck	lung
<b>Group A</b>										
1	L	11	1.4	3.0	2.9	2.7	0.2	56	-	-
	R#		2.5	4.3	5.6	4.9	0.0		-	
2	L	18	-	-	-	-	-	38	-	-
	R#		2.3	3.5	3.1	3.3	6.2		+	
3	L#	18	2.1	4.7	3.9	5.0	8.8	38	-	-
	R		2.0	2.6	2.3	2.5	4.8		-	
4	L	14	1.2	2.3	4.3	6.8	13.0	30	+	+
	R#		2.3	4.8	7.5	9.6	13.1		+	
5	L#	14	2.0	5.4	7.7	10.4	18.1	32	+	-
	R		1.4	3.0	4.2	5.0	8.8		+	
6	L	21	-	-	-	-	-	38	-	+
	R#		2.2	3.0	4.6	5.9	14.6		+	
<b>Group B</b>										
1	L	17	-	-	-	-	-	42	-	-
	R#		2.4	3.1	2.4	1.4	0.0		-	
2	L	11	2.4	2.7	1.7	0.7	0.0	76	-	-
	R#		3.2	5.2	4.3	1.9	0.0		-	
3	L	11	2.2	2.3	1.2	0.3	0.0	76	+	-
	R#		2.3	3.4	1.6	0.4	0.0		-	
4	L#	11	2.1	4.5	5.6	7.3	11.3	33	+	++
	R		1.2	4.1	5.0	7.3	11.3		+	
5	L#	11	2.2	5.2	7.2	8.1	14.3	42	+	+
	R		1.4	4.0	6.6	7.6	14.9		+	
6	L	11	0.6	1.9	2.9	3.9	7.7	34	+	-
	R#		3.1	6.0	7.5	18.1	27.0		+	
<b>Group C</b>										
1	L	14	2.5	5.3	9.6	13.3	15.0	23	+	++
	R#		2.9	5.6	10.0	13.1	15.2		+	
2	L	11	2.1	5.5	6.5	8.4	15.2	35	+	-
	R#		2.3	5.7	7.4	9.9	17.0		+	

L/R : Left / Right, # = IL-2 treated auricle; day 0 : start of IL-2 therapy, day  $\ddagger$  = day of sacrifice;  $\Delta T$  : time between tumour transplantation and start of IL-2 therapy;  $T \ddagger$  : time between start of IL-2 therapy and sacrifice;

\* : metastases microscopically confirmed: +/++ = some small (1-3 mm) / many large (8-15 mm) lung metastases

**Table 3.2.** Summary of the therapeutic effects

Group	N	Remission of primaries	Cures
<b>A (100,000U)</b>			
<b>Single tumour</b>	<b>2</b>	<b>0 / 2</b>	
<b>Twin tumours</b>	<b>4</b>	<b>1 / 4</b>	<b>1 / 6 (17%)</b>
<b>B (300,000U)</b>			
<b>Single tumour</b>	<b>1</b>	<b>1 / 1</b>	
<b>Twin tumours</b>	<b>5</b>	<b>2 / 5</b>	<b>2 / 6 (33%)</b>
<b>C (solvent)</b>			
<b>Twin tumours</b>	<b>2</b>	<b>0 / 2</b>	<b>0 / 2 (0%)</b>

N = number of animals

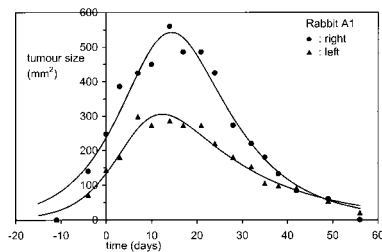
**Figure 3.1.**

Rabbit A1.  
Simultaneous regression of twin tumours at day 35 after peri-tumoural IL-2 injections of the right auricle.



**Figure 3.2.**

Rabbit A1.  
Fitted growth curves of both auricle tumours.



Peri-tumoural IL-2 treatment



**Figure 3.3.**

Rabbit C2, placebo.  
Progressive growth of twin tumours at day 35. Note bilateral swelling of parotid lymph nodes.

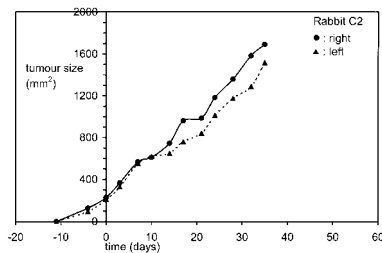


**Figure 3.4.**

Rabbit C2.  
Actual growth curves of both auricle tumours.

monary distress due to metastases. All parotid lymph nodes related to these 18 primaries were enlarged. Retromandibular lymph nodes were enlarged in 12 of these 18 tumours. Lung metastases were present in 5/10 (50%) of these animals. These metastases varied from some small (1-3 mm) nodules in 3 rabbits to many large (8-15 mm) nodules in 2 rabbits (Table 3.1). No metastases were found at other sites.

### 3.3.2.2 Rabbits with tumour remission

The 4 animals with a total of 7 primary tumours that regressed completely were killed at days 59, 67 and 87(2x) after transplantation, respectively. There was a nodular, palpable scar at the primary site. Small draining parotid lymph nodes were harvested in 5 of the 7 cases; they did not contain tumour. In one case no nodes were found. Finally, as mentioned before, in one case there was a large tumour mass in the parotid lymph node contra-lateral to the treated auricle tumour. No lung metastases were seen. At the injection site of the intra-muscular challenge in the thigh of the hind paw, the absence of tumour growth was confirmed microscopically.

### 3.3.3. Histopathology

#### 3.3.3.1 Tumour biopsies

As mentioned, biopsies were taken 3 days after completion of IL-2 treatment. All biopsies, both from controls and IL-2 treated tumours showed a variable degree of ischaemic tumour necrosis, which is typical for the Vx2 tumour. Vital tumour cells were already absent in 2 of the 6 biopsies (a biopsy of the non-treated tumour -A1- was not available) from the tumours that subsequently went into regression. This is notable, as measurable tumours were still present at day 21. So, the complete regression of a tumour nodule requires time after all cancer cells have died.

In contrast, all biopsies from the 18 progressively growing tumours still contained vital tumour cells. In large necrotic areas, blood vessels were seen surrounded by strands of vital tumour cells. The border between vital and necrotic tumour tissue was sharply demarcated. No inflammatory cells were seen at the tumour borders. A subcutaneous inflammatory infiltrate was present in the biopsies of both responders and non-responders. It consisted of neutrophilic ('pseudo-eosinophilic') granulocytes, lymphocytes, macrophages, and variable numbers of plasma cells.

In the biopsies of the responders, degeneration of tumour cells was observed particularly in the border areas adjacent to the inflammatory infiltrate. The degenerated tumour cells had a clear cytoplasm, blurred cell borders and occasionally pycnotic nuclei. Moreover, there was an increase of granulomatous tissue splitting up the tumour strands, leaving isolated degenerating tumour islands. The macrophages showed phagocytic activity, sometimes with giant cell formation. In addition, the thin-walled dilated blood vessels in the tumour were occasionally occluded by fibrinoid coagulations. Remarkably, there were no microscopical differences between regression of the IL-2 treated and the contra-lateral non-treated tumours.

#### 3.3.3.2 Primary tumours at autopsy

All progressively growing primary tumours showed massive invasion of the subcutis. In some cases the adjacent auricular tissues, i.e. cartilage and muscles were also invaded. Extensive necrosis was always observed. Type and morphologic features of this necrosis were similar as described for the biopsies.

There were 4 rabbits with complete remission of the primary tumour. Rabbits A1 and B1 were sacrificed at day 67 and 59, respectively. The primary sites contained necrotic areas with ghosts of tumour cells. These areas were surrounded by an infiltrate consisting mainly of plasma cells, foamy macrophages, giant cells, and few lymphocytes (Fig. 3.5). Rabbits B2 and B3 were sacrificed at day 87. No tumour tissue was present. Instead, dense fibrous scar tissue was noted containing throm-

Peri-tumoural IL-2 treatment

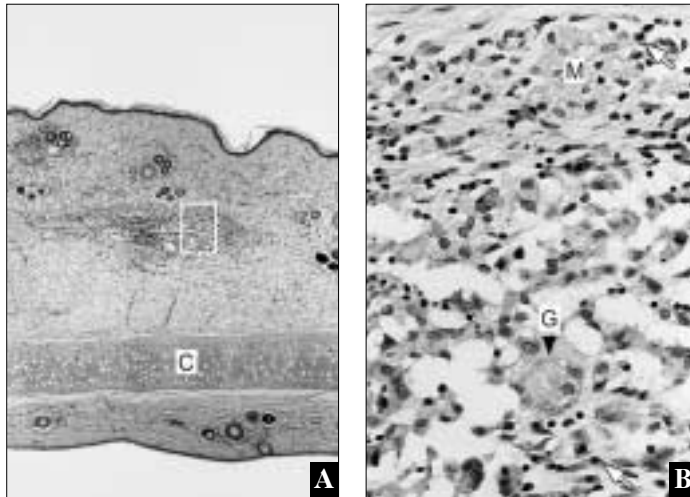


**Figure 3.5.**

Rabbit B1, 42 days after IL-2 therapy.

A: Microscopy of transverse section through the auricle at the site of the regressed tumour.

C = cartilage, original magnification 10x.

B: Detail of rectangular area.

Macrophages (M), plasma cells (white arrows), lymphocytes and a syncytial giant cell (G), original magnification 100x, HE-staining.

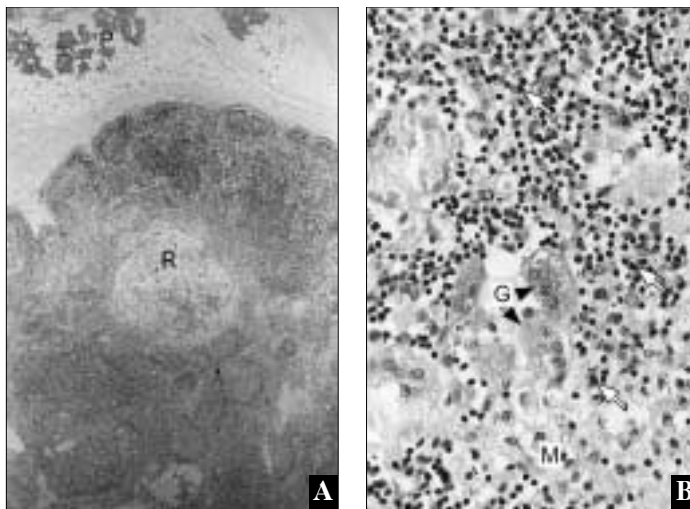


**Figure 3.6.**

Rabbit A1, 56 days after IL-2 therapy.

A: Microscopy of section through parotid lymph node showing a regressed metastasis (R). P = parotid salivary gland, original magnification 10x.

B: Detail of regressed metastasis.

Foamy macrophages (M), plasma cells (white arrows), lymphocytes and syncytial giant cells (G), Original magnification 100x, HE-staining.

bosed vessels, some lymphocytes and focal clusters of foamy macrophages packed with hemosiderin pigment.

### 3.3.3.3 Lymph nodes at autopsy

All lymph nodes showed a variable degree of lymphoid hyperplasia characterised by hyperplastic paracortical zones and enlarged follicles with marked germ centres. In the 10 animals with a total of 18 progressively growing primary tumours, metastases were microscopically confirmed in 16/18 (89%) of the parotid lymph nodes

and in 2/18 (11%) of the retromandibular lymph nodes.

The parotid lymph node of the rabbit B1 with complete regression of the primary tumour showed no evidence of vital or necrotic tumour cells. Bilaterally, the parotid lymph nodes of rabbit A1 with regression of both primary tumours were large and showed a hyperplastic appearance indicating a marked immune response. In some areas there were large fields with foamy macrophages indicating phagocytosis of necrotic debris (Fig. 3.6). This image was comparable to the histologic findings of the regressed primaries, suggesting the remission of a lymph node metastasis. Bilaterally, the parotid lymph nodes of rabbits B2 and B3, killed at day 87, showed a moderate lymphoid hyperplasia without evidence of tumour cells in all nodes but one. As mentioned, this was the lymph node contra-lateral to the IL-2 injected primary in rabbit B3 (Table 3.1), that showed progressive growth despite complete remission of both primaries.

### 3.4 Discussion

This study was primarily intended to assess whether any complete remissions could be obtained with IL-2 therapy in this model for head and neck cancer. The results were positive as complete tumour regressions could be obtained in 33% and cures in 25% of the rabbits after peritumoral administration of 100,000 or 300,000 U (Chiron) IL-2 during 5 consecutive days.

Carroll et al. [1995], injecting Vx2 carcinoma in the rabbit hind paw, failed to achieve complete remissions with a regimen of biweekly injections of 10,000 U (Hoffman-La Roche) IL-2. Possible explanations are:

1. Both the dose and the time intervals between IL-2 injections were not optimal [Den Otter et al., 1996].
2. Killing rabbits 1 week after completion of the IL-2 injections is too early to assess the effects of IL-2 therapy. In this study, the time point at which the first sign of remission was observed was highly variable, ranging from 0 to 10 days after completion of the therapy. Complete tumour regression took at least 6 weeks.
3. Initiating IL-2 treatment already at the day of tumour transplantation is ineffective. Maas et al. (1991) and Everse et al. [1996], using the SL2 lymphosarcoma model in DBA/2 mice, demonstrated that no therapeutic effect was observed if the interval between transplantation and the start of the IL-2 therapy is less than 7 days. In this study all IL-2 treatments started at least 11 days after transplantation, i.e. at the moment the tumours reached 2 cm<sup>2</sup> in size.

---

**Peri-tumoural IL-2 treatment**

The approach of linking IL-2 treatment to the tumour size instead of the time after transplantation, was chosen not only because of the different growth rate of tumours in different rabbits in the Vx2 model (chapter 5), but also because the tumour size is strongly correlated to the effect of the treatment in humans with HNSCC.

In a study with a LDLX40 adenocarcinoma in BALB/c mice, Liu et al. [1994] possibly did not obtain complete remissions because the mice were already killed 2 days after the last IL-2 injection, so the follow-up was too short. In a later study Liu et al. [1996] acquired 17% complete remissions 4 weeks after completion of IL-2 treatment in a breast cancer model using a LDLX43 adenocarcinoma in Wistar rats. Also Henriksson et al. [1992], using a prostatic adenocarcinoma in rats, did not achieve complete remissions with a continuous subcutaneous IL-2 infusion of  $1.1 \times 10^6$  Chiron U daily for 28 days. However, this cell line is a 'slow grower', as it requires even 3 months after transplantation to reach a treatable size. Such a tumour might also require a long regression period, whereas these authors stopped their observations already at the end of the IL-2 treatment. In the slowly growing, spontaneously occurring bovine ocular SCC, complete remission of IL-2 treated tumours also requires several months [Den Otter et al., 1993].

The effects of our study are comparable with the findings of Dubinett et al. [1993], using a line 1 alveolar cell carcinoma in BALB/c mice. They obtained a 24% cure rate injecting tumours twice daily with 50,000 Chiron Units per injection, which became apparent at about 10 days after the IL-2 treatment. Dubinett's experiment only differs from ours with respect to the continuation of the IL-2 treatment for 3 weeks, an extension of treatment that probably is unnecessary [Den Otter et al., 1996].

The differences in comparing and converting 'Hoffman-La Roche Units' and 'Chiron Units' to 'International Units'(IU) might be another explanation for the variability of the therapeutic effects in different IL-2 studies. According to Liu et al. [1996] 1 Chiron Unit has a comparable effectiveness of 6 IU, whereas Den Otter et al. [1996] suggest 1 Chiron Unit to be only as effective as about 0.1 IU.

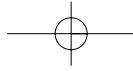
This study confirms the development of systemic therapeutic effects following local treatment with IL-2 [Maas et al., 1991], since both the IL-2-treated and the non-treated auricle tumours regressed. In addition, after a tumour challenge of cured animals the tumour did not take. The mechanism of the IL-2 induced tumour regression is as yet not fully understood. We assume that after tumour transplantation an early immune response develops, which is further boosted by IL-2 treatment. Indeed, a peri-tumoural infiltrate, consisting of macrophages, lymphocytes, and granulocytes was present in all biopsies. This results in a two-fold reaction:

1. Tumour cell degeneration, in particular at the tumour borders where the inflammatory infiltrate is present. This infiltrate gets a granulomatous character, which leads to splitting up of the tumour, resulting in necrosis and phagocytosis of tumour tissue.
2. The intra-tumoural vascular network may be vulnerable for IL-2 enhanced immune mechanisms. The clinically observed diminution of hyperaemia and purple discolouration around the tumour at the onset of tumour remission may be an indication of this IL-2-mediated vascular response. Furthermore, the rapidity of the tumour regression can only be explained if a vascular component is operating, affecting the intra-tumoural blood flow. Also De Mik et al. [1991] observed involvement of a vascular response in IL-2 induced tumour regression. They noted vascular dilatations, intra-luminal occlusions and features of stagnating circulation. This was also seen in some sections in the present study. However, we are not sure whether the latter is a primary cause of tumour necrosis or an epi-phenomenon.

Remarkably, in one rabbit a contra-lateral parotid lymph node metastasis persisted despite complete and permanent remission of both primary auricle tumours. Though unlikely, it is possible that this node contained a dedifferentiated Vx2 clone, resulting in a different immunogenic cell type. We are not aware of data discussing the development of such dedifferentiated Vx2 clones. Alternatively, the anti-tumour effectivity of the immune response at the primary site and in lymph node metastases might be different. Effects observed in this study mimic the histological changes found by Shah and Dickson [1978] after treating Vx2 hind limb tumours with local hyperthermia. These investigators postulated that the rabbits that died from metastases despite regression of the primary tumour had an 'inadequate' stimulation of their immune response. This finding supports the philosophy of treating both the primary lesion as well as the neck nodes with peri- or intra-tumoural IL-2 in humans [Vlock et al.,1994].

This pilot study shows that this Vx2 carcinoma model is suitable to investigate IL-2 treatment of HNSCC. The IL-2 treated primary tumour, the untreated primary tumour at a distant site, as well as draining lymph node metastases may regress. The mechanism of IL-2 mediated tumour regression is characterised by a granulomatous reaction causing slow tumour regression and it is likely that also inhibition of the blood flow is involved.

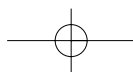
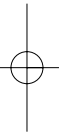
Because this model was developed to perform selective intra-arterial tumour embolisation with dextran hydrogel microspheres, also another treatment strategy, i.e. the controlled release of IL-2 from these microspheres perfusing the tumour, can be investigated.

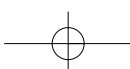
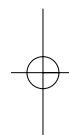


chapter

4

Intra-arterial embolisation therapy





## 4.1 Intra-arterial or regional therapy

### 4.1.1 Introduction

Anti-cancer therapy is potentially toxic to both neoplastic and normal tissues. So the therapeutic efficacy of anti-tumour treatment depends on the relative selectivity of a treatment modality for the tumour in preference to the normal tissues. For surgery this therapeutic selectivity, which is based on anatomic discrimination, becomes ineffective when an adequate tumour resection requires removal of normal tissues whose function is indispensable or irreplaceable. For chemotherapy and radiotherapy the therapeutic selectivity is based on physiologic and biochemical features that are more prevalent in rapidly dividing cancer cells than in normal cells. The goal of intra-arterial (i.a.) administration of chemotoxic drugs or radionuclides is to add anatomic selectivity to the inherent physiologic selectivity of anti-neoplastic agents [Collins, 1984; August, 1996]. Microspheres applied as intra-arterially infused embolisation particles can play a significant role in targeting these anti-neoplastic agents [Okamoto et al., 1985].

### 4.1.2 History and applications of intra-arterial chemotherapy

Following the discovery of various anti-microbiological agents at the beginning of the 20th century, reports on their i.a. administration appear in German literature. In 1914, Heddäus [1914] is one of the firsts to use the carotid artery for i.a. injections of antitoxin against tetanus. Glasser et al. [1945] give an overview on the history of i.a. therapy and present the first application of i.a. penicillin against infections of the extremities. In 1948 Kappert reviews various indications for i.a. treatment and preparations used for this purpose. Klopp et al. [1950] are the first to report on the i.a. injection of the anti-neoplastic agent nitrogen mustard Methyl Bis (B-Chloroethyl) Amine Hydrochloride ( $\text{HN}_2$ ) and confirm a complete regression following i.a.  $\text{HN}_2$  infusions into the external carotid artery in one of 7 patients with HNSCC.

Initially i.a. mono-chemotherapy is given with palliative intent [Sullivan and Daly, 1961]. In the 1970s and 1980s various treatment schedules based on the combination of multi-drug chemotherapy regimens and radiotherapy have been developed and used either as a sequential or as a concomitant (i.e. concurrent or simultaneous) treatment with curative intent. In his thesis, Noorman van der Dussen [1986] gives a thorough overview of these different modalities and their results. The combination of neck dissection and postoperative concomitant i.a. chemo-radiotherapy

induced a high percentage of complete remissions of non-resectable carcinomas, resulting in a survival rate of 20-30%.

However, the morbidity and mortality of the therapy were high and related to the combination of several factors:

1. I.a. catheter-technique related complications with downstream thrombosis, extravasation of cytostatic agents and dislocation of the tip.
2. Systemic toxicity with myelo-suppression.
3. Massive local tumour-necrosis with pus formation in combination with swallowing disorders and aspiration.

Advances in vascular interventional radiological techniques and availability of implantable injection ports made it possible to overcome the catheter related problems. Intra-arterial chemotherapy alone is still employed as palliative treatment of HNSCC [Eckardt and Kelber, 1994]. If curative treatment is planned, i.a. chemotherapy must be part of a multi-modality treatment. It can be combined with concurrent radiotherapy [Robbins et al., 1994] or used as an induction therapy with subsequent surgery [Kovács et al., 1999; Szabo et al., 1999]. In the beginning of the 1990s, the group of Robbins successfully initiated an organ preservation protocol to reduce dysfunction related to major oncological surgery [Robbins et al., 1994 and 1996]. The treatment consisted of repetitive superselective i.a. infusions of supradose cisplatin with simultaneous i.v. thiosulfate rescue and concomitant radiotherapy. With this protocol a 60-70% 2-year overall survival with an acceptable morbidity was obtained for advanced disease, which meant a renaissance of the i.a. chemotherapy for HNSCC. However, repeated i.a. catheter interventions carry the risk of dislodging arteriosclerotic plaques [Kovács et al., 1999] and a substantial amount of the supradose cisplatin still reaches the systemic circulation, urging the use of a thiosulfate rescue [Robbins et al., 1994].

#### 4.1.3 Pharmacokinetics

Regional drug delivery is an approach designed to improve an agent's pharmacokinetic profile by increasing tumour exposure and decreasing normal tissue exposure to the drug. Prerequisite for its success is that the relevant agent: 1) must be effective in the in-vivo tumour-microenvironment and 2) must reach the target cells in optimal quantities [Jain, 1995].

The overall selectivity for regional drug administration, i.e. the benefit of regional over systemic administration, is defined by the Ratio ( $R_d$ ) of the target site concentrations to the systemic concentrations:

$$R_d = R_{\text{target}} / R_{\text{systemic}}$$

and, based on a simple compartment model [Collins, 1984; August, 1996], can be written as:

$$R_d = (1 + Cl_{TB}/Q)/(1-E)$$

In which  $Cl_{TB}$  = the total body clearance

$E$  = the fraction extracted by the first pass and

$Q$  = the regional perfusion.

These latter three parameters i.e. the total body clearance, the fraction extracted by the first pass and the regional perfusion are the only three factors that affect the overall selectivity of the agent. Reducing the regional perfusion ( $Q$ ), thus enhancing the benefit of intra-arterial over i.v. infusion in the target area ( $R_d$ ), is the basic rationale to combine the chemotherapeutic agents with an emboliser [Lin et al., 1997]. This technique, called chemo-embolisation can be executed by two different approaches:

1. Mixing cytotoxic agents with iodised oil (Lipiodol) or with microspheres such as starch, gelfoam or polyvinyl foam.
2. The use of drug-carrier complexes or microcapsules slowly releasing its agents. Release of the drug can be obtained by spontaneous or induced biodegradation of the carrier or by diffusion of the drug from the microparticles.

Chemo-embolisation not only improves the overall selectivity, it will also reduce multiple vascular manipulations to a single procedure, with less morbidity for the main carotid branches both in terms of physical damage as well as chemotoxic irritation.

## 4.2 Embolisation particles for tumour treatment

### 4.2.1 Types of embolisation particles

A particle has been defined as anything that is small in relation to the space around it [Edmundson, 1967]. Thus electrons in an atom as well as stars in space are considered particles. Particles used for intra-arterial embolisation therapy may vary in size, shape and composition.

Polygonal fragments are the result of crushing [Muller and Rossier, 1951] or cutting [Harima et al., 1995] bulk material. Spherical fragments or microspheres are obtained e.g. by a solvent evaporation technique [Nijssen et al., 1999].

Particles can be classified as degradable or non-degradable. Degradable particles are usually polymer-based. Starch microspheres (Spherex<sup>®</sup>) consist of glucose polymers, being degraded by serum  $\alpha$ -amylases with a  $t_{1/2}$  of 15-30 min [Civalleri et al., 1989; Johansson, 1996]. Poly(L-lactic acid) microspheres degrade by

**Table 4.1.** Embolisation particles. Types, sizes and target organs.

Study	Type	Target <sup>1)</sup>	Size ( $\mu\text{m}$ ) <sup>2)</sup>
Embolisation-only particles			
Pillai 1991	Polystyrene	A Vx2 hind paw	27
Päuser 1996	Starch	A Vx2 liver	30-50
Anderson 1991	Albumin	A Rat liver sarcoma	(40 (18-54)
Lorelius 1984	Starch	A Vx2 liver	40 $\pm$ 20
Bastian 1998	PLA <sup>3)</sup>	A Rat liver hepatoma	$\geq$ 40
Meade 1987	'tracer'spheres	A Rat liver adenocarcinoma	$\geq$ 50
Päuser 1996	Gelfoam	A Vx2 liver	90
Lorelius 1984	Gelfoam	A Vx2 liver	80-200
Yang 1995a	Ethylcellulose	A Dog maxilla	50-301
Harima 1995	Gelfoam	A Vx2 uterus	$\pm$ 1,000
Civalleri 1989	Starch	H Liver tumours	40 $\pm$ 5
Johanson 1996	Starch	H Liver tumours	45
Layalle 1998	Gelfoam	H Bone metastases	150-250
Layalle 1998	PVA <sup>4)</sup> foam	H Bone metastases	$\pm$ 600
Latchaw 1977	PVA <sup>4)</sup> foam	H Vasc. Malform. HN <sup>5)</sup>	300-2,500
Radio-embolisation particles			
Turner 1994	<sup>166</sup> Ho-resin	A Pig liver	13 $\pm$ 2
Blanchard 1965	<sup>46</sup> Sn-resin/ceramic	A Vx2 liver	15 $\pm$ 3
Stribley 1981	<sup>57</sup> Co-resin	A Vx2 liver	15.3 $\pm$ 0.8
Ehrhardt 1987	<sup>90</sup> Y-resin	A Dog liver	15-30
Mumper 1991	<sup>166</sup> Ho-PLA <sup>3)</sup>	A Vx2 liver	10-75
Zimmerman 1995	<sup>90</sup> Y-resin	A Pig kidney	45-75
Kim 1962	<sup>90</sup> Y-ceramic	A Vx2 lung	60 $\pm$ 5
Andrews 1994	<sup>90</sup> Y-glass	H Liver tumours	22
Müller 1951	<sup>198</sup> Au-carbon	H Lung SCC	30-50
Yan 1993	<sup>90</sup> Y-glass	H Liver tumours	35 (30-50)
Lang 1971	<sup>198</sup> Au-carbon	H Lung SCC	812
Chemo-embolisation particles			
Burton 1992	Doxorubicine-resin	A Rabbit liver	17.5 $\pm$ 2.5
Yang 1995b	Cisplatin-ethylcellulose	A Dog maxilla	216-441
Bartkowski 1997	5 FU-PLA <sup>3)</sup>	A Rat liver hepatoma	$\geq$ 40
Spenlehauer 1988	Cisplatin PLA <sup>3)</sup>	- In vitro	100-200
Kato 1979+'80+'96	Mitomycin-ethylcellulose	H Various tumours + HNSCC	225 $\pm$ 55 (106-441)
Okamoto 1985	Cisplatin-ethylcellulose	H HNSCC	396 $\pm$ 119
Tomura 1996+'98	Carboplatin-ethylcellulose	H HNSCC	140-180

1)A = Animal, H = Human; 2)  $\geq$  = minimal size advised; 3) PLA = poly(L-lactic acid); 4) PVA = Poly vinyl alcohol;

5) HN = head and neck.

hydrolysis which may take weeks to months, dependent on crystallinity, porosity and surface size [Bergsma et al., 1993; Anderson and Shive, 1997]. Ethylcellulose, oxidised cellulose (Oxycel<sup>®</sup>) and gelatine sponge (Gelfoam<sup>®</sup>) particles are also metabolised in due time [Latchaw and Gold, 1979; Kato et al., 1980].

Resin-based particles [Stribley et al., 1981; Zimmerman et al., 1995], polyvinyl alcohol foam particles and glass or carbon microspheres are presumed biocompatible or bio-inert and do not degrade in-vivo [Latchaw and Gold, 1979; Nakhgevary et al., 1988].

Non-degradable particles are preferably applied to carry radionuclides in order to prevent leaching of radioactivity outside the tumour region. Carriers of chemotherapeutic drugs are often biodegradable to release the encapsulated agents.

#### 4.2.2 Size of embolisation particles

The size of microspheres used in various embolisation studies varies considerably and ranges from 10 to 2,500  $\mu\text{m}$ . An overview is given in Table 4.1. The average particle size used for embolisation of visceral organs varies from 15 to about 75  $\mu\text{m}$ , whereas the particle size used for embolisation in the head and neck area ranges from 100 to about 500  $\mu\text{m}$ .

Theoretically, particles have to be small enough to create a diffuse distribution throughout the whole tumour and have to be large enough to prevent them from spilling to the systemic circulation. This includes either the venous circulation with spill to the lungs or the collateral arterial system with possible stray emboli to other organs. Three vessel-related variables can influence the spill of microspheres to the lungs and stray emboli to other organs:

1. The structure of the tumour vessels itself.
2. The presence of arterio-venous (AV) shunts.
3. The presence of arterio-arteriolar (AA) connections.

Tumour vessels are different from normal vessels [Bloemendal et al., 1998]. They often contain abnormal, irregular capillary-like distended vessels of a large size [Stewart et al., 1959; Blanchard et al., 1965].

Spill of microspheres to the lungs via AV shunts and to other organs via AA connections may occur at any site. However, the consequences of spill via AA connections depend on the organ that is embolised. In the head and neck area the consequences of stray emboli are more serious than elsewhere: Emboli may lead to permanent ophthalmic or neurologic deficits [Latchaw et al., 1979; Braun et al., 1985; Mames et al., 1991; Morrissey, 1997]. Side effects may also be better recognised in humans than in animals. Fear for these stray emboli could explain the employment of relatively large sized particles (over 100  $\mu\text{m}$ ) in human HNSCC

embolisation [Okamoto et al., 1985; Kato et al., 1996]. However, it is of doubt if these large particles can cause a diffuse tumour-embolisation or merely get stuck in the feeding arterioles before even reaching the tumour. Moreover it is questionable if particles of a larger size will avoid stray emboli to the brain as e.g. the middle meningeal artery has an average diameter of at least 500  $\mu\text{m}$  in humans. Prevention of stray emboli can be achieved by occlusion of non-tumour branches: Ligation of non-tumour branches is performed in animal embolisation studies [Päuser et al., 1996; Harima et al., 1996]. In humans, coil embolisation is a method of eliminating unwanted perfusion during i.a. chemotherapy [McCarter et al., 1995; Kato et al., 1996]. In the head and neck region, AA shunts connecting the internal and external carotid system can be visualised during arteriography and occluded if present [Tomura et al., 1996].

In practice, the technical process of fabrication primarily dictates the particle size. A solvent evaporation technique e.g. yields particles ranging in size from 10-200  $\mu\text{m}$ . Selected sizes can be obtained by sieving these microspheres through differently sized sieves, although a substantial yield of the total production is lost in this way [Spenehauer et al., 1988; Nijssen et al., 1999].

#### 4.2.3 analysis of particle size

Because individual particles of a sample are rarely uniform in size it is useful to define an average particle size to be able to compare different samples. In practice the arrhythmic mean, defined as the sum of the variables X divided by the total frequency F of the variables of a sample is most useful [Edmundson, 1967]:

$$\text{Arrhythmic mean} = \Sigma X/F$$

One can define different means, dependent on the properties of the particle that is taken into account, such as its diameter, its surface or its volume. Two of these play an important role in the description of microspheres used for i.a. embolisation of tumours.

1. The length-number or ordinary arrhythmic mean diameter: It is the size of most frequent occurrence and a satisfactory definition of average particle size if the size range is narrow and normally distributed.
2. The volume-weighted or weight moment mean diameter: This is the largest of the averages and gives a mean diameter that corresponds with the mean volume or weight of the particles.

If the size range is broad and not normally distributed, both mean diameters should be given when describing the dimension of the particles used [Edmundson, 1967]. A standard deviation or standard error of this mean may be added. However, in most studies the definition of the mean particle size is not given. This makes comparison of results difficult.

## 4.3 Current applications of i.a. embolisation therapy

### 4.3.1 Embolisation without active anti-tumour pharmaceuticals

With respect to oncologic treatment, arterial embolisation can be performed to facilitate subsequent surgical excision of highly vascular tumours to reduce operative blood loss. Or as palliative measure for tumours that cause troublesome bleeding or pain despite radiotherapy. Tumours of the kidney and bone metastasis are regularly embolised for these reasons. This therapy is intended as a temporary occlusion of the feeding arteriolar vessels, rather than a diffuse embolisation of the tumour as a whole. This is illustrated by the fact that the effect of these embolisations is short-lasting as collateral vascular supply takes over rather quickly [Almgard, 1977; Miller, 1995; Layable, 1998].

### 4.3.2 Chemo-embolisation

To date, patients with unresectable liver and pancreatic cancer seem better off with regional therapy and the application of chemo-embolisation has been well documented to include controlled studies. Especially the combined use of cytotoxic drugs with degradable starch microspheres gives better responses than chemotherapy alone, although the survival rate has not shown significant improvement [Johansson, 1996; August, 1996; Lin et al., 1997; Aigner, 1998]. Apart from the pharmacokinetic benefit of co-injecting drugs with microspheres certain drugs such as mitomycin and adriamycin are claimed to be even more effective under hypoxic conditions which prevail during embolisation treatment [Johansson, 1996; Aigner, 1998].

Selective chemo-embolisation of irresectable chest wall recurrences from breast cancer or fungating primary breast cancers showed 83% complete remissions [Aigner, 1998]. Coil embolisation of the distal internal mammary artery is effective in eliminating unwanted perfusion of cytotoxic agents to normal tissues [McCarter et al., 1995].

### 4.3.3 Radio-embolisation

Intra-arterial radionuclide therapy is an internal radiation therapy, using microspheres as carrier for selective delivery of radio-pharmaceuticals into tumours, commonly addressed as 'radio-embolisation'. Most frequently used radio-isotopes are the beta-emitters yttrium-90 ( $^{90}\text{Y}$ ), rhenium-188 ( $^{188}\text{Re}$ ) and holmium-166 ( $^{166}\text{Ho}$ ).

#### 4.3.3.1 History

One of the first reports on anti-tumour treatment with internal radiotherapeutic agents was by Müller [1946] on intra-tumoural injection of a suspension of radiozinc ( $^{63}\text{Zn}$ ) in patients with uterus carcinoma. Müller and Rossier [1951] described the first selective radio-embolisation of lung carcinoma with radiogold ( $^{198}\text{Au}$ ) absorbed on carbon particles. Kim et al. [1962] reported on the application of ceramic microspheres containing  $^{90}\text{Y}$  for various inoperable tumours.

#### 4.3.3.2 Recent applications

Major advances in radio-pharmaceutical techniques over the past decade have resulted in improved methods of delivery and therapeutic ratios [Novell et al., 1991]. Nowadays, radio-embolisation of unresectable primary hepatocellular carcinoma is considered an equally effective treatment modality as chemo-embolisation but tolerance seems better with fewer side effects [Raoul et al., 1997; Novell and Hilson, 1994].

Radio-embolisation of the liver can be achieved either with iodine-131 lipiodol and gelatine sponge-particles [Raoul et al., 1997] or with  $^{90}\text{Y}$  and  $^{166}\text{Ho}$  incorporated in resin, glass or poly-lactic acid microspheres. In theory,  $^{90}\text{Y}$  is a more suitable isotope based on its greater beta-energy and range. Leaching of free  $^{90}\text{Y}$  with accumulation in bone, resulting in myelosuppression, hampered the application of  $^{90}\text{Y}$ -containing microspheres. This problem is recently solved [Yan et al., 1993], but the risk of shunting of the spheres into the systemic circulation leading to pulmonary fibrosis still prevents wide clinical use of these particles.

To overcome the problems of high density and non-biodegradability of these  $^{90}\text{Y}$ -microspheres,  $^{166}\text{Ho}$  containing poly(L-lactic-acid) ( $^{166}\text{HoPLA}$ ) microspheres were developed [Mumper et al., 1991] and are nowadays tested in various animal studies [Bastian et al., 1998; Nijsen et al., 1999]. These spheres are designed to maintain their integrity until decay of  $^{166}\text{Ho}$  is complete. Because they are of low density, these  $^{166}\text{HoPLA}$  spheres are more easily suspended in aqueous media as compared to ceramic microspheres, allowing a more uniform distribution within the tumour [Nijsen et al., 1999].

Though sophisticated molecular carriers such as monoclonal antibodies and radioactive growth factor inhibitors, are being developed to get nuclear agents to their effector sites, these approaches are still limited in effectiveness because of the inability to deposit significant quantities of radioactivity in solid cancers. Administering radionuclides in microspheres by a radiological catheter may be fast, effective and safe [Novell and Hilson, 1994; Zimmerman et al., 1995].

#### 4.3.4 Embolisation of head and neck tumours

In head and neck oncology, superselective endovascular embolisation without active anti-tumour pharmaceuticals is used in the management of haemorrhage in patients with malignant disease [Morrissey et al., 1997] or in the treatment of vascular malformations [Braun et al., 1985; Enjolras and Mulliken, 1996].

In Japan, chemo-embolisation with carboplatin-, mitomycin- or peplomycin-containing microspheres called 'microcapsules', plays a significant role in regional chemotherapy. Though being a controversial treatment modality, it is considered a technique of choice for palliation of advanced tumours with acceptable morbidity [Tomura et al., 1998; Kato et al., 1996]. Until now, to our knowledge no studies on radio-embolisation of head and neck tumours were performed.

### 4.4 Possible strategies for embolisation-therapy of head and neck cancer

Embolisation particles for HNSCC can be applied in three possible ways:

1. Application of inactive degradable microspheres in combination with currently used protocols that combine i.a. chemotherapy with external beam irradiation such as the RadPlat protocol of Robbins et al. [1997]. Degradable starch or poly(L-lactic acid) microspheres are potential candidates. A maximum regional advantage should be achieved by a suboptimal dose of these spheres, producing a partial vascular blockade [Johansson, 1996].
2. Application of microspheres as carriers that slowly release either classical chemo-therapeutic drugs such as the platinum-based complexes, or drugs that act as local biologic response modifier or inhibit angiogenesis. Dextran hydrogel microspheres with controlled degradation [Hennink et al., 1996; Franssen et al., 1999] can play a role here.
3. Application of microspheres for internal radionuclide therapy, especially those containing beta-emitting isotopes. The holmium-166 poly(L-lactic acid) microspheres [Mumper et al., 1991; Nijssen et al., 1999] seem an attractive option.

As far as the size of the microspheres is concerned, additional studies will have to clarify if the particle-size should match the size currently used for embolisation of hepatic tumours and therefore would be in the range of 15-75  $\mu\text{m}$ , or that the size should be much larger in the range of 100-500  $\mu\text{m}$  to match the particle size currently used for chemo-embolisation of HNSCC.

It is appropriate to test the retention of microspheres smaller than  $100\ \mu\text{m}$  in the Vx2 rabbit auricle model first because the diameter of the tumour vessels of the Vx2 carcinoma is smaller than  $100\ \mu\text{m}$  [Stewart et al., 1959; Blanchard et al., 1965] and most other Vx2-embolisation studies employ particles sized between 13 and  $90\ \mu\text{m}$  (see Table 4.1). Besides, the preparation of dextran hydrogel and  $^{166}\text{HoPLA}$  microspheres via the solvent evaporation technique yields an average particle size in the range of  $10\text{-}100\ \mu\text{m}$  [Franssen et al., 1997; Nijssen et al., 1999].

Other prerequisites, to achieve an optimal intra-arterial embolisation of tumours with radioactive microspheres [Latchaw and Gold, 1979; Novell et al., 1991] are:

1. The vascular anatomy of the tumour is amenable for deposition of particles.
2. Availability of a technology to superselectively apply the particles.
3. Availability of particles with a high and stable load of tracer for imaging.
4. An appropriate sizing of particles to obtain maximal trapping in tumours with minimal shunting.
5. Optimal characteristics of the isotope with respect to chemical inertness, range and half-life of ionising radiation.

These aspects are addressed in the following studies by:

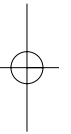
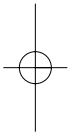
1. Analysing whether the Vx2 tumour vasculature is suitable for deposition of labelled particles. Tumour angiogenesis of Vx2 tumours implanted into the auricle must be observed beforehand (Chapter 5).
2. Developing a technique for super-selective infusion of microsphere-suspensions via the caudal auricular artery and evaluating the retention of microspheres in the cannulation system (Chapters 5 and 7).
3. The labelling of dextran hydrogel microspheres with a radioactive technetium-99m tracer and the application of holmium-166 that emits 6.2% of its energy as gamma-photons (Chapter 6).
4. The analysis of the entrapment of microspheres of a different size in the Vx2 rabbit auricle model (Chapters 6 and 7).
5. The assessment of the application of degradable holmium-166 poly(L-lactic-acid) microspheres for embolisation of HNSCC, while also studying the leaching of free holmium-166 in urine and faeces (Chapter 7).



chapter

5

The Vx2 carcinoma in the rabbit auricle  
as an experimental model  
for intra-arterial embolisation  
of head and neck squamous cell carcinoma



---

R.J.J. van Es, O. Franssen, H.E.J. Dullens, M.R. Bernsen, F. Bosman,  
W.E. Hennink, P.J. Slootweg

Laboratory Animals 1999;33:175-184.



## Abstract

**Introduction:** There is a need for the development of a new head and neck cancer model to study the effects of novel intra-arterial therapies.

**Materials and methods:** The Vx2 carcinoma cell line is transplanted into both auricles of New Zealand White rabbits. The speed of tumour growth is assessed. The study is focussed on the vascular anatomy of the rabbit auricle and the effects of intra-arterial embolisation of the carcinomas with dextran hydrogel microspheres.

**Results:** During the phase of exponential growth the tumour-surface doubling-time was  $7.1 \pm 2.0$  days. Standard deviation in growth of the tumours was significantly larger between separate animals than between tumours growing in the left and right auricle of each individual animal (2.0 versus 0.65 days). A fresh cell suspension containing at least  $10 \cdot 10^6$  vital tumour cells was necessary to yield a tumour-take of 85%. The caudal auricular artery perfuses the caudal half of the external ear and is very suitable for macroscopic cannulation. Histological evaluation shows, that the use of dextran hydrogel microspheres of at least 25 micrometers in combination with ligation of non-tumour perfusing branches of the central auricular artery yields diffuse embolisation of the Vx2 carcinoma.

**Conclusion:** This rabbit Vx2 auricle carcinoma model can be of use in further studies to optimise particle size and dosage for embolisation as well as to evaluate the effect of different anti-neoplastic drugs, slowly released by controlled degradation of dextran microspheres.

We thank W. den Otter for placing laboratory support at our disposal, A. Versluis and H. Boere for taking care of the rabbits, P. Rothengatter for the photography and P. Egyedi for his innovative ideas and valuable remarks in preparing this manuscript.

## 5.1 Introduction

The role of regional or intra-arterial (i.a.) chemo- and immuno-therapy in the treatment of head and neck squamous cell carcinoma (HNSCC) in humans remains controversial [Harker and Stephens, 1992]. The i.a. embolisation of malignant tumours with biodegradable microspheres containing anti-tumour drugs is considered to be one of the most effective ways of selective anti-tumour therapy [Okamoto et al., 1985]. It precludes the need for indwelling arterial catheters and prevents its associated morbidity with continuous long-term infusion systems [Conn and Langer, 1978; Schouwenburg et al., 1980]. However, controlled degradation of microspheres used for tumour embolisation was not possible until now. Dextran hydrogels are especially developed for the controlled release of pharmaceutically active compounds, either by diffusion [Hennink et al., 1996] or by degradation [Franssen et al., 1997].

As stated in chapter 1.3, basically three types of animal tumour models exist for HNSCC: Spontaneously occurring tumours, tumours induced by the topical application of carcinogens and tumours induced via transplantable cell lines. The transplantation of the Vx2 cell line [Kidd and Rous, 1940] has frequently been used to study novel i.a. chemotherapy strategies in various organs of the rabbit [Davidson et al., 1986; Harima et al., 1996; Päuser et al., 1996]. Vx2 tumour growth and angiogenesis can be studied in detail in the rabbit auricle [Tromberg et al., 1990].

The aim of the following study is twofold:

1. To develop an experimental HNSCC model in the rabbit, that is easy to handle and does not depend on microsurgery, in which the effects of i.a. therapy can be studied.
2. To assess the possible use of dextran hydrogel microspheres for i.a. tumour embolisation in this model.

We present an investigation on the arterial supply of the auricle of New Zealand White (NZW) rabbits and describe a technique of its i.a. cannulation. The transplantation and growth of the Vx2 carcinoma in the auricle as well as its embolisation with dextran hydrogel microspheres is evaluated.

## 5.2 Materials and methods

### 5.2.1 Animals

Adult female NZW rabbits were used as described in chapter 2.2.1.

### 5.2.2 Vascular anatomy of the rabbit auricle

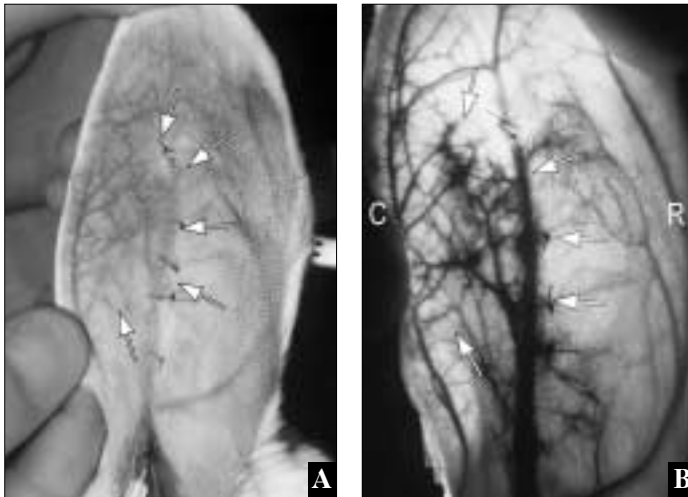
To get insight in the vascular supply of the auricle, two rabbits were sacrificed. Details of interest for our study were subsequently corroborated in the ensuing experiments reported in this article. The caudal auricular artery emerges from the superficial temporal artery [Barone et al., 1973]. At the dorsocaudal base of the auricle, the caudal auricular artery lies deep to the external ear muscles. At the point where the artery emerges from under the superior margin of the cutaneous auricular muscles, the caudal auricular vein lies superficial and frequently medial to the artery. Sometimes 2 or even 3 veins are encountered. The great auricular nerve is also situated superficially to the artery and external ear muscles. The main stem of the artery traverses to the apex of the auricle, in the axis, as central or intermediate auricular artery. The anterior or rostral margin of the auricle is supplied via a separate rostral marginal artery. In the apex region anastomoses between both marginal and central vessels exist.

Infusion of a methylene blue dye solution shows that the caudal two-thirds of the auricle are vascularised by the caudal auricular artery. Selective ligation of macroscopically visible arterial branches to the rostral half of the auricle, results in selective perfusion of a region between the central artery and the caudal margin (Fig. 5.1). This region was chosen for tumour implantation to study the effects of i.a. embolisation.

### 5.2.3 Tumour cells

The Vx2 tumour cells were propagated by intramuscular passage as described in chapter 2.2.2. Cell suspensions were used either fresh, i.e. within 2 hours, or cryopreserved for later use. The number of cells in suspension was counted using a haemocytometer. Viability of cells was estimated by Trypan blue exclusion. Cryopreservation was performed by freezing cells down in ice-cold RPMI 1640 [Gibco, Grand Island NY, USA], containing 20% FCS and 10% DMSO at a concentration of  $1-3 \cdot 10^8$  cells/ml. The cell suspension was kept in a freezing container (Cryo 1°C, Nalgene®, USA) at  $-70^\circ\text{C}$  for at least 4 hours before storage in liquid nitrogen [Morgan and Darling, 1993].

## Embolisation of the Vx2 model

**Figure 5.1.**

Injection of methylene blue dye in the left central auricular artery after ligation of distal and rostral branches. Note the area of perfusion between midline and caudal margin (arrows). External (A) and transmitting (B) light source. C=caudal margin, R=rostral margin.

**5.2.4 Embolisation particles**

Dextran hydrogel microspheres were prepared at the Utrecht Institute for Pharmaceutical Sciences (Department of Pharmaceutics, Faculty of Pharmacy, Utrecht University, the Netherlands) according the following protocol: Deoxygenised aqueous solutions of methacrylated dextran (degree of substitution, i.e. the number of methacrylates per 100 glucopyranose residues = 4, 1g, 40% w/w), synthesised according to Van Dijk-Wolthuis et al. [1997a] and polyethylene glycol (PEG,  $M_w$  20.000, 0.1g, 24% w/w) are vigorously mixed for 2 minutes with a vortex under an Argon atmosphere. Part of this primary emulsion (0.25g) is added to a PEG solution ( $M_w$  4.000, 4.75g, 24% w/w) immediately after mixing. The emulsion is gently homogenated by hand. Subsequently, potassium peroxydisulfate (180  $\mu$ l, 50mg/ml) and N,N,N',N'-tetramethyl ethylenediamine (100  $\mu$ l 20% v/v, pH neutralised with 4M HCL) are added and the mixture is incubated without stirring for 30 min at 37°C to allow polymerisation of the methacrylic moieties in the dextran chain. Thus obtained microspheres are then sieved (sieve: Storck-Veco, Eerbeek, Holland; mesh 10  $\mu$ m) to separate the smaller from the large particles.

Particle size was analysed by a model 770 AccuSizer (Particle Sizing Systems, Santa Barbara, California, USA) and expressed in micrometers as the 'number mean diameter' (num) i.e. the ordinary arithmetic mean diameter of the particles, and the 'volume mean diameter' (vol), i.e. the diameter corresponding to the mean volume of the particles [Edmundson, 1967].

### 5.2.5 Analgesia, sedation and euthanasia

For details on analgesia, sedation and euthanasia is referred to chapter 2.2.4.

### 5.2.6 Tumour induction

All hair was removed from the auricle by shaving the skin with a pair of clippers. To induce tumours a 0.10-0.15 ml suspension (in RPMI 1640), containing  $4-24 \cdot 10^6$  vital cells, was injected (with a 0.5 mm needle) s.c. into the dorsal lateral portion (i.e. between the central auricular artery and caudal margin) of the middle third of both auricles (fresh suspensions: 10 rabbits; cryopreserved suspensions: 5 rabbits). Composition of the cell suspensions was checked through cytopins stained with Haematoxylin and Eosin (HE). More than 95% of the cells were of the carcinoma type.

### 5.2.7 Evaluation of tumour growth and statistics

To evaluate speed of growth, the size of 12 tumours (five paired and two single tumours, in 7 rabbits) was recorded in time (t, days) by two-dimensional measurements with callipers and presented as surface area (A, cm<sup>2</sup>). Based on a mathematical model assuming the tumour to grow exponentially with a fixed growth rate [Hasenclever et al., 1996], speed of growth was characterised by a 'Tumour-surface doubling-time' (T, days), i.e. the time in which the tumour surface has doubled in size (from  $A_0$  to  $2 \cdot A_0$ ).

During the phase of exponential tumour growth, T was estimated by the best fitting curve that applied to the following function of A:

$$[1] \quad A(t) = A_0 \cdot 2^{t/T}$$

Standard deviation (Sd) of T was calculated for all tumours. For the five paired tumours an 'intra-rabbit' standard deviation (Sd') was calculated, according to

$$[2] \quad Sd' = \sqrt{\{[\sum_{i=1}^n (T_{left,i} - T_{right,i})^2] / 2n\}}$$

where  $T_{left,i}$  and  $T_{right,i}$  are the Tumour-surface doubling-times of each left and right ear respectively and n is the number of paired tumours, i.e. 5 in this case.

The F-test [Armitage and Berry, 1988] was used to assess significance of the difference between Sd and Sd'. Statistics used were by SPSS for windows release 6.1.

To evaluate tumour growth and development of metastases, 5 rabbits (one rabbit per time point) were sacrificed at days 3, 7, 10, 14 and 21 after transplantation. All other rabbits that showed tumour growth were sacrificed between 5 and 9 weeks after transplantation. To depict the vascularisation of the external ear and peritumoural blood vessels, the ear was placed on the flashlight with its medial side (TTL Electronic flashlight type Metz 45CL4; Camera: Nikon F4; Objective: Mikro-Nikkor 105mm F2.8, Diaphragm F22, picture size 1:2).

**Embolisation of the Vx2 model**

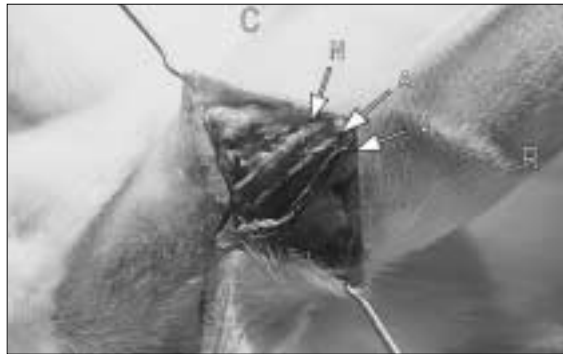


**Figure 5.2.**  
Exposure of left central auricular artery (A). Note the relation to the great auricular nerve (N), and central auricular vein (V). C=caudal margin, R=rostral margin.



**Figure 5.3.**  
Control of tumour perfusion of the left auricle with i.a. methylene blue dye. C=caudal margin, R=rostral margin.

**5.2.8 Embolisation**

Procedure: after shaving and disinfection of the auricle and its base, a cutaneous incision is made parallel and slightly lateral to the caudal auricular vein. The vein is kept aside and the artery can be found in the layer between the vein and the cartilage (auricular concha), emerging deep from the upper margin of the cutaneous auricular musculature (Fig. 5.2). Slight tapping and some drops of lidocaine 2% help to prevent arterial spasm. The arterial diameter at this site is suitable for macroscopic cannulation with a 0.6 mm Microflex<sup>®</sup> needle infusion set (Vycon, Belgium) or preferably, to avoid the risk of perforation, an Abbocath<sup>®</sup> catheter (Abbott, Sligo, Republic of Ireland). The cannula is fixed with a peri-arterial suture and is subsequently sutured to the skin to prevent inadvertent displacement. Selective tumour perfusion is confirmed using methylene blue dye 4 mg/ml in glucose 5% (Fig. 5.3).

Embolisation with dextran hydrogel microspheres of various particle sizes (Table 5.1) was performed in 7 tumours (in 4 rabbits: no.'s 6353, 6503, 6576 and 6577 respectively on day 22 to 43 after transplantation). Sieved particles (mesh 10  $\mu\text{m}$ ) were used in rabbit 6576 and 6577. Each tumour was embolised with 10-160 mg (wet weight) microspheres in 1 ml phosphate buffer solution. Embolised rabbits were sacrificed 41-50 days after transplantation.

### 5.2.9 Evaluation of embolisation

After sacrificing, the animals were autopsied. Thoracic and abdominal organs were inspected. To verify presence of tumour and microspheres, tissue samples from the primary site, lymph nodes, lungs, spleen and lumbar backbone marrow were fixed in formalin. Sections were embedded in paraffin and histologically evaluated after staining with HE and Periodic Acid Schiff (PAS). Success of tumour embolisation was judged on the basis of dispersion of microspheres in and around the tumour and classified as 'poor' (i.e. hardly any microspheres retained in tumour vasculature), 'diffusely good' (i.e. a diffuse and uniform dispersion of microspheres in vessels in and around vital tumour tissue), or 'intermediate' (i.e. in some parts of the sections, tumour vessels retain microspheres).

## 5.3 Results

### 5.3.1 Tumour growth

#### 5.3.1.1 Primary site

In the 10 auricles (in 5 rabbits) injected with a thawed cell suspension, only 4/10 (40%) a tumour developed. Vitality of thawed cell suspensions was about 10%, containing 10 - 20.10<sup>6</sup> vital cells.

In the 20 auricles injected with fresh cell suspensions, in 17/20 (85%) a tumour developed. Vitality of fresh cell suspensions was in all cases over 50%. The auricles that developed a tumour, had been injected with 6 - 24.10<sup>6</sup> vital cells. The 3 auricles that did not show progressive tumour growth received 6.10<sup>6</sup> (two auricles) and 10.10<sup>6</sup> (one auricle) vital cells respectively.

Tumour-surface doubling-time (T) varied between 4.5 and 9.9 days (mean 7.1  $\pm$  2.0 days) in all animals. Contrary to the standard deviation (Sd) of 2.0 days between rabbits, the standard deviation between tumours in both auricles of the same animal (Sd') was only 0.65 days. The difference between Sd and Sd' was statistically significant ( $p < 0.025$ ).

Embolisation of the Vx2 model

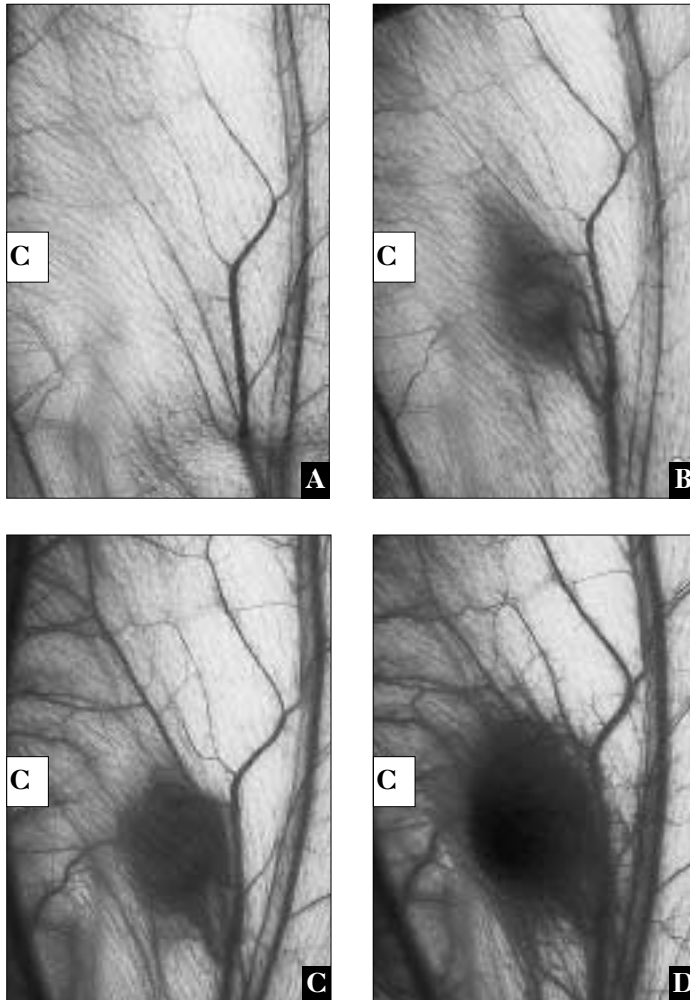


**Figure 5.4. (A-D)**  
 Development of tumour vessel bed before implantation (A) and at a tumour size of 16 (B), 42 (C), 110 (D) mm<sup>2</sup> respectively. Note that the structure of pre-existing vessels remains unchanged. C=caudal margin.

In one case development of tumour vasculature was followed until a tumour surface of 110 mm<sup>2</sup> was reached (Figs. 5.4a-d). Pre-existing vascular architecture did not change during neovascularisation of the tumour.

**5.3.1.2 Metastatic disease**

Microscopic first level lymph node metastases were encountered in the parotid of 2 rabbits killed at 3 and 14 days after transplantation. A single microscopic lung metastasis was found in the rabbit killed 10 days after transplantation.

In the four rabbits sacrificed more than 5 weeks after transplantation, lymph nodes

**Table 5.1.** Data on embolised rabbits

Rabbit no. <sup>1)</sup>	sieving mesh( $\mu\text{m}$ )	particle size( $\mu\text{m}$ )		arterial ligation <sup>2)</sup>	embolisation results <sup>3)</sup>	
		num.	vol.			
<b>6353</b>	<b>L</b>	<b>no</b>	<b>5.4</b>	<b>22.3</b>	<b>no</b>	<b>poor</b>
<b>6503</b>	<b>L</b>	<b>no</b>	<b>3.1</b>	<b>61.6</b>	<b>no</b>	<b>poor</b>
	<b>R</b>	<b>no</b>	<b>3.1</b>	<b>61.6</b>	<b>yes</b>	<b>intermediate</b>
<b>6576</b>	<b>L</b>	<b>&gt;10</b>	<b>13.0</b>	<b>26.5</b>	<b>yes</b>	<b>poor</b>
	<b>R</b>	<b>&gt;10</b>	<b>13.0</b>	<b>26.5</b>	<b>mult.</b>	<b>intermediate</b>
<b>6577</b>	<b>L</b>	<b>&gt;10</b>	<b>9.8</b>	<b>28.4</b>	<b>mult.</b>	<b>diffusely good</b>
	<b>R</b>	<b>&gt;10</b>	<b>10.2</b>	<b>48.0</b>	<b>mult.</b>	<b>diffusely good (+necrosis)</b>

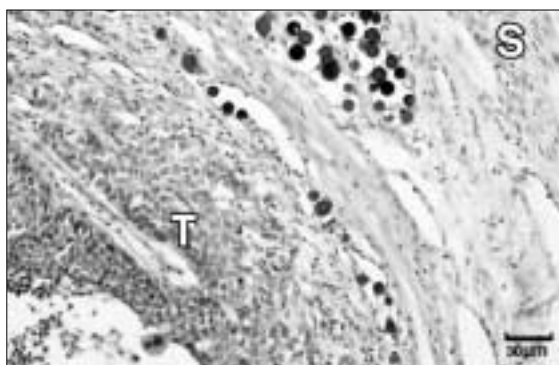
<sup>1)</sup>L=Left auricle; R=Right auricle

<sup>2)</sup>yes = central artery distal to the tumour only; mult. = multiple non-tumour branches

<sup>3)</sup>poor = hardly any microspheres retained; intermediate = some retention of microspheres; good = diffuse dispersion of microspheres

**Figure 5.5.**

Microscopy of tumour tissue after embolisation. Dextran hydrogel microspheres around the tumour (T) and in the stroma (S). Original magnification 50x, PAS stain.



in the parotid area became palpable from the 4th week on. All regional lymph nodes and lungs proved to contain metastatic SCC at autopsy. Two rabbits, that did not develop tumours in the auricles, showed tachypnea, loss of animal spirits, loss of appetite and loss of weight (8.6% and 15.3% respectively) 9 weeks after injection of thawed tumour cells, and were therefore sacrificed. At autopsy massive lung metastases were found. No metastases were found at other sites.

### 5.3.2 Embolisation study

Data on particle size and results are summarised in Table 5.1. Dextran hydrogels stain highly PAS-positive and microspheres are easily detected in histological slides. In the first two rabbits (no.'s 6353 and 6503) embolisation was poor. In the lungs thromboemboli and alveolar edema was observed, though the animals were clinically well. Sieving the particles (mesh diameter: 10  $\mu\text{m}$ ) as well as ligation of the central artery distally from the tumour and branches that perfuse non-tumour regions, resulted in better embolisation (Fig.5.5). In these rabbits (no.'s 6576 and 6577) microspheres still could be found in the lungs, resulting in some septal inflammatory infiltrate, but alveoli were normally distended without edema. Judgement of dispersion of microspheres 21 days after the injection of rabbit no. 6577 was difficult because of extensive tumour necrosis, as a result of the i.a. embolisation. In rabbit no. 6577 some microspheres were found around a regional (parotid) lymph node metastasis. No microspheres were observed in other tissues.

## 5.4 Discussion

In this auricle Vx2 SCC model, the response rate of subcutaneous transplantation was 85% when fresh, and only 40% when cryopreserved tumour cell suspensions were used, most likely because of a poor recovery from storage in liquid nitrogen, resulting in a cell viability of only 10%. The many dead cells injected may have had an immunisation effect stimulating an effective immune response, which prevented outgrowth of tumour. Failures of transplantation in this study occurred when  $10 \cdot 10^6$  vital cells or less were injected. Only Wagner [1994] reports a response rate of 100% using  $5 \cdot 10^6$  cells intramuscularly in the hind limb. Davidson et al. [1986] using  $5 \cdot 10^6$  cells intramuscularly in the hind limb, Tromberg et al. [1990] using  $10 \cdot 10^6$  cells subcutaneously in the auricle, Pauser et al. [1996] using  $10 \cdot 10^6$  cells intrahepatically and Harima et al. [1996] using  $100 \cdot 10^6$  cells intramuscularly in the uterus do not report their response rates explicitly. In contrast to muscle or the liver, to create a small subcutaneous vesicle in the auricle, the maximum injectable volume is about 0.1 ml. This demands a suspension of at least  $100 \cdot 10^6$  vital cells per millilitre. We advise to use at least  $20 \cdot 10^6$  vital cells, and to prevent an unfavourable balance between vital and necrotic cells as occurred in using our cryopreserved tumour suspensions. In contrast to Schouwenburg et al. [1980], who used tumour fragments for implantation, like others [Davidson et al., 1986; Tromberg et al., 1990; Wagner et al., 1994;

Harima et al., 1996; Päufer et al., 1996] we preferred injection of tumour suspensions to prevent disruption of the vascular architecture of the auricle, which might interfere with the i.a. embolisation study. The injection of suspensions, however, has the disadvantage of possible leakage of cells i.v. or intra-lymphatically. This mechanism might explain our observation of a micrometastasis, soon after tumour induction, in the lymph node (3 days) and lung (14 days). It can also explain the massive lung metastases despite absence of tumour growth in the auricle in 2 animals.

In contrast to Tromberg et al. [1990] who used the dorsal medial portion of the auricle as implantation site to study photodynamic therapy, we chose the dorsal lateral part of the auricle. In this area perfusion shows to be mainly dependent on the caudal auricular artery, whereas the medial portion also receives branches from the rostral auricular artery. The model allows for accurate measurement of tumour size and good assessment of the development of lymph node metastases.

In this Vx2 auricle model cannulation of the superficially lying caudal auricular artery without the aid of a microscope is easy: general anaesthesia is therefore not necessary, in contrast to other models [Davidson et al., 1986; Schouwenburg et al., 1980]. Even with a large auricular tumour mass the rabbits did not seem to be troubled, which might very well be so in case of large hind limb tumours. Because of the invariable development of lung metastases, we feel that, in the benefit of the animals' well being, termination of studies with this model has to be done within 8 to 10 weeks after tumour transplantation.

Being aware of the simplification of reality using the mathematical growth model of Hasenclever et al. [1996], the estimated Tumour-doubling-time (T) of 7.1 days corresponds well with the findings of Muckle and Dickson [1971], describing Vx2 tumours in thigh-muscles of male NZW rabbits. Like their data, we also find a considerable variation of T between animals. We are of opinion that the implantation of the Vx2 tumour in both auricles allows for a better comparison between the embolised and the contralateral 'control' tumour than a control tumour in another animal, because variation in T proved significantly larger between animals than between two auricles (2.0 vs 0.65 days). Moreover, also others [Schouwenburg et al., 1986; Davidson et al. 1986] stressed the importance of a model with bilaterally implanted tumours, that allows for comparison of drug distribution between the regionally embolised tumour and the contra-lateral control tumour, where exposure is to systemic drug levels only.

As there is a substantial difference in speed of tumour growth between animals, in contrast to others [Päufer et al., 1996, Harima et al., 1996, Tromberg et al., 1990] we believe that timing of intervention should be dictated by the size of the tumour instead of by a fixed time span after transplantation of the tumour. The finding, that

---

**Embolisation of the Vx2 model**

pre-existing vascular architecture is not changed by newly developed blood vessels that perfuse the tumour, makes the timing of i.a. embolisation independent of the moment of tumour induction.

In the embolisation models of the liver [Päuser et al., 1996] and the uterus [Harima et al., 1996] the organ-specific artery is used and non-tumour branches are ligated to enhance the efficiency of embolisation. In our model, macroscopical ligation of non-tumour branches is easily performed with the aid of methylene blue dye, because of the translucency of the auricle.

The Vx2 SCC is surrounded by large irregular capillary-like blood vessels [Stewart et al., 1959; Blanchard et al., 1965]. The diameter of microspheres to be used for tumour embolisation has to be small enough to obtain a uniform dispersion of particles in and around the tumour, but has to be large enough to prevent spillage of particles to the lungs. This might in part explain the large variance of particle sizes used for embolisation in literature: Mumper et al. [1991] use polylactic acid particles of  $23.6 \pm 4.9 \mu\text{m}$  for internal radiation, and Päuser et al. [1996] use starch particles with a diameter of 30 to 50  $\mu\text{m}$  for chemo embolisation of the rabbit liver. Okamoto et al. [1985] use cisplatin microcapsules of  $396 \pm 119 \mu\text{m}$  in humans with head and neck cancer. These investigators however, did not report on histopathology of lung tissues following their embolisation. This might be due to the fact, that particles used are not easily visible by light microscopy. Dextran microspheres used in this study, are easily detected with a PAS stain.

Small particles with a diameter characterised by a number weighted mean  $< 9 \mu\text{m}$  traverse the tumour capillary bed and induce microemboli with edema in the lungs. The use of larger particles in combination with ligation of non-tumour branches enhances the success of diffuse tumour embolisation and prevents lung edema. Yet, microspheres were found in lung septa. Adverse effects from these microspheres will be dictated by the anti-tumour drugs to be enclosed, because the toxicity of the dextran hydrogel itself is low [Van Dijk-Wolthuis, 1997b].

It can be concluded that the Vx2 carcinoma in the rabbit auricle is suitable to be used as an experimental head and neck SCC model particularly to study the effects of intra arterial anti-tumour therapy using dextran hydrogel microspheres as embolisation particles. Future studies with this model will have to establish the optimal size and dosage of the microspheres. Thereafter the effects of controlled release of different anti-tumour drugs from these microspheres can be evaluated.

As dextran hydrogels are developed for the controlled release of proteins and peptides, the use of these particles as a carrier for a wide range of immuno-stimulating drugs, such as interleukins and interferons, might add a new dimension to the field of anti-tumour therapy.

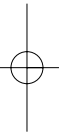
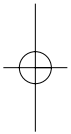




chapter

6

Establishment of an optimal size of  
microspheres for embolisation of the  
rabbit Vx2 head and neck cancer model



---

R.J.J. van Es, J.F.W. Nijsen, H.F.J. Dullens, M. Kicken, A. van der Bilt, W. Hennink,  
R. Koole, P.J. Slootweg

Journal of Cranio-Maxillofacial Surgery (in press)



## Abstract

**Introduction:** Intra-arterial embolisation of unresectable malignant tumours with biodegradable microspheres is an effective way of selective anti-tumour therapy. Possible candidates are Dextran hydrogel (Dex) microspheres for chemo-embolisation and Holmium-166 poly(L-lactic acid) ( $^{166}\text{HoPLA}$ ) microspheres for radio-embolisation. This study was performed to investigate the distribution of intra-arterially injected microspheres both in-vivo and histologically in order to establish an optimal size of particles for embolisation of head and neck tumours.

**Materials and Methods:** Twenty rabbits with Vx2 auricle tumours were embolised via the caudal auricular artery with 3 different batches Dex and 1 batch  $^{166}\text{HoPLA}$  microspheres varying in size from 19 to 66  $\mu\text{m}$ . Dex microspheres were labelled with  $^{99\text{m}}\text{Tc}$  in 6 cases. The proportion of microspheres entrapped in the tumour was measured with a gamma camera. The distribution of microspheres around the primary tumour and spill of particles to lungs or other organs was analysed on histological sections.

**Results:** The 19  $\mu\text{m}$   $^{166}\text{HoPLA}$  particles used for embolisation of liver tumours proved inadequate for embolisation as 51% spilled to the lungs, whereas over 95% of the 40-66  $\mu\text{m}$  Dex microspheres were retained within the primary tumour area. Dex20 and Dex30 microspheres tended to be more evenly distributed throughout the primary tumour. Particle density in lung tissues proved significantly lower for the Dex50 group. In 2 rabbits of the Dex20 group stray emboli to the brain occurred.

**Conclusion:** The results of this investigation show that both Dextran hydrogel and holmium-166 poly(L-lactic acid) microspheres are potential candidates for embolisation of head and neck cancer. In future studies, present arterio-arteriolar connections should be identified and occluded. Particles with a number weighted mean size of at least 40  $\mu\text{m}$  and a volume weighted mean size up to 70  $\mu\text{m}$  should be employed.

The authors thank Henny IJzerman, Maarten Gerrits, Alice van Dongen and Fred van het Schip of the department of Nuclear Medicine, Okke Franssen and Jenny Cadée of the department of Pharmaceutics, Jan Nico den Breejen of the Radionuclids Laboratory and Adri Versluis of the Animal Department for their substantial contribution to this study. We also thank Bram van der Meijs for his efforts in analysing the data.

## 6.1 Introduction

Intra-arterial (i.a.) embolisation of malignant tumours with biodegradable microspheres containing anti-tumour drugs is considered to be one of the most effective ways of selective anti-tumour therapy [Kato et al., 1994]. However, the optimal size of microspheres for embolisation of head and neck tumours still has to be established. On the one hand particles have to be small enough to create a diffuse distribution throughout the tumour and on the other hand particles have to be large enough to prevent them from spilling to the systemic circulation. The latter includes either the venous circulation with spill to the lungs, or the collateral arterial system with stray emboli to important neural structures. Dextran hydrogel (Dex) microspheres are promising candidates because of their controllable degradation and property to show a sustained release of pharmaceutically active drugs [Stenekes et al., 1998; Franssen et al., 1999]. Diffuse distribution of these microspheres in and around tumour tissue following i.a. injection has been demonstrated in a Vx2 head and neck cancer model of the rabbit (Chapter 5). Radio-embolisation is considered an effective treatment modality for unresectable primary hepatocellular carcinoma [Novell and Hilson, 1994]. Radioactive holmium-166-poly(L-lactic acid) ( $^{166}\text{HoPLA}$ ) microspheres that are especially developed for treatment of these tumours [Mumper et al., 1991; Nijsen et al., 1999], might be equally suitable for treatment of unresectable head and neck cancer.

The particle size used in several liver embolisation studies varies between 10 and 50  $\mu\text{m}$  [Stribley et al., 1983; Lorelius et al., 1984; Pillai et al., 1991; Pauser et al., 1996; Bastian et al., 1998]. Embolisation with  $^{166}\text{HoPLA}$  of rabbit liver tumours proved successful with a particle diameter of  $24 \pm 5 \mu\text{m}$  [Mumper et al., 1991]. For chemo-embolisation of head and neck cancer, ethylcellulose particles with a much larger size of 140-440  $\mu\text{m}$  have been used [Yang et al., 1995; Kato et al., 1996; Tomura et al., 1998].

The embolisation experiments described in this chapter evaluates the biodistribution of four available, differently sized batches of microspheres in a rabbit Vx2 head and neck cancer model: Three batches Dex microspheres, of which a part was labelled with radioactive  $^{99\text{m}}\text{Tc}$  ( $^{99\text{m}}\text{Tc}$ ) and one batch  $^{166}\text{HoPLA}$  microspheres. The distribution of microspheres in the tumour, the lungs and brain is analysed both in-vivo with a gamma camera as well as histologically after sacrifice. The results of these experiments are important for the development of future treatment strategies based upon tumour embolisation of head and neck cancer.

## 6.2 Materials and methods

### 6.2.1 Animal tumour model

Tumours were induced by injection of Vx2 carcinoma cells into the auricles of 20 adult female NZW rabbits as described in chapter 2.2.2. Tumours were embolised when they reached a size of 4 cm<sup>2</sup>. During all experiments sedation and analgesia was achieved with a mixture of fentanyl 0.315mg/ml and fluanisone 10mg/ml (Hypnorm<sup>®</sup>, Janssen Cilag).

### 6.2.2 Embolisation particles

Dex microspheres were obtained from the Utrecht Institute for Pharmaceutical Sciences and prepared as described by Stenekes et al. [1998]. The degree of methacrylate substitution (i.e. the number of methacrylate groups per 100 glucopyranose units) was 4 and the equilibrium water content of the dextran microspheres was 40%. Three differently sized batches were available. They were prepared by separating particles through different sieves of 20 μm (Dex20), 30 μm (Dex30), 50 μm (Dex50) to exclude smaller particles. A 100 μm sieve was used to exclude larger particles.

<sup>166</sup>HoPLA microspheres were prepared at the Department of Nuclear medicine of the University Medical Center, Utrecht as described by Nijsen et al. [1999]. The available batch is routinely used for experimental radio-embolisation of the liver in tumour bearing rats.

### 6.2.3 Radioactive labelling

To study biodistribution of Dex in-vivo, two batches of Dex (Dex20 and Dex50) were labelled with 30 MBq <sup>99m</sup>TcO<sub>4</sub>. The batch was only used if the percentage of <sup>99m</sup>TcO<sub>4</sub> leaking from microspheres in 1 hour was less than 10%.

<sup>99m</sup>Tc labelled Dex microspheres were prepared according to the following protocol:

- Dex microspheres are suspended in 5 ml aquadest and centrifuged (Hettich Rotanta<sup>®</sup>) for two cycles at 1000 rpm during 5 min.
- Resuspension of the pellet in 1 ml aquadest and perfusion with N<sub>2</sub> gas during 30 min at room temperature.
- Addition of 5 μm(l SnCl<sub>2</sub>-solution (SnCl<sub>2</sub>·2H<sub>2</sub>O, 30 mg/ml concentrated HCl) and 30MBq <sup>99m</sup>TcO<sub>4</sub> in 1 ml 0.9% NaCl.
- Labelling for one hour while stirring at room temperature.
- Centrifugation (Hettich Rotanta<sup>®</sup>) at 2000 rpm during 5 min and determina-

## Size of microspheres for embolisation

**Table 6.1.** Number of animals that received different batches of microspheres

Batch	Regular study	Radionuclide study		Total
	non-radioactive	<sup>99m</sup> Tc-label	free <sup>99m</sup> Tc	
<b>Dex20</b>	<b>4</b>	<b>3</b>		<b>7</b>
<b>Dex30</b>	<b>4</b>			<b>4</b>
<b>Dex50</b>		<b>3</b>	<b>3</b>	<b>6</b>
<b><sup>166</sup>HoPLA</b>		<b>3</b>		<b>3</b>
<b>Total</b>	<b>8</b>	<b>9</b>	<b>3</b>	<b>20</b>

tion of labelling percentage, calculated according to the following equation:  
 Labelling percentage = (Activity of Microsphere pellet / Activity of  
 Microsphere pellet + Supernatant) x 100%.

- If labelling percentage is at least 90%: Resuspension of the labelled microsphere pellet in 1.0 ml 0.9% NaCl and aspiration in a 2 ml syringe.

**6.2.4 Particle size analysis**

The actual particle size of the available batches was analysed by a model 770 AccuSizer (Particle Sizing Systems, Santa Barbara, California, USA) and expressed in micrometers as the 'number weighted mean' diameter i.e. the ordinary arithmetic mean diameter of the particles, and the 'volume weighted mean' diameter, i.e. the diameter corresponding to the mean volume of the particles [Edmundson, 1967].

**6.2.5 Embolisation Experiments**

Twenty auricle tumours were embolised with the 4 different batches of embolisation particles by injecting microspheres following cannulation of the caudal auricular artery (Table 6.1). In each experiment a total of 0.7-1.4 ml 0.9% NaCl solution was used containing 50 mg Dex or <sup>166</sup>HoPLA microspheres. Eight rabbits received non-radioactive Dex microspheres.

Experiments for evaluating the radioactive biodistribution of the different microspheres were carried out with 12 animals divided into 4 groups:

1. Group I (n=3): <sup>99m</sup>Tc-labelled Dex20
2. Group II (n=3): <sup>99m</sup>Tc-labelled Dex50
3. Group III (n=3): Dex50 mixed with free 20 MBq <sup>99m</sup>Tc
4. Group IV (n=3): <sup>166</sup>HoPLA

Group III was added to verify possible leaching of <sup>99m</sup>Tc from Dex microspheres in-vivo.

Biodistribution of radioactivity was monitored by a gamma camera immediately after embolisation and 1 hour later in case of  $^{99m}\text{Tc}$ -labelling and 24 hours later in case of  $^{166}\text{Ho}$ -labelling.

#### 6.2.6 Radionuclide imaging

All data were acquired with a gamma camera (Elscont<sup>®</sup>) interfaced to a computer (Apex 609R, Elscint Ltd., Israel). A low energy, high-resolution collimator was used. The rabbits were positioned prone and the field of view included the auricle, carrying the tumour and the torso (Fig. 6.1). The activity generated from identical rectangular 'Regions of Interest', superimposed over each auricle, the lungs and the abdomen, was determined. Data were corrected for radioactive decay and the acquisition time. If the activity from the embolised tumour overshadowed the activity from the lungs (i.e. if the overflow correction of the gamma camera arrested the acquisition time before 600 s), the embolised auricle was covered and a separate image of the lungs was acquired (Fig. 6.3b).

#### 6.2.7 Analysis of imaging

The relative portion (in percent) of labelled microspheres entrapped in the tumour was calculated according to the following equation:

$$[1] \text{ Portion entrapped microspheres} = \left\{ \frac{\text{Activity tumour}}{\text{Activity (tumour} + \text{lung)}} \right\} \times 100\%.$$

Because free  $^{99m}\text{Tc}$  is excreted via the kidneys into the bladder, the relative portion (in percent) of entrapped free  $^{99m}\text{Tc}$  in the tumour was calculated according to the following equation:

$$[2] \text{ Portion entrapped free } ^{99m}\text{Tc} = \left\{ \frac{\text{Activity tumour}}{\text{Activity (tumour} + \text{lung} + \text{abdomen)}} \right\} \times 100\%.$$

The portion entrapped microspheres was measured immediately after embolisation ( $t_1$ ) and 1 or 24 hours later ( $t_2$ ), for  $^{99m}\text{Tc}$ -labelled Dex or  $^{166}\text{Ho}$ PLA microspheres respectively. The percentage of microspheres leaking from the tumour in due time was calculated according to the following equation:

$$[3] \text{ Leakage} = 1 - \left( \frac{\text{portion entrapped } t_2}{\text{portion entrapped } t_1} \right) \times 100\%.$$

Differences between groups were tested with a general linear model repeated measures procedure (repeated measures ANOVA).

#### 6.2.8 Autopsy and histological preparation

One day after completion of the embolisation experiments, the rabbits were sacrificed by i.v. injection of 2 ml pentobarbital 200 mg/ml (Euthesate<sup>®</sup>). The tumour-bearing auricles and inflated lung specimens were dissected and fixed in 10%

### Size of microspheres for embolisation

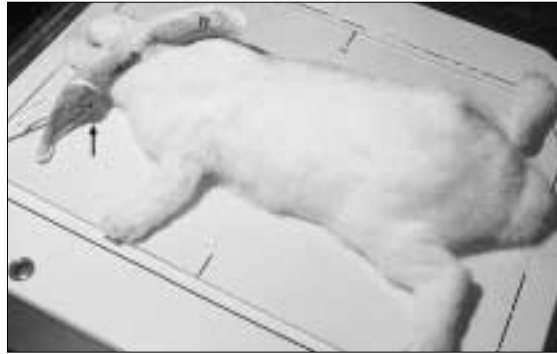


**Figure 6.1.**

Position of the rabbit on the gamma camera during nuclear imaging. Arrow indicates embolised tumour.

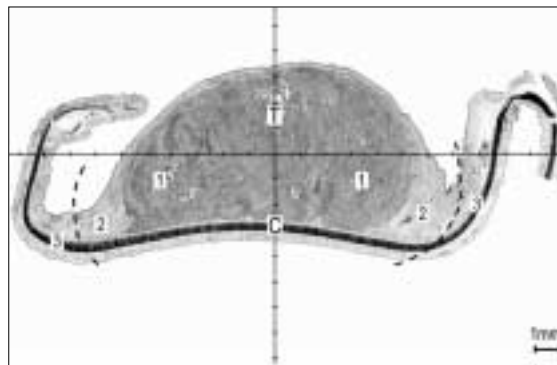


**Figure 6.2.**

Transverse histological section through the auricular tumour with Areas 1, 2 and 3 (see text). Dotted line marks the 2mm zone between Area 2 and 3. PAS stain. T = tumour, C = Cartilage.

formaldehyde solution for histological examination.

Tissue samples were prepared for paraffin sectioning according to established methods. Three slices (thickness 3-5mm) were taken perpendicular to the auricular axis from the whole-embolised tumour: One proximal, one middle and one distal section. One sample was taken from each lung lobe. Brain sections (anterior, middle and posterior) were taken from two animals with neurological signs (see 6.3.3 Clinical observations). Sections were stained with HE and PAS, allowing better detection of the carbohydrate Dex microspheres

#### 6.2.9 Analysis of histology

##### 6.2.9.1 Distribution of microspheres around the primary tumour

Tumour cross-sections were represented schematically as in Fig. 6.2. The number of particles was counted in three distinct areas by using a grid meter under the light microscope [Pillai et al., 1991]: Area 1 = within the tumour; Area 2 = immediately around the tumour within 2 mm from the tumour border. Area 3 = distant from the tumour, i.e. > 2 mm from the tumour border. The 2 mm area was chosen

arbitrarily, based on the mean range of  $\beta$ -energy from holmium-166 in tissue, being 1 to 2 mm [Turner et al., 1994]. For each batch, the distribution of particles in these 3 Areas was determined for each tumour section (proximal, middle and distal) and presented as a percentage of all particles counted. If Area 2 could not be determined reliably, particles were only scored being in- or outside the tumour, i.e. Area 2 and 3 were lumped together versus Area 1.  $^{166}\text{HoPLA}$  particles do not stain and proved difficult to detect within a dense peri-tumoural inflammatory infiltrate. Because of unreliable visualisation of  $^{166}\text{HoPLA}$  particles in auricular sections, these measurements were not feasible and excluded from analysis.

Univariate ANOVA was used to determine significant differences in distribution of microspheres between different batches Dex, different Areas 1-3 and different tumour sections (proximal, middle and distal).

#### 6.2.9.2 Spill of microspheres to lungs and brain

Particle size in lung and brain sections was measured by using a grid-meter under the light microscope [Pillai et al., 1991] and specified in categories of  $5\ \mu\text{m}$  ranging from 10 to  $80\ \mu\text{m}$ . The total surface of the sectional slides was estimated by using a grid-meter. Particle density was defined as: Number of particles per category divided by the total surface of the sections (in  $\text{cm}^2$ ). Differences in particle density of lung tissue were determined with Student's *t*-test for different batches of microspheres. Particle density and distribution of microspheres in the brain were determined for the two rabbits with neurological signs.

## 6.3 Results

### 6.3.1 Particle size analysis

Number weighted mean and volume weighted mean diameters of the sieved batches are summarised in Table 6.2. On average, the number weighted mean diameters are 19, 40, 50 and  $60\ \mu\text{m}$  and the volume weighted mean diameters are 50, 72, 77 and  $90\ \mu\text{m}$  for  $^{166}\text{HoPLA}$ , Dex20, Dex30 and Dex50 respectively. Note that the number weighted mean diameter of the  $^{166}\text{HoPLA}$  particles is  $19\ \mu\text{m}$  and much smaller than the  $40\ \mu\text{m}$  of the Dex20 particles despite the use of the same sieve size to separate small particles.

**Size of microspheres for embolisation**

**Table 6.2.** Particle size analysis of available batches of microspheres

Batch	Sieve size ( $\mu\text{m}$ )	Num. wt. mean $\pm$ sd ( $\mu\text{m}$ )	Vol. wt. mean $\pm$ sd ( $\mu\text{m}$ )
<b><math>^{166}\text{HoPLA}</math></b>	<b>20-50</b>	<b>18.8 <math>\pm</math> 10.8</b>	<b>50.4 <math>\pm</math> 35.5</b>
<b>Dex20</b>	<b>20-100</b>	<b>39.5 <math>\pm</math> 19.3</b>	<b>72.1 <math>\pm</math> 27.9</b>
<b>Dex30</b>	<b>30-100</b>	<b>49.8 <math>\pm</math> 19.4</b>	<b>77.0 <math>\pm</math> 30.0</b>
<b>Dex50</b>	<b>50-100</b>	<b>66.4 <math>\pm</math> 21.1</b>	<b>90.2 <math>\pm</math> 30.8</b>

**Table 6.3.** Percentage of injected dose entrapped within the primary tumour

Group	Microspheres	$T_0=0$ hour	$T_1=1\text{h} / 24\text{h}$	$T_0 - T_1$
		Mean $\pm$ sd (%)	Mean $\pm$ sd (%)	Leakage (%)
<b>I</b>	<b><math>^{99\text{m}}\text{Tc}</math>-labelled Dex50</b>	<b>98.7 <math>\pm</math> 0.70</b>	<b>97.4 <math>\pm</math> 1.46</b>	<b>1.32</b>
<b>II</b>	<b><math>^{99\text{m}}\text{Tc}</math>-labelled Dex20</b>	<b>97.1 <math>\pm</math> 2.01</b>	<b>96.2 <math>\pm</math> 2.34</b>	<b>0.92</b>
<b>III</b>	<b>Dex 50 + Free <math>^{99\text{m}}\text{Tc}</math></b>	<b>46.2 <math>\pm</math> 13.1**</b>	<b>25.3 <math>\pm</math> 7.2**</b>	<b>45.1</b>
<b>IV</b>	<b><math>^{166}\text{HoPLA}</math></b>	<b>52.7 <math>\pm</math> 26.58*</b>	<b>48.7 <math>\pm</math> 27.63*</b>	<b>7.59</b>

Differences vs. Groups I and II:  $p < 0.05$  (\*) and  $p < 0.01$  (\*\*)

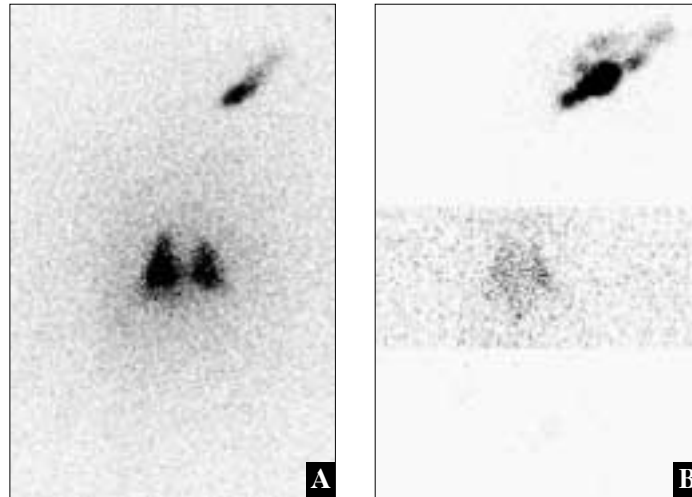
**6.3.2 Radionuclide imaging**

The percentages of microspheres entrapped in the primary tumour immediately after injection, after 1 hour for  $^{99\text{m}}\text{Tc}$ -labelled Dex microspheres and after 24 hours for  $^{166}\text{HoPLA}$  microspheres are shown in Table 6.3.

There was a significant difference the portion of radioactivity entrapped in the tumour between Dex20 and Dex50 microspheres (Group I and II) on the one hand and Dex50 microspheres with free  $^{99\text{m}}\text{Tc}$  or  $^{166}\text{HoPLA}$  microspheres (Group III and IV) on the other hand. Over 95% of the Dex20 and over 97% of the Dex50 microspheres was retained in the tumour whereas about 50% of the  $^{166}\text{HoPLA}$  microspheres spilled to the lungs (Figure 6.3).

Less than 1.5% of the Dex microspheres and 7.5% of the  $^{166}\text{HoPLA}$  microspheres leaked from the tumour in due time. Dex50 microspheres retained 46% of the free  $^{99\text{m}}\text{Tc}$  initially, indicating an occlusion of vessels with stasis of intra-vascular fluids. Almost half of this activity was washed out in one hour and excreted via the kidneys.

**Figure 6.3.**  
Gamma camera images of the  
auricle and lungs.  
A:  $^{166}\text{HoPLA}$  microspheres.  
Note the heavy activity of  
spilled particles in the lungs.  
B:  $^{99\text{m}}\text{Tc}$ -labelled Dex50  
microspheres. Combined image:  
The acquisition time of the  
inserted lung area is six times  
longer (see text).



### 6.3.3 Clinical observations

Two (10%) of the 20 rabbits showed neurological signs after recovery from their sedation, consisting of a tendency to spin around their longitudinal axis with a vertical ocular nystagm. One animal died spontaneously during the night, the other was sacrificed as planned after 24 hours. Both rabbits had received Dex20 microspheres. Both brains were autopsied. From one of these animals also liver and kidney tissues were harvested.

### 6.3.4 Histology

#### 6.3.4.1 Primary tumours

Microspheres tended to cluster within the larger vessels in and around the tumour, rather than being uniformly dispersed throughout the capillaries. A significant difference in distribution of Dex particles in different Areas was found in only the proximal sections of the tumours (Table 6.4): In groups Dex30 and Dex50, 28% and only 1% of the particles was found within the tumour tissue, i.e. Area 1 respectively. In groups Dex20 and Dex50, 60% and 25% of the particles was found within 2 mm of the tumour border (i.e. Area 1+2) respectively. No other differences between the batches were found. When comparing the proximal, middle and distal sections, the Dex20 and Dex30 microspheres tended to be more evenly distributed throughout the tumour as a whole. However, the Dex50 spheres still distributed fairly well in the three sections with 25, 60 and 90% of the particles lying within 2 mm of the tumour border respectively.

## Size of microspheres for embolisation

**Table 6.4.** Mean percentage of particles found inside tumour (Area 1) or within 2 mm of tumour margin (Area 1+2)

	Tumour	Proximal section	Middle section	Distal section	Total
<b>Dex20</b>	<b>Area 1</b>	<b>14.4% ± 18.0</b>	<b>41.1% ± 25.8</b>	<b>21.1% ± 32.1</b>	<b>25.5% ± 27.4</b>
	<b>Area 1+2</b>	<b>59.4% ± 29.2**</b>	<b>80.0% ± 21.9</b>	<b>83.4% ± 13.2</b>	<b>74.9% ± 23.4</b>
<b>Dex30</b>	<b>Area 1</b>	<b>27.6% ± 21.2*</b>	<b>45.0% ± 35.7</b>	<b>20.6% ± 9.7</b>	<b>30.1% ± 23.9</b>
<b>Dex50</b>	<b>Area 1</b>	<b>1.1% ± 1.8*</b>	<b>15.5% ± 23.6</b>	<b>49.3% ± 30.2</b>	<b>25.2% ± 30.3</b>
	<b>Area 1+2</b>	<b>24.8% ± 7.6**</b>	<b>60.4% ± 27.6</b>	<b>89.5% ± 12.8</b>	<b>63.4% ± 31.3</b>

differences: \*p<0.05, Dex30 vs. Dex50; \*\*p<0.1, Dex20 vs. Dex50

**6.3.4.2 Lungs**

Significant differences in particle density were found between Dex20, Dex30 and Dex50 in each category of microsphere diameter up to 40  $\mu\text{m}$  (Figs. 6.4 and 6.5). The density of  $^{166}\text{HoPLA}$  particles in the lung was 4 to 6 times higher in comparison with the Dex Groups, and even reached 13/cm<sup>2</sup> in the 25  $\mu\text{m}$  category (Fig. 6.5). Only in the Dex50 Group, particle density did not exceed 0.25/cm<sup>2</sup> in any category.

**6.3.4.3 Brain, liver, spleen, kidney**

In the rabbits with neurological signs, both hemispheres (i.e. both the embolised and the contra-lateral side) contained microspheres. Particle density reached 4.0/cm<sup>2</sup> in the 20  $\mu\text{m}$  category. Also particles as large as 75  $\mu\text{m}$  were found (Fig. 6.6). However, no microspheres were found in liver, kidney and spleen tissue sections.

**6.4 Discussion**

The results of this study show that intra-arterial embolisation of the Vx2 rabbit head and neck cancer model is not effective with 19  $\mu\text{m}$   $^{166}\text{HoPLA}$  microspheres routinely used for embolisation of liver tumours, as over 50% of the particles is spilled to the lungs. They also show that Dex microspheres with a number weighted mean diameter of 40-66  $\mu\text{m}$  are effectively entrapped in the primary tumour with less than 5% spill to the lungs.

**Figure 6.4.**  
 Particle density in lung tissue per category of sphere diameter for Dex microspheres. Significant differences ( $p < 0.05$ ), \*: between Dex20 and Dex30, \*\*: between Dex20 and Dex50, \*\*\*: between Dex30 and Dex50.

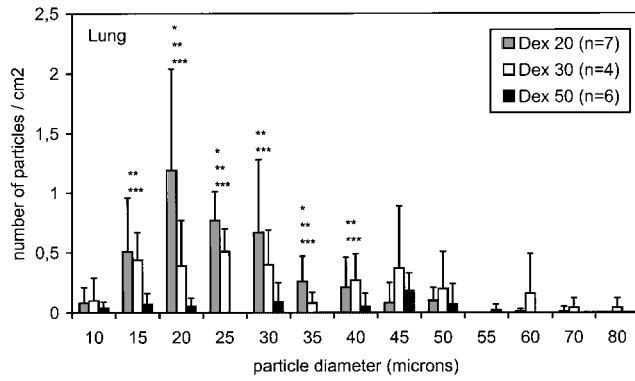


**Figure 6.5.**  
 Particle density in lung tissue per category of sphere diameter for  $^{166}\text{HoPLA}$  microspheres. Note difference in scale compared to Fig. 6.4. \*: significant differences ( $p < 0.05$ ) between  $^{166}\text{HoPLA}$  and all Dex Groups.

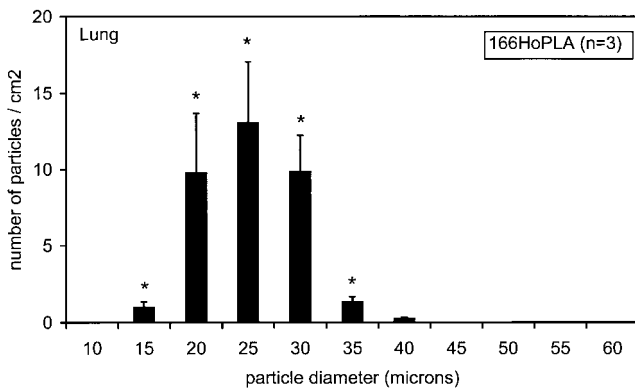
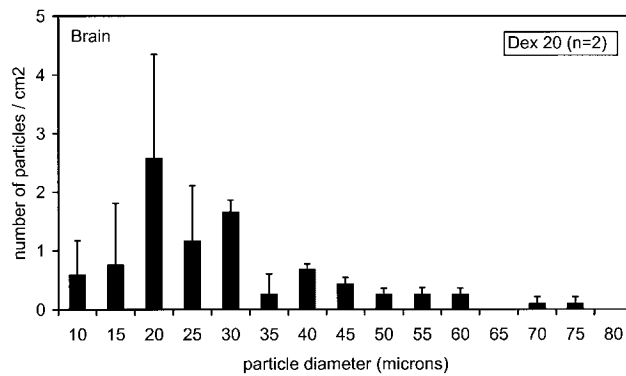


**Figure 6.6.**  
 Particle density in brain tissue per category of sphere diameter for two animals with neurological signs.



---

**Size of microspheres for embolisation**

As discussed in paragraph 4.2.2, three vessel-related variables can influence the spill of microspheres to the lungs and stray emboli to other organs:

1. The structure of the tumour vessels itself.
2. Arterio-venous (AV) shunts in the organ in which the tumour grows.
3. Arterio-arteriolar (AA) connections in the organ in which the tumour grows.

Re-1. Like other tumours, the Vx2 tumour is known to induce the development of a dilated capillary-like vasculature [Stewart et al., 1959; Blanchard et al., 1965].

Re-2. On AV shunt size in laboratory animals only scanty data are available. With respect to this auricle tumour model, the observations of Grant [1930] are of interest. He has described the presence of about 1 AV communication/mm<sup>2</sup> in the rabbit's auricle with an external size of 20-70  $\mu\text{m}$ . Kim et al. [1962] mentioned the presence AV shunts in various organs in the dog up to 50  $\mu\text{m}$  in size, but these accounted for less than 5% of the total flow.

These factors explain why the used batches <sup>99m</sup>Tc-labelled Dex (with a number weighted mean diameter of 40 to 66  $\mu\text{m}$  on average) were all effectively entrapped in the primary tumour with less than 5% spill to the lungs, whereas more than 50% of the 19  $\mu\text{m}$  <sup>166</sup>HoPLA microspheres spilled to the lungs. Histological analysis showed that up to a particle size of 40  $\mu\text{m}$  Dex50 particles spilled even significantly less to the lungs as compared to the Dex20 and Dex30 Groups.

Re-3. AA connections are known to be present between the caudal and rostral auricular artery of the rabbit auricle and rabbits have an intact circle of Willis [Barone et al., 1973], but no information exists about the size of these connections. These connections may explain the occurrence of stray emboli to both hemispheres in the two rabbits with neurological signs after infusion of Dex20 microspheres: Retrograde flow of microspheres via the rostral auricular artery and external carotid into the internal carotid, circle of Willis and both hemispheres. Because in the brain particles up to a size of 75  $\mu\text{m}$  were found, AA shunts in the tumour or in the auricle must be at least of this calibre. Retrograde flow was limited to the carotid bifurcation and did not reach the aorta because no particles were found in liver, spleen or kidney samples.

There is also less risk of retrograde flow if injection pressure is maintained below the systolic blood pressure, which is 100 mmHg on average in adult rabbits [Manning et al., 1994]. We did not control injection pressure in our study.

Stray emboli to the brain did not occur in the <sup>166</sup>HoPLA Group despite massive spill of particles to the lungs. This could be explained by the fact that small particles obstruct AV shunts less effectively, resulting in a lower infusion pressure and less risk of retrograde flow via AA connections. Moreover the number of animals in the <sup>166</sup>HoPLA Group was smaller than in the Dex20 Group and apparently all spilled

$^{166}\text{HoPLA}$  particles were effectively entrapped within the pulmonary vessels. Prevention of stray emboli in this model was achieved by macroscopical ligation of non-tumour branches as visualised with the aid of methylene blue dye. This has been done in other animal embolisation studies [Päuser et al., 1996; Harima et al., 1996], as well as in humans where coil embolisation is a method of eliminating unwanted perfusion during i.a. infusions [McCarter et al., 1995]. In the head and neck region, AA shunts connecting the internal and external carotid system can be visualised during arteriography and occluded if present [Tomura et al., 1996].

Our study further shows that it is not sufficient to mention only the mesh size of the used sieves to compare different batches of particles. The actual particle size has to be expressed in number and volume weighted mean values [Edmundson, 1967]. The substantial differences in biodistribution between the  $^{166}\text{HoPLA}$  batch sieved between 20-50  $\mu\text{m}$  and the Dex20 batch sieved between 20-100  $\mu\text{m}$  can be explained by the differences in the actual particle size, being 19  $\mu\text{m}$  vs. 40  $\mu\text{m}$  and 50  $\mu\text{m}$  vs. 72  $\mu\text{m}$  for number and volume weighted means respectively. Differences in physico-chemical properties between the Dex and  $^{166}\text{HoPLA}$  spheres as well as differences in the sieving processes itself in the different institutions may have caused these differences in particle size.

We realise that the diameter of microspheres measured in 7  $\mu\text{m}$  histological slides does not represent the real size of the spheres. Theoretically, the size of the observed sphere segments should be corrected [Pahlplatz et al., 1995]. Assuming an infinite number of measurements (over a thousand in this study), this correction is applicable to all measurements of all batches. Therefore the conclusions concerning differences found between the Dex20, Dex30 and Dex50 Groups are not substantially influenced.

Our study also confirms that drug retention in the tumour can effectively be enhanced by mixing cytotoxic agents with microspheres [Lorelius et al., 1984]: One hour after embolisation with Dex50 microspheres mixed with free  $^{99\text{m}}\text{Tc}$  (Group III), still 25% of the free  $^{99\text{m}}\text{Tc}$  was retained within the tumour. But when drugs are slowly released from microspheres as represented by  $^{99\text{m}}\text{Tc}$ -labelling (Groups I and II), primary retention of anticancer drugs is more effective and exceeds the 95%.

Considering the optimal particle size for tumour embolisation two different philosophies exist: 1): 'Use the smallest particles that will not penetrate to the venous circulation' [Stribley et al., 1983]. This statement holds true for embolisation of e.g. liver tumours, as stray emboli via collateral arteries are of less concern

---

**Size of microspheres for embolisation**

---

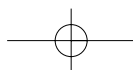
and entrapment of small particles in the liver vessel network seems highly effective. The particle size used in several liver embolisation studies varies between 10 and 50  $\mu\text{m}$  [Stribley et al., 1983; Lorelius et al., 1984; Mumper et al., 1991; Pillai et al., 1991; Pauser et al., 1996]. However, in a thorough distribution-study, Bastian et al. [1997] conclude that a mean particle diameter of at least 40  $\mu\text{m}$  is required to prevent spill to the lungs and spleen. Their lung sections contained high concentrations of particles smaller than 40  $\mu\text{m}$ . These findings correspond well with the good entrapment of Dex particles in our study and the significant increase of lung particle density below the 40  $\mu\text{m}$  category.

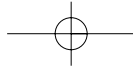
Philosophy 2): 'Use the largest microspheres that will not decrease the curative effect of (chemo-) embolisation' [Yang et al., 1995]. This philosophy could be true for embolisation head and neck cancers, since the consequences of stray emboli to important neural structures are detrimental. It might explain the use of chemo-embolisation particles with an exceptionally large size of 140-440  $\mu\text{m}$  as used by others [Yang et al., 1995; Kato et al., 1996; Tomura et al., 1998]. However, it is of doubt if this large size will avoid stray emboli to the brain in humans as e.g. the middle meningeal artery has an average diameter of at least 500  $\mu\text{m}$ . Our study demonstrates that such a large size is not necessary to prevent spill to the lungs. With a particle size of 40-66  $\mu\text{m}$ , over 95% of the microspheres can be retained in the tumour. Moreover, in our study the distribution of microspheres within 2 mm from the tumour border dropped from 60% to 25% in the proximal sections, when using particles of 66  $\mu\text{m}$  (Dex50) instead of 40  $\mu\text{m}$  (Dex20). It is questionable if very large (>100  $\mu\text{m}$ ) particles still can cause a diffuse tumour-embolisation or merely get stuck in the feeding arterioles before even reaching the tumour. This not only will allow collateral supply to take over, but also might block the infusion pathway resulting in a higher infusion pressure with even more risk of retrograde flow and stray emboli to the brain.

It is concluded that embolisation of this rabbit Vx2 head and neck cancer model is ineffective with 19  $\mu\text{m}$   $^{166}\text{HoPLA}$  microspheres but shows optimal (>95%) entrapment of 40-66  $\mu\text{m}$  dextran hydrogel microspheres with a fair particle distribution in and around the tumour. These dextran hydrogel microspheres, developed for sustained release of pharmaceutically active anti-tumour drugs, can be labelled effectively with radioactive  $^{99\text{m}}\text{Tc}$  to study their biodistribution. Embolisation particles for this animal model should therefore ideally have a number weighted mean size of at least 40  $\mu\text{m}$  and a volume weighted mean size up to 70  $\mu\text{m}$ . The occurrence of stray emboli to the brain is a serious complication which demands present arterio-arteriolar connections to be detected and ligated or occluded.



Future embolisation studies will have to focus on the effects of embolisation on tumour growth itself. Either larger sized batches  $^{166}\text{HoPLA}$  containing therapeutic doses of radioactivity or dextran hydrogel microspheres containing chemo- or immuno-therapeutic drugs are promising candidates.

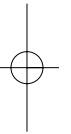




chapter

7

Effect of intra-arterial embolisation of the  
rabbit Vx2 head and neck cancer model with  
radioactive holmium-166 poly(L-lactic acid)  
microspheres



---

R.J.J. van Es, J.F.W. Nijsen, A.D. van het Schip,  
H.F.J. Dullens, P.J. Slootweg, R. Koole

International Journal of Oral & Maxillofacial Surgery (Submitted)



## Abstract

**Introduction:** Interstitial radiotherapy is an effective treatment modality against head and neck cancer. Radioactive holmium-166 labelled poly(L-lactic acid) ( $^{166}\text{HoPLA}$ ) microspheres could be applied as radio-embolisers.

**Materials and methods:** Twenty-two NZW rabbits with Vx2 squamous cell carcinomas transplanted into the auricles were intra-arterially (i.a.) embolised with radioactive and inactive HoPLA microspheres with a mean diameter of 38-80  $\mu\text{m}$ . The effects on tumour growth, the efficiency of i.a. infusion, the efficacy of retention of microspheres in the primary tumour and the excretion of free holmium-166 were analysed.

**Results:** Radio-embolisation induced 79% complete tumour remissions. Over 95% of the microspheres was retained in the tumour and the leaching of holmium-166 was less than 0.1% in 2 days. The injection efficiency was not optimal, as 40% of the microspheres was retained in the cannulation system. Arterio-arteriolar connections should be detected and closed prior to embolisation to prevent stray emboli into the brain.

**Conclusion:**  $^{166}\text{HoPLA}$  microspheres with a diameter of 38-80  $\mu\text{m}$  are promising candidates for future studies on radio-embolisation of unresectable head and neck cancer.

The authors thank Maarten Gerrits, Sander Zielhuis and Alice van Dongen of the department of Nuclear Medicine for their help in analysing the scintigraphic images. We thank Jenny Cadée of the department of Pharmaceutics for sizing the microspheres, Mark Konijnenberg of Mallinckrodt Medical b.v. Petten for calculating irradiation doses to the tumours, Peggy Adema of BARD Benelux n.v. for supplying the infusion systems, Andries van der Bilt for the statistical analysis and Peter Rothengatter for the photography. Finally, we thank and Jan Nico den Breejen of the Radionuclids Laboratory, Adri Versluis of the Animal Department and Bram van der Meijs and Marc Kicken for their help in performing the animal experiments.

## 7.1 Introduction

Today's interstitial radiotherapy represents a highly effective treatment modality available to the head and neck oncologist, with the advantage that it allows delivery of a high local dose of radiation to the tumour without destroying local anatomy or inducing xerostomia. However, a major concern is the problem of dose inhomogeneity due to errors in source placement related to technical difficulties during implantation and there is the risk of tumour seeding along the implantation tract [Close et al., 1993; Podd et al., 1994]. Moreover, the long half-life and the high gamma energy of frequently used radiochemicals such as iridium-192 and iodine-125 lead to significant exposure of medical staff to radiation. These drawbacks, can be circumvented by intra-arterial (i.a.) embolisation of the tumour with beta-emitting isotopes. There is a recent revival of the interest in i.a. anti-tumour therapies in the management of oral cancer [Kovács et al., 1999]. Also chemo-embolisation of head and neck cancer has proven an effective therapeutic option in the hands of several groups [Tomura et al., 1998; Kato et al., 1996].

I.a. embolisation of unresectable primary hepatocellular carcinoma and hepatic metastases with radioactive biodegradable microspheres is nowadays considered an effective treatment modality [Novell and Hilson, 1994]. Neutron-activated holmium-166 is a beta-emitter ( $E_{\text{max}}=1.84$  MeV) with radiotherapeutic properties appropriate for therapy and a short physical half-life of 26.8 hours, that also emits photons (81 keV, 6.2%) suitable for gamma imaging. Holmium-166 labelled poly(L-lactic acid) ( $^{166}\text{HoPLA}$ ) microspheres have especially been developed for radio-embolisation of such liver malignancies [Nijsen et al., 1999].

Up to now, no reports exist about the experimental radio-embolisation of head and neck cancer. We have described a Vx2 head and neck cancer model of the rabbit that is suitable for studying effects of i.a. tumour embolisation (chapter 5). However,  $^{166}\text{HoPLA}$  microspheres sieved between 20 and 50  $\mu\text{m}$  used for embolisation of liver tumours, have proven to be too small for embolisation of this head and neck cancer model because 50% of the radioactivity spilled to the lungs (chapter 6). To evaluate the effects of radio-embolisation on tumour growth in the Vx2 rabbit model we performed the present study with larger sized  $^{166}\text{HoPLA}$  microspheres, sieved between 50 and 70  $\mu\text{m}$ .

As the effectiveness of treatment depends on the administration of microspheres and retention of radioactivity in the primary tumour, the following technical items were also addressed:

1. The efficiency of i.a. infusion of  $^{166}\text{HoPLA}$  microsphere suspensions.
2. The efficacy of retention of these  $^{166}\text{HoPLA}$  microspheres within the primary tumour.
3. The leaching of free holmium-166( $^{166}\text{Ho}$ ) into urine and faeces.

## 7.2 Materials and methods

### 7.2.1 Animal tumour model

Vx2 auricle carcinomas were induced as described in chapter 2.2.2. Single tumours were induced in 8 rabbits and twin tumours (i.e. into both auricles) were induced in 14 rabbits. Sedation and analgesia during experiments is described in chapter 2.2.4.

### 7.2.2 Microspheres

Inactive  $^{165}\text{HoPLA}$  batches were sieved between 50 and 70  $\mu\text{m}$  resulting in a number weighted mean diameter of 38.2  $\mu\text{m}$  and a volume weighted mean diameter of 80.2  $\mu\text{m}$  (model 770 Accusizer<sup>®</sup>, Particle sizing Systems, Santa Barbara, California USA). Radioactive  $^{166}\text{HoPLA}$  microspheres were prepared at the Department of Nuclear Medicine of the University Medical Center Utrecht, as described by Nijsen et al. [1999].

Batches for infusion were prepared by dissolving the microspheres in 0.9% NaCl with 4% modified gelatine (Gelofusine<sup>®</sup>, Vifor Medical SA, Switzerland) to retard sedimentation of the particles. The total volume was 0.8 ml per batch. The radioactivity of each batch was maintained between 60 and 80 MBq to attain a therapeutic tumour dose [Stabin and Konijnenberg, 2000]. Each batch contained 55 mg of microspheres on average.

### 7.2.3 Embolisation experiment

Of the 22 animals, 15 rabbits received radioactive  $^{166}\text{HoPLA}$  microspheres and 7 rabbits received inactive  $^{165}\text{HoPLA}$  microspheres. The 14 contra-lateral twin tumours were not treated and served as controls. Auricle tumours were embolised after reaching a surface area of 4  $\text{cm}^2$ , by injecting the microsphere suspension via the caudal auricular artery as described in chapter 5. In summary: After skin inci-

#### Embolisation with $^{166}\text{HoPLA}$ microspheres

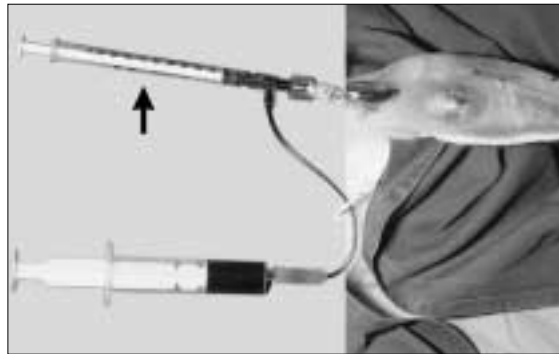


**Figure 7.1.**

Cannulated caudal auricular artery and connection of syringes with methylene blue dye and  $^{166}\text{HoPLA}$  microspheres.

sion and exposure of the caudal auricular artery, cannulation was performed with an Abbocath<sup>®</sup> cannula (Abbott, Ireland). A T-shaped extension set of a Per-Q-Cath<sup>®</sup> catheter (Bard Access Systems, USA) was connected to the i.a. cannula onto which both the syringe for infusion of methylene blue dye (2 mg/ml) and the syringe containing the suspension of the microspheres were connected (Fig. 7.1). Selective perfusion of the tumour region was achieved by ligation of macroscopically visible arterial branches to the rostral half of the auricle. The microsphere suspension was injected after vigorous shaking, to prevent sedimentation. The catheter and the syringe were repeatedly and carefully flushed in an attempt to clear the whole cannulation system from retained particles. The wound was closed after removal of the catheter and the whole cannulation system was checked for retained microspheres (see 7.2.5). Gamma camera imaging of the  $^{166}\text{HoPLA}$  treated rabbits was performed straight after embolisation and 24 hours later. Animals were sacrificed 6 weeks after embolisation or earlier in case of progressive disease with signs of pain or distress as described in chapter 2.2.4.

#### 7.2.4 Evaluation of tumour growth, histopathological investigation and statistics

The primary tumour size was measured with callipers in two dimensions and recorded as surface area ( $A$ ,  $\text{cm}^2$ ) three times a week. At autopsy the primary tumour or the site in the auricle where it regressed, was excised. Enlarged draining lymph nodes in the parotid, retromandibular and cervical area were collected and their number was recorded. Thoracic and abdominal organs were inspected for the presence of metastasis or embolisation sequelae. A slice of each lung lobe and fragments of the liver, spleen and kidney were removed. In case of neurological signs, samples of both cerebral hemispheres were removed. All tissues were placed in 10% buffered formalin and paraffin sections ( $5 \mu\text{m}$ ) were prepared. Sections were

stained with haematoxylin and eosin and studied by an experienced pathologist to confirm or exclude the presence of tumour cells.

To determine significant differences in tumour growth between the radioactive  $^{166}\text{HoPLA}$  group, the inactive  $^{165}\text{HoPLA}$  group and the Control tumours Student's t-test was used. For these three groups tumour response was categorised at autopsy according to the following definitions:

Complete Remission (CR)	= histologically confirmed absence of tumour.
Partial Remission (PR)	= over 50% tumour remission in size, but histological presence of vital tumour cells.
Stable Disease (SD)	= 0 - 50% tumour remission.
Progressive Disease (PD)	= progressive tumour growth.

Differences of tumour response and differences in number and size of lymph node and lung metastases between groups were tested with a chi-square test.

#### **7.2.5 Efficiency of intra-arterial microsphere infusion**

The radioactivity retained in the removed cannulation system, was measured in a low-background gamma counter (Tobor<sup>®</sup>, Nuclear-Chicago, USA) and corrected for decay using the time of injection as the activity reference time. The injected dose was defined as:

$$[1] \text{ Injected dose} = (\text{activity prepared}) - (\text{activity retained in the cannulation system}).$$

Efficiency of injection was represented as a percentage of the total radioactivity prepared in the batch, using the following equation:

$$[2] \text{ Injection efficiency} = (\text{Injected dose}/\text{Activity prepared}) \times 100\%.$$

#### **7.2.6 Nuclear imaging of rabbits**

All scintigrams were acquired on a gamma camera (Elscont<sup>®</sup>) interfaced to a computer (Apex 609R, Elscint Ltd., Israel). A low energy, high-resolution collimator was used. The rabbits were positioned prone and the field of view included the auricle tumour and torso. The activity generated from identical rectangular Regions of Interest (ROI), superimposed over each auricle and thorax, was determined.

### 7.2.7 Retention of microspheres in the primary tumour

The relative amount (in percentage) of microspheres entrapped in the tumour was calculated according to the following equation:

$$[3] \text{ Percentage entrapped} = \left\{ \frac{\text{Activity tumour}}{\text{Activity (tumour + lung + abdomen)}} \right\} \times 100\%.$$

The percentage of entrapped microspheres was measured immediately after embolisation ( $t_1$ ) and 1 day later ( $t_2$ ). The percentage of microspheres leaking from the tumour in due time was calculated by the following equation:

$$[4] \text{ Leakage} = (1 - \text{percentage entrapped } t_2 / \text{percentage entrapped } t_1) \times 100\%.$$

### 7.2.8 Leaching of $^{166}\text{Ho}$ in urine and faeces

All urine and faeces produced by rabbits embolised with radioactive  $^{166}\text{HoPLA}$  was collected separately the first and second day after embolisation, to test for the presence of free  $^{166}\text{Ho}$ . Radioactivity in these samples was measured with the low-background gamma counter, corrected for background radiation and decay, and expressed as a percentage of the injected dose.

## 7.3 Results

### 7.3.1 Embolisation and tumour growth

The effects of embolisation on tumour growth are summarised in Table 7.1 and Fig. 7.2. One animal that died from stray emboli to the brain (see 7.3.2 Systemic effects) was excluded, leaving 21 rabbits for analysis. Embolisation proved a highly effective anti-tumour treatment resulting in 79-86% complete remissions. There was a significant difference in complete remissions between embolised and control tumours but not among the two treatment groups themselves (Table 7.1). Also 8/14 (57%) of the contra-lateral control-tumours regressed simultaneously with the embolised primary tumours. Regression of a control tumour occurred only in case of remission of the treated tumour. Tumour growth curves showed this same pattern (Fig. 7.2). The tumour size differed significantly between treated and control tumours, but the remission curve of the tumours treated with radioactive  $^{166}\text{HoPLA}$  ran parallel to the curve of the inactive  $^{165}\text{HoPLA}$  group. Clinical images depicting effects of radio-embolisation on tumour growth are presented in Figs. 7.3 A-D.

No differences in development of lymph node metastases were observed between the groups (Table 7.2). Lymph node metastases were found in 29-43% of the

**Table 7.1.** Primary tumour growth of embolised and control tumours.

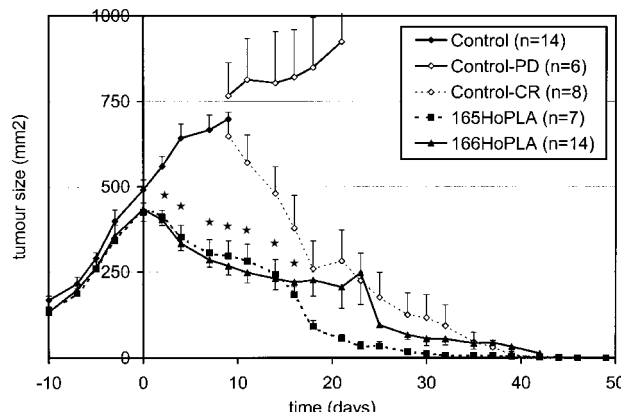
	<sup>166</sup> HoPLA n=14	<sup>165</sup> HoPLA n=7	Controls n=14
<b>CR</b>	<b>11 (79%)</b>	<b>6 (86%)</b>	<b>8 (57%)*</b>
<b>PR</b>	<b>2 (14%)</b>	<b>1 (14%)</b>	<b>0</b>
<b>SD</b>	<b>0</b>	<b>0</b>	<b>0</b>
<b>PD</b>	<b>1 ( 7%)</b>	<b>0</b>	<b>6 (43%)*</b>

CR = complete remission ; PR = partial remission; SD = stable disease; PD = progressive disease.

\* Significant difference between controls and <sup>166</sup>HoPLA/<sup>165</sup>HoPLA groups.

**Figure 7.2.**

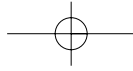
Tumour growth curves of treated and control tumours; Day 0 = day of embolisation. At day 10 a distinction is made between control tumours with progressive disease (PD) or with complete remission (CR).  
★ Significant differences (p<0.01) in tumour size between controls and treated tumours (t-test).



autopsies. In some neck nodes related to regressed primary tumours, histological changes suggesting regression of metastases were observed. These consisted of fields with foamy macrophages and syncytial giant cells indicating phagocytosis of necrotic cells. Lung metastases were seen in only one rabbit treated with <sup>166</sup>HoPLA and in one with <sup>165</sup>HoPLA microspheres.

### 7.3.2 Systemic effects

One out of the 22 embolised rabbits died because of the complications of stray emboli to the brain. Because this animal belonged to the radioactive <sup>166</sup>HoPLA group, phosphorous plate images (i.e. organographs) of tumour sections and visceral organs could be obtained (Figs. 7.4 and 7.5). The tumour sections showed a diffuse distribution of radioactivity throughout the whole primary tumour. Also



Embolisation with  $^{166}\text{HoPLA}$  microspheres

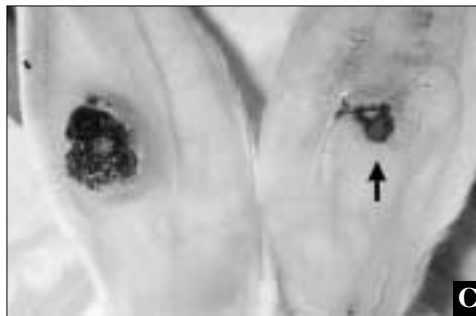
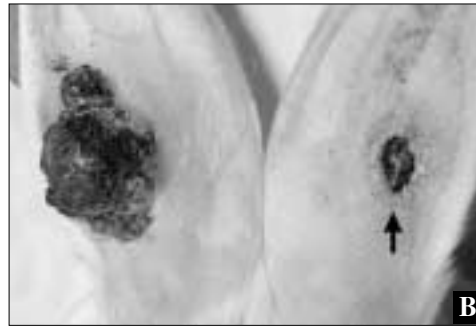


**Figure 7.3.**

Vx2 auricle tumours.

A: Typical situation at the start of embolisation.

B: 2 weeks after embolisation with progressive growth of the control tumour and remission of embolised tumour.

C: or arrested growth of the control tumour and remission of the embolised tumour.

D: 6 weeks after embolisation with complete remission of both the treated and control tumours.

Arrow indicates embolised tumour.

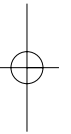


**Table 7.2.** Lymph node metastases of embolised and control tumours

	<sup>166</sup> HoPLA n=14	<sup>165</sup> HoPLA n=7	Controls n=14
<b>Present</b>	<b>5 (36%)</b>	<b>2 (29%)</b>	<b>6 (43%)</b>

**Figure 7.4.**

Rabbit with stray emboli to the brain. Organograph of transverse tumour sections perpendicular to the long axis of the auricle. Note diffuse activity in and around the primary tumour (T). The activity via an arteriolar connection into the rostral auricular artery is indicated with an arrow.

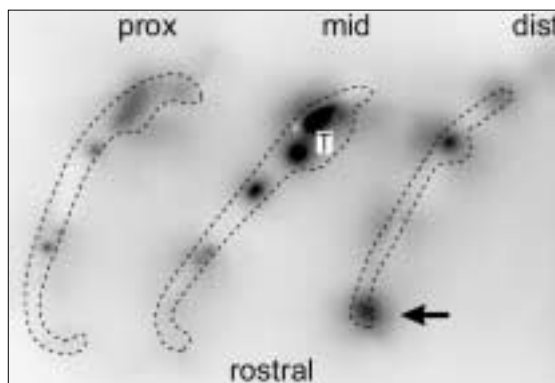
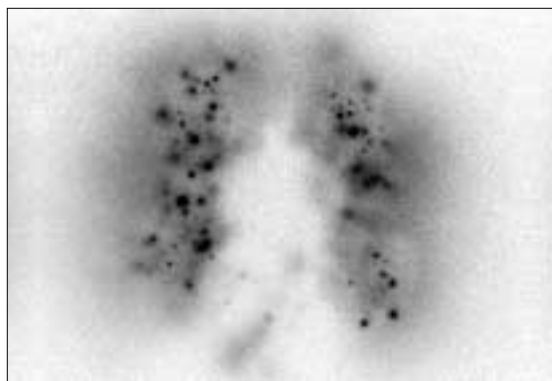


**Figure 7.5.**

Rabbit with stray emboli to the brain. Organograph of the lungs. Note clusters of radioactivity from spilled particles.



activity in the rostral auricular artery could be recognised (Fig. 7.4, arrow), which explained the mechanism of stray emboli to the brain via arterio-arteriolar connections in the auricle and retrograde flow via the rostral auricular artery into the carotid artery. Of the visceral organs, only the lungs contained <sup>166</sup>HoPLA particles (Fig. 7.5). They contained 6.6% of the injected dose, which proved the largest spill to the lungs of all animals treated (see 7.3.4).

Embolisation with  $^{166}\text{HoPLA}$  microspheres**Table 7.3.**  $^{166}\text{Ho}$  excretion in faeces and urine in promillage of the injected dose

	Faeces $\pm$ sem (‰)	Urine $\pm$ sem (‰)	Total $\pm$ sem (‰)
<b>24 hours</b>	<b>0.03 <math>\pm</math> 0.008</b>	<b>0.27 <math>\pm</math> 0.33</b>	
<b>48 hours</b>	<b>0.03 <math>\pm</math> 0.007</b>	<b>0.11 <math>\pm</math> 0.20</b>	
<b>Total</b>	<b>0.06 <math>\pm</math> 0.012</b>	<b>0.38 <math>\pm</math> 0.48</b>	<b>0.44 <math>\pm</math> 0.06</b>

Apart from the brain tissues of the one rabbit that died from stray emboli, no adverse reactions were seen in other tissues. Particularly the lung sections did not show sequelae of the 4% spilled microspheres, neither with respect to vascular occlusion nor with respect to irradiation damage.

**7.3.3 Efficiency of microsphere injection**

The efficiency with which the microsphere suspension could be injected intra-arterially was  $61.1 \pm 16.0\%$  (range 33-87%). Thus, about 40% of the microspheres was retained within the infusion system and did not reach the tumour. It resulted in an average injected dose of 34.2 MBq in 33 mg of microspheres.

**7.3.4 Retention of microspheres in the primary tumour**

Immediately after embolisation on average  $96.5 \pm 1.4\%$  (range 93.4 - 98.5%) of the injected  $^{166}\text{HoPLA}$  microspheres was retained at the site of the primary tumour. After 24 h the relative activity entrapped was  $97.3 \pm 0.8\%$ . Apparently no leakage of microspheres from the primary tumour occurred after embolisation.

**7.3.5 Leaching of  $^{166}\text{Ho}$  in urine and faeces**

Activity of  $^{166}\text{Ho}$  in faeces and urine is summarised in Table 7.3. The total activity excreted 48 h after embolisation was  $0.44 \pm 0.06\%$  (range 0.18 - 0.94‰) of the injected dose. Activity of  $^{166}\text{Ho}$  found in urine was about 6 times higher than in faeces.

## 7.4 Discussion

### 7.4.1 Effects on tumour growth

Our study shows that the i.a. infusion of HoPLA microspheres with a mean diameter of 38-80  $\mu\text{m}$  is very effective in inducing complete remissions of primary tumours in this Vx2 head and neck cancer model. As no differences between the  $^{166}\text{HoPLA}$  and  $^{165}\text{HoPLA}$  groups were found, the addition of irradiation appeared not to add to tumour remission in this animal model. This can be explained by an inefficient infusion of the microspheres resulting in an insufficient injected dose. Because, on average, 40% of the radioactivity was retained in the infusion system, only 35 MBq entered the primary tumour. This injected dose is too low to achieve a Tumour Control Probability of 95% [Briesmeister, 1977; Stabin and Konijnenberg, 2000]. On the other hand, a remission of 80% following embolisation with inactive  $^{165}\text{HoPLA}$  microspheres leaves little room for the discrimination of additional effects from irradiation. Another more likely explanation is the high sensitivity of the Vx2 carcinoma to vascular occlusion following embolisation. Indeed, Yoshikawa et al. [1994] could induce regression of Vx2 limb tumours after one week of repeated daily embolisation with starch microspheres (that degrade within 40 minutes). They demonstrated that this anti-tumour effect is due to the phenomenon of ischemia-and-reperfusion injury.

To imitate the situation in humans, superselective radio-embolisation should ideally be performed on large Vx2 tumours transplanted into the mouth or pharynx of the animal. This option is both ethically unacceptable and technically, even in rabbits, difficult. For that reason, the Vx2 model of tongue cancer described by Matsumoto et al. [1999] was not applicable in our situation. Their treatment started when tumours were still small. Moreover, the physical condition of control rabbits with tongue tumours over 10  $\text{cm}^3$  was not reported in their study.

Our study also shows that the use of a twin tumour model in which a non-treated contra-lateral tumour acts as a control tumour has its drawbacks, as more than 50% of the control tumours regressed simultaneously with the embolised tumours. Twin tumours models have also been used by others [Schouwenburg et al., 1980; Karanfilian et al., 1982; Everse et al., 1997]. Schouwenburg et al. [1980] and Karanfilian et al. [1982] used contra-lateral auricle tumours as controls in rat carcinoma models for i.a. chemotherapy. They attributed growth inhibition of the contra-lateral side to exposure of systemic anti-tumour drug levels. Everse et al. [1997] however, used a twin-lymphoma model in mice to underscore the systemic

#### Embolisation with $^{166}\text{HoPLA}$ microspheres

effects of immuno-modulation following IL-2 therapy. Also the Vx2 tumour is immunogenic as it responds to local IL-2 therapy (chapter 3).

The embolisation in our study caused extensive ischemic necrosis of the treated tumours, which possibly led to a massive presentation of Vx2 tumour antigens and an effective stimulation of the immune system known as concomitant immunity. This mechanism could also explain the regression of metastases found in some lymph nodes. Further discussion of this phenomenon lies beyond the purpose of this study.

#### 7.4.2 Efficiency of injection

A significant practical problem in administering micro particles is their tendency to settle quickly in the injection vehicles and to clump in the syringe or cannulation system. This problem of enhanced sedimentation seems to be frequently encountered as reported on the internet (<http://www.biogeltech.com/research.html>) but to our knowledge has never been quantified in literature. Our injection efficiency was 61% despite adding methylcellulose as injection vehicle. Most particles were retained in niches at the transition of the catheter to the cannula. Quick sedimentation of glass microspheres is a well-known problem attributed to their high density of 3.3 g/ml which accounts for significant variations in doses administered [Ehrhardt and Day, 1987; Mumper et al., 1991]. Though the density of  $^{166}\text{HoPLA}$  is much lower (1.4 g/ml), agitation of the solution during injection as well as repeated flushing of the cannula system has been advised by others [Bastian et al., 1998; Turner et al., 1994] and was carried out during our experiments. However, we did not control the flow rate to create a laminar flow [Mumper et al., 1991]. In future studies an overdose of about 40% should be taken into account when using the present infusion system.

#### 7.4.3 Efficacy of microsphere retention

Retention of the  $^{166}\text{HoPLA}$  microspheres prepared for this study proved highly efficient with over 95% entrapment at the primary tumour site. It is comparable with the 94.5% retention of  $^{166}\text{HoPLA}$  microspheres (diameter 24  $\mu\text{m}$ ) in rabbit Vx2 liver tumours [Mumper et al., 1991] and the 94.5-98.5% entrapment of yttrium-90 glass microspheres (diameter 22  $\mu\text{m}$ ) in human liver tumours [Andrews et al., 1994]. Although Turner et al. [1994] obtained 99.99% entrapment of even smaller  $^{166}\text{Ho}$ -resin microspheres (diameter  $13 \pm 2 \mu\text{m}$ ) in pigs, the livers in their model did not contain tumours. Entrapment of microspheres might be better in normal tissues because tumours induce capillary-like distended vessels [Van Es et al., 1999].

After 24 h, the portion of entrapped microspheres was slightly higher than immediately after embolisation (97.3% vs 96.5%). Though well within the limits of variation, it could be explained by a partial washout of some very small particles spilled to the lungs. In the previous study (chapter 6) with dextran hydrogel microspheres of a comparable size, a subsequent leaking of microspheres from the embolised tumour of 1% was observed. Retention of these microspheres was 96.2 % and consistent with the findings in this study.

The microspheres spilled to the lungs tend cluster in vessels as also observed by others [Bastian et al., 1998; Muller and Rossier, 1951]. Our organograph of the lungs of the rabbit that died from brain emboli is comparable to the findings of Muller and Rossier [1951] after i.v. injections of  $^{198}\text{Au}$  microparticles (diameter 30-50  $\mu\text{m}$ ) in rabbits. No post-irradiation sequelae were observed at autopsy in this study, probably because lung tissues received at most 1.5 MBq. Yan et al. [1993] did not find pulmonary changes after pathological examination of rabbits infused with 1480 MBq  $^{99}\text{Y}$ trium-glass microspheres, an injected dose 20 times higher than in our study.

The organograph of the auricle tumour sections shows good dose homogeneity due to an even distribution of the  $^{166}\text{Ho}$ PLA microspheres in and around the whole primary tumour.

The occurrence of stray emboli to the brain is a well-known and serious complication following embolisation of head and neck lesions. It can not be prevented by the use of larger microspheres, as in humans stray emboli also occur with particles measuring 300-2,500  $\mu\text{m}$  [Latchaw and Gold, 1979]. Therefore, unwanted embolisation into other arterial channels should be avoided by:

1. Detection and closure of non-tumour arterial branches, as was carried out in our study with methylene blue dye and tying up the vessels. This can also be performed in humans by e.g. coil embolisation [Andrews et al., 1994; McCarter et al., 1995].
2. The use of a balloon catheter to prevent potential reflux. In our study the injected artery was exposed and the infusion cannula was tied, making reflux impossible.

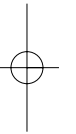
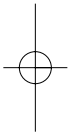
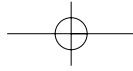
The following measures might further minimise unwanted embolisation:

1. Prevention of over-embolisation by incorporating a maximum of radioactivity in the aliquot of microspheres to be injected and monitoring the flow rate with fluoroscopy.
2. Monitoring of injection pressure and keeping it below the average blood pressure.

**7.4.4 Leaching of  $^{166}\text{Ho}$  in faeces and urine**

The excretion of  $^{166}\text{Ho}$  found in our study is below the arbitrary limit of 0.1% of the injected dose after two half-lives as posed by Ehrhardt and Day [1987]. It is comparable to the 1.6% leaching found by Nijsen et al. [1999] after 192 h incubation in liver homogenate, but lower than the 5.5% after 144 h found in vivo by Mumper et al. [1991]. A different rate of biodegradation or resorption of the  $^{166}\text{Ho}$ PLA spheres because of a different crystallinity might explain these differences. Our  $^{166}\text{Ho}$ PLA spheres degrade slowly as no substantial resorption of the particles was noted 42 days after embolisation.

It is concluded that  $^{166}\text{Ho}$ PLA microspheres with a mean diameter of 38-80  $\mu\text{m}$  are promising candidates for future studies on radio-embolisation of unresectable head and neck cancer. Embolisation induced 79-86% complete primary tumour remissions, over 95% of the particles was retained in the primary tumour and leaching of  $^{166}\text{Ho}$  in urine and faeces was minimal. However, the injection efficiency should be optimised because 40% of the microspheres was retained in the cannulation system. Arterio-arteriolar connections should be carefully detected and closed to prevent stray emboli into the brain. The fact that this Vx2 tumour is highly sensitive to vascular occlusion should be kept in mind in future radio-embolisation studies because it makes assessment of the additive value of irradiation difficult. Furthermore, the purported immunogenic nature of the Vx2 carcinoma renders contra-lateral tumours less ideal as non-treated controls because of systemic concomitant anti-tumour activity.

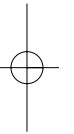
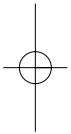


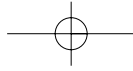


chapter

8

Summary, discussion and conclusions





## 8.1 Summary and general discussion

Advanced stage oral and oropharyngeal carcinomas have a disappointingly low survival rate, which has not improved substantially for the last two decades. Conventional treatment still consists of surgery, radiotherapy and chemotherapy or a combination of these modalities. In view of its increasing incidence and failure of preventive measures, there is a need for the development of new treatment strategies against this disease. The aim of this thesis has been to make a contribution to this.

An overview of alternative treatment modalities against Head and Neck Squamous Cell Carcinoma (HNSCC) is presented in **chapter 1**. To test these modalities, animal cancer models are necessary. Disadvantages of models currently used to test new loco-regional treatment strategies against HNSCC are discussed. Attention is focussed on the transplantable Vx2 Squamous Cell Carcinoma (SCC) as it was felt that transplantation of this tumour into the rabbit auricle would render a suitable HNSCC animal model.

The development of a Vx2 HNSCC model and evaluation of its biologic behaviour in terms of tumour take-rate and development of metastases is described in **chapter 2**. Two groups of New Zealand White rabbits received either subcutaneous injections of Vx2 suspensions (group S) or solid Vx2 pieces (group P) into both auricles. The tumour take-rate was recorded. Sacrifice took place at various times after transplantation. At autopsy, the size of the primary tumours and of lymph node, lung and other metastases were assessed. The tumour take-rate in group S and P was 78% and 59% respectively. The elapsed time after transplantation and the maximal size of the tumours that regressed spontaneously was significantly different between the two groups and amounted  $83 \pm 7 \text{ mm}^2$  at  $10.4 \pm 1.6$  days for group S and  $243 \pm 30 \text{ mm}^2$  at  $20.9 \pm 2.0$  days for group P, respectively. Four weeks after transplantation, more than 90% of the necks in both groups contained lymph node metastases. There was a trend ( $p=0.14$ ) for a higher incidence of lung metastases in group S compared to group P (47% vs. 14%). Metastases at other sites were rarely seen (less than 5%). A significant correlation ( $p=0.02$ ) between weight loss and the size of lung metastases was found. It is concluded that transplantation of Vx2 tumour cell suspensions into both auricles renders a model for loco-regional disease which mimics the biologic behaviour of HNSCC in humans and in which anti-tumour regimens against both the primary tumour and lymph node metastases can be tested.

Regarding the technique of tumour grafting, subcutaneous transplantation of freshly prepared Vx2 cell suspensions in this model with at least  $20 \cdot 10^6$  vital cells gave the

best results. With fresh cell suspensions the tumour take-rate was 78-85%. The transplantation of thawed Vx2 suspensions (see **chapter 5**) or solid Vx2 pieces into the auricle yielded worse take-rates of 40-59% respectively, which might be explained by the induction of anti-tumour immunity by transplanted dead Vx2 cells at this site [Förg et al., 1998]. Development of artificially created metastases following injection of Vx2 suspensions [Gadeholt-Göthlin and Göthlin, 1995], apparently did not play a substantial role in this model.

The effects of local interleukin-2 (IL-2) immune-therapy on the Vx2 HNSCC model are described in **chapter 3**. A regimen of peri-tumoural IL-2 that appeared optimal in murine tumour models [Den Otter et al., 1996] was applied. Treatment started when the surface area of one of the bilaterally implanted tumours exceeded 2 cm<sup>2</sup>. In 4/12 (33%) rabbits the treated primary tumours regressed completely, simultaneously with the non-treated contra-lateral tumours. Also metastases in draining lymph nodes of both treated and untreated primary tumours regressed in three of these animals. Three (25%) of all 12 treated animals were cured. Tumour cells subsequently injected in the cured animals did not result in new tumour growth. Histology of regressing tumours in cured cases showed an active granulomatous reaction with a histiocytic response, splitting up of tumour islands, and obstruction of blood vessels with fibrin thrombi. These findings indicate both a local and a systemic effect of IL-2 in the Vx2 auricle SCC model. The effects of peri-tumoural IL-2 therapy appeared similar to the effects observed following i.a. embolisation of the Vx2 tumour with inactive poly(L-lactic acid) microspheres (see **chapter 7**): Successful embolisation of one tumour induced a simultaneous regression of 57% of the contra-lateral control tumours. Therefore, this Vx2 HNSCC model is suitable to demonstrate the induction of an effective systemic immune response against the Vx2 tumour which results in tumour rejection at another site [Maas et al., 1991]. The induction of this immune response probably is preceded by ischemic necrosis of the Vx2 tumour [Yoshikawa et al., 1994]. This study shows that it is not permitted to use a contra-lateral auricle tumour as independent intra-animal control, because a local treatment of the index tumour that generates necrosis, will frequently induce a immune-mediated regression of also the non-treated control tumour.

Various aspects of the application of intra-arterial (i.a.) anti-cancer therapy are discussed in **chapter 4**. Because there is a pharmacokinetic rationale for the application of intra-arterially infused embolisation particles in tumour treatment, an overview of available embolisation particles is given. Attention is focussed on existing chemo- and radio-embolisation therapies. Potential strategies for the application of embolisation-therapies against HNSCC are given. Prerequisites that are necessary to be

---

**Summary, discussion and conclusions**

---

addressed in animal studies, are discussed.

The second purpose of the study was the application of the Vx2 auricle SCC model in the development of new loco-regional treatment strategies against HNSCC, based on i.a. infusion of micro-particles as carriers for anti-tumour drugs.

Attention is focussed on growth speed of the Vx2 SCC tumours in **chapter 5**. Also a technique for i.a. tumour perfusion is presented and the effects of i.a. embolisation of the Vx2 auricle SCC model with Dextran hydrogel (Dex) microspheres are analysed. During the exponential growth phase, the tumour-surface doubling-time was  $7.1 \pm 2.0$  days. Standard deviation in growth of the tumours was significantly larger between separate animals than between tumours growing in the left and right auricle of each individual animal (2.0 vs. 0.65 days).

The caudal auricular artery perfuses the caudal half of the external ear and proved to be suitable for macroscopic cannulation. Histological evaluation showed, that the use of Dex microspheres of at least  $25 \mu\text{m}$  in combination with ligation of branches from the central auricular artery that do not perfuse the tumour, yielded a diffuse embolisation of the Vx2 tumour. It is concluded that this Vx2 auricle SCC tumour model can be used in further studies to optimise particle size and dosage for embolisation as well as to evaluate the effects of either different anti-neoplastic drugs, slowly released by controlled degradation of Dex microspheres or embolisation particles containing radionuclides.

The distribution of i.a. injected microspheres is investigated both in-vivo as well as histologically in **chapter 6**, in order to determine an optimal size of particles for embolisation of head and neck tumours. Rabbits with Vx2 auricle tumours were embolised via the caudal auricular artery with available batches Dex and holmium-166 labelled poly(L-lactic acid) ( $^{166}\text{HoPLA}$ ) microspheres, varying in size from 19 to  $66 \mu\text{m}$ . Dex microspheres were additionally labelled with  $^{99\text{m}}\text{Tc}$ . The proportion of microspheres entrapped in the tumour was measured with a gamma camera. The distribution of microspheres around the primary tumour and spill of particles to lungs or other organs was analysed on histological sections. The  $19 \mu\text{m}$   $^{166}\text{HoPLA}$  particles proved inadequate for embolisation as 51% of the particles spilled to the lungs, whereas over 95% of the  $40\text{-}66 \mu\text{m}$  Dex microspheres was retained within the primary tumour area. With  $66 \mu\text{m}$  microspheres the deposition of particles in lung tissues proved significantly lower, but particles of this size showed a decreased deposition of microspheres directly around the target tumour. The results of this investigation showed that particles with a mean size of at least  $40 \mu\text{m}$  should be employed, to prevent substantial spill to the lungs. Microspheres of sizes over  $100 \mu\text{m}$  as used for chemo-embolisation of HNSCC in humans [Kato et al., 1994; Tomura et al., 1998] cannot be used in this Vx2 auricle SCC model,

because these large particles get stuck in the feeding arterioles before reaching the tumour.

Of the 44 rabbits embolised in this study, 3(7%) developed neurological signs. In these animals microspheres were found in brain tissue and ophthalmic vessels. It appeared to be due to arterio-arterial connections between the caudal and rostral auricular artery, which were not detected and occluded. The inadvertent spill of microspheres into the brain or eyes via arterio-arteriolar connections is a well-known sequel of tumour embolisation in the head and neck area in humans [Latchaw and Gold, 1979; Braun et al., 1985; Mames et al., 1991]. As injection pressure was not monitored in this model, a too high pressure could have resulted in retrograde flow of microspheres into the internal carotid artery. Possibly, also fluoroscopy could effectively detect stray emboli in future studies [Latchaw and Gold, 1979].

The long-term effects of embolisation of the Vx2 auricle SCC model with radioactive  $^{166}\text{HoPLA}$  microspheres are reported in **chapter 7**. The effects of embolisation on tumour growth, the efficiency of intra-arterial infusion of microspheres, the efficacy of retention of spheres in the primary tumour and the excretion of free  $^{166}\text{Ho}$  in faeces and urine were analysed. Radio-embolisation induced 78% tumour remissions. More than 95% of the microspheres were retained in the tumour and the leaching of free  $^{166}\text{Ho}$  was less than 0.1% in 2 days. However, 40% of the particles retained in the cannulation system due to enhanced sedimentation. It is concluded that these  $^{166}\text{HoPLA}$  microspheres with a diameter between 40 and 80  $\mu\text{m}$ , are promising candidates for future studies on radio-embolisation of unresectable head and neck cancer. However, also inactive HoPLA microspheres induced remissions of the target tumour as well as non-treated contra-lateral control tumours (see also **chapter 3**). Therefore, the additional effects of irradiation following embolisation of the rabbit Vx2 auricle SCC model are difficult to discern, because the Vx2 tumour is highly sensitive to ischemia and reperfusion injury [Yoshikawa et al., 1994].

## 8.2 Final conclusions

- Transplantation of the Vx2 SCC cell-line into the rabbit auricle renders an animal tumour model that mimics the behaviour of HNSCC in humans, with over 90% lymph node metastases after 4 weeks, 47% lung metastases after 5-10 weeks and less than 5% metastases at other sites.
- Success of transplantation is around 80% with freshly prepared Vx2 SCC cell-suspensions and significantly better than with solid tumour pieces or thawed, cryo-preserved suspensions.
- The tumour-surface doubling-time of Vx2 SCC auricle tumours in NZW rabbits is  $7.1 \pm 2.0$  days. Standard deviation of growth speed is significantly larger between separate animals than between separate tumours within the same animal.
- Repeated daily peri-tumoural IL-2 injections induce a systemic anti-tumour activity with regression of 25% of the treated primary tumours simultaneously with non-treated control tumours and lymph node metastases.
- Employment of an intra-individual Vx2 SCC control tumour to evaluate effects of local tumour treatment is not permitted because of the development of a systemic anti-tumour immune response in the animal.
- With cannulation of the caudal auricular artery and ligation of branches that do not supply the tumour, a regional perfusion of Vx2 SCC tumours in the dorso-caudal side of the auricle is obtained.
- The optimal particle size for embolisation of Vx2 auricle tumours is about  $40 \mu\text{m}$  in number- and  $70 \mu\text{m}$  in volume-weighted means respectively. Smaller particles shunt to the lungs while larger particles disperse less favourable around the tumour.
- The Vx2 tumour is highly sensitive to vascular occlusion following i.a. embolisation. This makes it difficult to discern the additional effects of irradiation following radio-embolisation.
- Sedimentation of holmium-166 labelled poly(L-lactic acid) ( $^{166}\text{HoPLA}$ ) microspheres accounts for retention of 40% of the particles in the cannulation system.
- In 7% of all Vx2 SCC auricle tumour-embolisation procedures, inadvertent spill of microspheres into the rabbit brain occurred via arterio-arteriolar connections.
- The leaching of free holmium-166 from  $^{166}\text{HoPLA}$  microspheres is less than 0.1% after twice its half-life.

### 8.3 Suggestions for further research

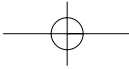
There is a need for clinical and experimental studies to assess the efficacy of various new treatment strategies against oral and oropharyngeal cancer. Attention will have to focus on combinations of the conventional triad of surgery, chemotherapy and radiology with novel therapies as multi-modality immune-therapy, inhibition of angio-genesis and genetic engineering.

The rabbit Vx2 auricle SCC model developed in this study can be used in the future:

1. To get better insight in the patho-fysiology of head and neck cancer, such as metastatic spread and immune reactivity.
2. To further evaluate the possible applications of new treatment strategies against head and neck cancer.

Future embolisation studies must establish whether the 40-80  $\mu\text{m}$  microspheres employed in this investigation are also optimal for oral and oropharyngeal SCC in humans. Attention must be paid to identification and occlusion of arterio-arteriolar connections and the injection pressure should be monitored to prevent stray emboli. The dextran hydrogel microspheres are primarily suited for controlled release of immunoglobulins instead of small chemotherapeutic drugs such as cisplatinium. They may be applied either intra-arterially or peri-tumourally, for prolonged release of e.g. immune-stimulating proteins that have a short in-vivo half-life.

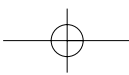
The radioactive  $^{166}\text{HoPLA}$  microspheres are promising candidates for future studies. They can be applied as intra-arterial radionuclide therapy for inoperable tumours either with curative intent or as palliation. Aspects concerning calculation of the appropriate tumour dose, efficiency of infusion of the microspheres and prevention of stray emboli to the brain have to be addressed. Peri-tumoural injection of these microspheres for palliation of recurrent tumours is another possible application worth to be investigated.

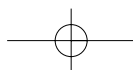
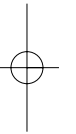
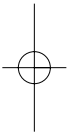
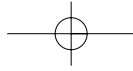


chapter

9

Samenvatting





## 9.0 Samenvatting

De overleving na behandeling van uitgebreide mondholte- en oropharynx-carcinomen is teleurstellend en is de afgelopen 20 jaar nauwelijks verbeterd. Gezien de jaarlijks toenemende incidentie van de ziekte en het falen van preventieve maatregelen is er behoefte aan de ontwikkeling van nieuwe behandelstrategieën. De gebruikelijke behandeling bestaat nog altijd uit operatie, bestraling en chemotherapie of een combinatie hiervan. In **Hoofdstuk 1** wordt een overzicht van diverse behandel mogelijkheden tegen het Plaveisel Cel Carcinoom in het Hoofd-Hals gebied (PCCHH) gegeven. Teneinde nieuwe vormen van behandelingen te testen zijn diermodellen nodig. Momenteel gebruikte diermodellen worden besproken en speciale aandacht is er voor het transplanteerbare Vx2 plaveiselcel carcinoom (PCC) in het konijn.

Het primaire doel van deze studie is te evalueren of transplantatie van dit Vx2 PCC naar het oor van het konijn een geschikt diermodel oplevert om nieuwe loco-regionale behandel mogelijkheden voor het PCCHH te testen.

In **Hoofdstuk 2** wordt de ontwikkeling van een Vx2 PCC tumor model en de evaluatie van het biologische gedrag ervan voor wat betreft succes van transplantatie en de ontwikkeling van lymfeklier- en longmetastasen, beschreven. Twee groepen New Zealand White konijnen ontvingen ofwel subcutaan injecties van Vx2 celsuspensies (groep S) ofwel solide Vx2 brokjes (groep P) in beide oorschelpen. De dieren werden gedood op verschillende tijdstippen na tumor transplantatie. Bij obductie werden de afmetingen van de primaire tumor, van de lymfeklieren en van longmetastasen vastgesteld. Bij spontane tumor remissie werd de maximale omvang van de tumor en het tijdstip waarop deze optrad vastgelegd. Het succes van tumor transplantatie bedroeg 78% en 59% in respectievelijk groep S en P. Indien regressie optrad, waren de maximale omvang van de tumor en het tijdstip waarop regressie begon, significant verschillend tussen groep S en P: respectievelijk  $83 \pm 7 \text{ mm}^2$  op  $10,4 \pm 1,6$  dagen en  $243 \pm 30 \text{ mm}^2$  op  $20,9 \pm 2,0$  dagen. Ontwikkeling van lymfekliermetastasen was niet verschillend in beide groepen. In groep P en S werden na 4 weken in meer dan 90% van de gevallen halsklier metastasen aangetroffen. Er was een geringe neiging ( $p=0,14$ ) voor het optreden van meer longmetastasen in groep S vergeleken met groep P (47% vs. 14%). Er was een positieve correlatie tussen gewichtsverlies van het dier en de omvang van longmetastasen. Transplantatie van de Vx2 tumor cellijn naar beide oorschelpen levert een succesvol PCCHH model voor loco-regionale ziekte op, waarin tumorbehandelingen gericht op zowel de primaire tumor als lymfeklier metastasen kan worden getest. Transplantatie met

tumorbokjes of celsuspensies die ingevroren zijn geweest (**Hoofdstuk 5**) wordt niet aanbevolen omdat dan het transplantatiesucces laag is.

In **Hoofdstuk 3** wordt beschreven hoe het konijn Vx2 tumormodel is gebruikt, om de effecten van een lokale immuun-behandeling met interleukine-2 (IL-2) te testen. Peritumorale IL-2 behandeling werd gestart zodra één van de bilateraal getransplanteerde tumoren groter dan 2 cm<sup>2</sup> was. In 4/12 (33%) van de konijnen trad complete regressie op van de behandelde primaire tumor, tegelijkertijd met regressie van de niet behandelde contra-laterale controle-tumor. Ook metastasen in drainerende lymfeklieren gingen in regressie. Drie (25%) van de 12 behandelde dieren konden worden genezen. Tumorcellen opnieuw geïnjecteerd in de eenmaal genezen dieren leidde niet tot nieuwe tumorgroei. Histologie van de in regressie gegane tumoren van de genezen dieren, toonde een actieve granulomateuze reactie met een histiocytair component, het opsplitsen van tumor in kleine eilandjes en obstructie van bloedvaten door fibrine trombi. Deze bevindingen demonstreren zowel een lokaal als systemisch therapeutisch effect van het gebruikte IL-2 regime bij dit Vx2 carcinoommodel.

Een vergelijkbare simultane regressie van de contra-laterale controle-tumoren trad ook op na embolisatie-behandeling zonder IL-2 toediening (**Hoofdstuk 7**). Mogelijke oorzaak hiervan is een door necrotisch tumorweefsel opgewekte immuunreactie die de controle-tumor doet verdwijnen. Dit neveneffect betekent dat een 2<sup>e</sup> contra-laterale Vx2 tumor niet gebruikt kan worden als controle voor beoordeling van het effect van een lokale therapie op de behandelde tumor in hetzelfde konijn.

In **Hoofdstuk 4** worden verschillende aspecten van de toepassing van intra-arteriële, ook wel regionale anti-tumor therapie besproken. Omdat er een farmacokinetische basis is voor toepassing van intra-arteriële infusie van microbolletjes als tumorbehandeling, wordt een overzicht gegeven van beschikbare deeltjes voor intra-arteriële embolisatie. Aandacht wordt m.n. gericht op reeds bestaande therapieën van chemo-embolisatie en radio-embolisatie buiten het hoofd-hals gebied. Mogelijke strategieën voor toepassing van embolisatie behandeling tegen het PCCHH, alsmede de voorwaarden die nodig zijn voor verdere dierproeven, worden besproken.

In **Hoofdstuk 5** is er aandacht voor de groeisnelheid van de Vx2 tumor in de oorschelp. Een techniek voor de selectieve intra-arteriële tumorperfusie wordt gepresenteerd en de effecten van intra-arteriële embolisatie van dit Vx2 oorschelp PCC model met dextraan hydrogel microbolletjes worden geanalyseerd. Tijdens de fase van exponentiele groei blijkt de tumor-oppervlakte verdubbelingstijd  $7,0 \pm 2,0$  dagen. Standaarddeviatie van de groei van de tumoren blijkt significant groter tussen twee afzonderlijke dieren, dan tussen twee tumoren in beide oren van hetzelfde

---

**Samenvatting**

dier (2,0 vs 0,65 dagen). De arteria auricularis caudalis blijkt de caudale helft van de oorschelp van het konijn te perfunderen en is geschikt voor macroscopische canulatie. Histologisch onderzoek laat zien dat een combinatie van dextran hydrogel microbolletjes van tenminste 25  $\mu\text{m}$  in diameter met het onderbinden van arteria auricularis centralis-takken die de tumor niet perfunderen, noodzakelijk is om een diffuse embolisatie van het Vx2 carcinoom te verkrijgen. Dit Vx2 tumormodel blijkt bruikbaar voor verdere studies waarin de partikelgrootte en de dosering benodigd voor embolisatie, worden geoptimaliseerd. Vervolgens kunnen dan de effecten van ofwel verschillende chemotherapeutica die langzaam door gecontroleerde degradatie van dextran microsferen worden afgegeven, ofwel radioactieve microbolletjes worden geëvalueerd.

In **Hoofdstuk 6** wordt de distributie van intra-arterieel geïnjecteerde microbolletjes verder onderzocht om tot een optimale afmeting van de bolletjes voor embolisatie van hoofd-hals tumoren te komen. Konijnen met Vx2 oorschelp carcinomen worden geëmboliseerd via de arteria auricularis caudalis met dextran hydrogel of holmium-166 poly(L-lactic acid) ( $^{166}\text{HoPLA}$ ) microbolletjes, die in grootte variëren van 19 tot 66  $\mu\text{m}$ . Een deel van de dextran hydrogel bolletjes wordt gelabeld met  $^{99\text{m}}\text{Tc}$  Technetium. De hoeveelheid microbolletjes die in de tumor vastloopt, wordt gemeten met behulp van een gamma camera. De distributie van bolletjes rondom de primaire tumor en het verlies van bolletjes naar de long en andere organen, wordt ook histologisch beoordeeld. De 19  $\mu\text{m}$   $^{166}\text{HoPLA}$  bolletjes die normaal voor leverembolisatie worden gebruikt, blijken ongeschikt voor embolisatie in dit model, omdat 51% van de deeltjes doorschiet naar de long. Daarentegen blijft meer dan 95% van de 40 tot 66  $\mu\text{m}$  dextran hydrogel bolletjes wel goed in de primaire tumor hangen. Bij grotere microbolletjes is de partikel-dichtheid in het longweefsel significant lager, maar wordt de distributie rondom de primaire tumor ongunstiger. In 2 konijnen die geëmboliseerd werden met 40  $\mu\text{m}$  microbolletjes ontstonden emboliën op afstand in het brein, ten gevolge van arterio-arteriolaire verbindingen. De resultaten van dit onderzoek laten zien dat zowel dextran hydrogel als  $^{166}\text{HoPLA}$  microbolletjes geschikte kandidaten zijn voor embolisatie van hoofd-hals tumoren. Deeltjes met een gemiddelde diameter van 40-70  $\mu\text{m}$  geven het beste resultaat om doorschieten naar de longen te verhinderen. De distributie van grotere deeltjes rondom de tumor is ongunstiger.

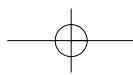
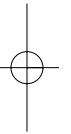
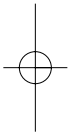
In **Hoofdstuk 7** worden de lange termijn effecten van embolisatie van het Vx2 oorschelp PCC model met radioactieve en inactieve holmium-gelabelde poly(L-lactic acid) microbolletjes besproken. Beoordeeld worden zowel de effecten van embolisatie op tumorgroei als het rendement van intra-arteriële infusie van microbolletjes en de efficiëntie van het blijven hangen van bolletjes in de primaire tumor.

De uitscheiding van vrij holmium-166 wordt vastgesteld. De radioembolisatie resulteert in 78% remissie van primaire tumoren. Meer dan 95% van de bolletjes blijkt vast te lopen in het tumorvaatblad en de lekkage van holmium-166 is minder dan 0,1% in 2 dagen. Echter, het rendement van de infusie van bolletjes moet verbeterd worden, omdat bijna 40% van de deeltjes achter blijft in de canulatiesysteem t.g.v. sedimentatie van de partikels. De conclusie is dat  $^{166}\text{HoPLA}$  microbolletjes met een aantal, respectievelijk volume gewogen gemiddelde van 40 en 80  $\mu\text{m}$  veelbelovende kandidaten zijn voor toekomstige toepassing als radioembolisatie van niet-resectabele hoofd-hals tumoren. Het Vx2 oorschelp PCC model leent zich echter minder goed voor embolisatie, omdat ook bij embolisatie met niet-actieve microbolletjes complete remissies van zowel de primaire als contralaterale controle tumoren werden verkregen, hetgeen wijst op de inductie van een systemische immuunreactie in het konijn na unilaterale tumornecrose.

In **Hoofdstuk 8** worden de bevindingen van de voorliggende studies samengevat en bediscussieerd. Met name is er aandacht voor de inductie van een systemische immuunreactie en wordt gesproken over aspecten van ongewenste embolisatie op afstand. Er wordt afgesloten met het bespreken van mogelijkheden voor toekomstige studies.



## References



## References

- Aigner KR.** Intra-arterial infusion: overview and novel approaches. *Semin Surg Oncol* 1998;14:248-253.
- Almgård LE, Slezak P.** Treatment of renal adenocarcinoma by embolisation. A follow-up of 38 cases. *Eur Urol* 1977;3:279-281.
- Almond P.** Physics of radiotherapy of head and neck tumours. In: *Comprehensive Management of head and neck tumours* (Thawley SE, Panje WR, Batsakis JG, Lindberg RD eds.) WB Saunders Company, Philadelphia, 2nd ed. 1999:124-140.
- Andersen JH, Angerson WJ, Willmott N, Kerr DJ, McArdle, Cooke TG.** Regional delivery of microspheres to liver metastases: the effects of particle size and concentration on intrahepatic distribution. *Br J Cancer* 1991;64:1031-1034.
- Anderson JM, Shive MS.** Biodegradation and biocompatibility of PLA and PLGA microspheres. *Adv Drug Del Rev* 1997;28:5-24.
- Andrews JC, Walker SC, Ackermann RJ, Cotton LA, Ensminger WD, Shapiro B.** Hepatic radioembolization with yttrium-90 containing glass microspheres: preliminary results and clinical follow-up. *J Nucl Med* 1994;35:1637-1644.
- Armitage P, Berry G.** Comparison of two variances. In: *Statistical methods in medical research*. Oxford: Blackwell scientific publications 2nd ed. 1988:112-115.
- August DA.** Theoretic and Experimental Aspects of Regional Liver Infusion. *Surg Oncol Clin North Am* 1996;5:399-409.
- Balemans LT, Steerenberg PA, Kremer BH, Koppenhagen FJ, De Mulder PH, Den Otter W.** Specific tumor memory induced by polyethylene-glycol-modified interleukin-2 requires both helper and cytotoxic T cells. *Cancer Immunol Immunother* 1995;40:125-131.
- Bastian P, Bartkowski R, Kohler H, Kissel T.** Chemo-embolization of experimental liver metastases. Part I: distribution of biodegradable microspheres of different sizes in an animal model for the locoregional therapy. *Eur J Pharm Biopharm* 1998;46:243-254.
- Batsakis JG.** Pathology of tumors of the oral cavity. In: *Comprehensive management of head and neck tumours* (Thawley SE, Panje WR, Batsakis JG, Lindberg RD eds.) WB Saunders Company, Philadelphia, 2nd ed. 1999: 632-672.
- Barone R, Pavaux C, Blin PC, Cuq P.** *Atlas d'anatomie du Lapin*. Paris: Masson & Cie éditeurs, 1973.
- Bergsma EJ, Rozema FR, Bos RRM, De Bruijn WC.** Foreign body reactions to resorbable poly(l-lactide) bone plates and screws used for fixation of unstable zygo-

## References

- matic fractures. *J Oral Maxillofac Surg* 1993;51:666-670.
- Biel MA.** Photodynamic therapy of head and neck cancers. *Semin Surg Oncol* 1995;11:355-359.
- Blanchard RJW, Grotenhuis I, LaFave JW, Perry JF.** Blood supply to hepatic V2 carcinoma implants as measured by radioactive microspheres. *Proc Soc Ex Biol Med* 1965;118:465-468.
- Bloemendal HJ, Logtenberg T, Voest EE.** New strategies in anti-vascular cancer therapy. *European Journal of Clinical Investigation* 1999;29:802-809.
- Bolman C, De Vries H.** Psycho-social determinants and motivational phases in smoking behavior of cardiac in-patients. *Preventive Medicine* 1998;27:738-747.
- Bradford CR and Carey TE.** Molecular biology of head and neck tumors In: *Comprehensive management of head and neck tumours* (Thawley SE, Panje WR, Batsakis JG, Lindberg RD eds.) WB Saunders Company, Philadelphia, 2nd ed. 1999: 321-342.
- Braun IF, Levy S, Hoffman JC.** The use of transarterial microembolization in the management of hemangiomas of the perioral region. *J Oral Maxillofac Surg* 1985;43:239-248.
- Brem H, Folkman J.** Inhibition of tumour angiogenesis mediated by cartilage. *J Exp Med* 1975;141: 427-439.
- Briesmeister JF.** MNCP- A general Monte Carlo code for neutron and photon transport. Version 3A. Los Alamos, NM: Los Alamos National Laboratory LA-12625-M, 1997.
- Bruland OS.** Cancer therapy with radiolabeled antibodies. An overview. *Acta Oncol* 1995;34:1085-1094.
- Carroll WR, Bunge FR, Wolf GT, Carey TE, McClatchey KD, Poore J.** Perilesional interleukin-2 in the VX-2 carcinoma in rabbits: a preliminary investigation. *Otolaryngol Head Neck Surg* 1995;112:430-436.
- Civalleri D, Scopinaro G, Balletto N, Claudiani F, DeCian F, Camerini G, DePaoli M, Bonalumi U.** Changes in vascularity of liver tumours after hepatic arterial embolization with degradable starch microspheres. *Br J Surg* 1989;76:699-703.
- Claessen AM, Bloemena E, Bril H, Meijer CJ, Scheper RJ.** Locoregional administration of etoposide, but not of interleukin 2, facilitates active specific immunization in guinea pigs with advanced carcinoma. *Cancer Res* 1992;52:2440-2446.
- Clayman GL, El-Naggar AK, Merrit J et al.** Adenovirus mediated p53 gene transfer in patients with advanced recurrent head and neck squamous cell carcinoma. *J Clin Oncol* 1998;16:2221-2232.
- Cloos J, Spitz MR, Schantz SP, Hsu TC, Zhang ZF, Tobi H, Braakhuis BJ, Snow GB.** Genetic susceptibility to head and neck squamous cell carcinoma. *J Natl Cancer*

Inst 1996;17;88:530-535.

**Close LG, Morrish TN, Nguyen P.** Intraoperative versus interstitial radiotherapy: a comparison of morbidity in the head and neck. *Laryngoscope* 1993;103:231-246.

**Collins JM.** Pharmacologic rationale of drug delivery. *J Clin Oncol* 1984;2:498-504.

**Conlon KC, Bading JR, McDermott EWM, Corbally MT, Tolvo AJ, Brennan MF.** Extremity metabolism in the cachectic, VX-2 carcinoma-bearing rabbit. *J Surg Res* 1993;55:330-337.

**Conn H, Langer R.** Continuous long-term intra-arterial infusion in the unstrained rabbit. *Laboratory Animal Science* 1978;28:598-602.

**Davidson T, Wallace J, Carnochan P.** The rabbit as an experimental model for regional chemotherapy. Intra-arterial hindlimb infusion. *Laboratory Animals* 1986; 20:343-346.

**Davis WE, Zitsch III RP.** Statistics of head and neck cancer. In: *Comprehensive management of head and neck tumours* (Thawley SE, Panje WR, Batsakis JG, Lindberg RD eds.) WB Saunders Company, Philadelphia 2nd ed. 1999:283-295.

**Day GL, Blot WJ.** Second primary tumors in patients with oral cancer. *Cancer* 1992;70:14-19.

**De Mik JJ, Koten JW, Maas RA, Dullens HF, Den Otter W.** Tumour regression by IL-2 mediated stagnation of blood flow. *In Vivo* 1991;5:679-684.

**DeNardo SJ, Kroger LA, DeNardo GL.** A new era for radiolabeled antibodies in cancer? *Curr Opin Immunol* 1999;11:563-569.

**Den Otter W, Hill FWG, Klein WR, Koten JW, Steerenberg PA, De Mulder PHM, Rutten VPMG, Ruitenber EJ.** Low doses of interleukin-2 can cure large bovine ocular squamous-cell carcinoma. *Anticancer Research* 1993;13:2453-2456.

**Den Otter W, De Groot JW, Bernsen MR, Heintz APM, Maas R, Hordijk GJ, Hill FWG, Klein WR, Ruitenber EJ, Rutten VPMG.** Optimal regimens for local IL-2 tumour therapy. *Int J Cancer* 1996;66:400-403.

**Donaldson RC.** Methotrexate plus Bacillus Calmetto-Guérin (BCG) and Isonazid in the treatment of cancer of the head and neck. *American J Surg* 1972;124:527-534.

**Dougherty TJ, Gomer CJ, Henderson BW, Jori G, Kessel D, Korbelik M, Moan J, Peng Q.** Photodynamic therapy. *J Natl Cancer Inst* 1998;90:889-905.

**Dubinett SM, Patrone L, Tobias J, Cochran AJ, Wen DR, McBride WH.** Intratumoral interleukin-2 immunotherapy: activation of tumor-infiltrating and splenic lymphocytes in vivo. *Cancer Immunol Immunother* 1993;36:156-162.

**Easty DM, Easty GC.** Establishment of an in vitro cell line from the rabbit VX2 carcinoma. *Virchows Arch B (Cell Pathol)* 1982;39:333-337.

**Eckardt A, Kelber A.** Palliative, intraarterial chemotherapy for advanced head and neck cancer using an implantable port system. *J Oral Maxillofac Surg* 1994;52:1243-1246.

**Edmundson IC.** Particle size analysis. In: *Advances in pharmaceutical sciences* (Bean

## References

- HS, Becket AH and Carless JF eds.) London: Academic Press, 1967:95-179.
- Edwards JM, O'Donell TF, Johnson H, Rutt D, Kinmouth JB.** Endolymphatic BCG therapy in the rabbit VX2 tumour. *Surg Forum* 1975;26:147-149.
- Egilmez NK, Jong YS, Iwanuma Y, Jacob JS, Santos CA, Chen FA, Mathiowitz E, Bankert RB.** Cytokine immunotherapy of cancer with controlled release of biodegradable microspheres in a human tumor xenograft/SCID mouse model. *Cancer Immunol Immunother* 1998;46:21-24.
- Egilmez NK, Jong YS, Hess SD, Jacob JS, Mathiowitz E, Bankert RB.** Cytokines delivered by biodegradable microspheres promote effective suppression of human tumors by human peripheral blood lymphocytes in the SCID-Winn model. *J Immunother* 2000;23:190-195.
- Ehrhardt GJ, Day DE.** Therapeutic use of  $^{90}\text{Y}$  microspheres. *Nucl Med Biol* 1987;14:233-242.
- Ell C, Gossner L.** Photodynamic therapy. *Recent Results. Cancer Res* 2000;155:175-181.
- Enjolras O, Mulliken JB.** Vascular cutaneous anomalies in children: malformations and hemangiomas. *Pediatr Surg Int* 1996;11:290-295.
- Everse LA, Bernsen MR, Dullens HFJ, Den Otter W.** The success of locoregional, low-dose recombinant interleukin-2 therapy in tumor-bearing mice is dependent on the time of rIL-2 administration. *J Exp Ther Oncol* 1996;1:231-236.
- Everse LA, Renes IB, Jörgenliemk-Schulz IM, Rutgers DH, Bernsen MR, Dullens HFJ, Den Otter W, Battermann JJ.** Local low-dose interleukin-2 induces systemic immunity when combined with radiotherapy of cancer. A preclinical study. *Int J Cancer* 1997;72:1003-1007.
- Fidler IJ.** Modulation of the Organ Microenvironment for treatment of cancer metastasis. *J National Cancer Institute* 1995;87:1588-1592.
- Folkman J.** Fighting Cancer by Attacking Its Blood Supply. *Scientific American* 1996;sept:116-119.
- Förg P, Von Hoegen P, Dalemans W, Schirmacher V.** Superiority of the ear pinna over muscle tissue as site for DNA vaccination. *Gene Therapy* 1998;5:789-797.
- Foulkes WD, Brunet JS, Sieh W, Black MJ, Shenouda G, Narod SA.** Familial risks of squamous cell carcinoma of the head and neck: retrospective case-control study. *BMJ* 1996;313:716-721.
- Franssen O, Vos OP, Hennink WE.** Delayed release of a model protein from enzymatically-degrading dextran hydrogels. *J Controlled Release* 1997;44:237-245.
- Franssen O, Stenekes, RJH, Hennink WE.** Controlled release of a model protein from enzymatically-degrading dextran microspheres. *J Controlled Release* 1999;59:219-228.

- Franzke A, Buer J, Atzpodien J.** Interleukin-2 in cancer therapy: recent advances. *Exp Opin Invest Drugs* 1994;3:597-619.
- Fukazawa H, Ohashi Y, Sekiyama S, Hoshi H, Abe M, Takahashi M, Sato T.** Multidisciplinary treatment of head and neck cancer using BCG, OK-432, and GE-132 as biologic response modifiers. *Head Neck* 1994;16:30-38.
- Gadeholt-Göthlin G, Göthlin JH:** Comparison of nephrectomy and/or doxorubicin treatment in rabbit renal VX-2 Carcinoma. *J Surg Oncol* 1995;58:134.
- Galasko CSB, Haynes DW.** Survival of VX2 carcinoma cells in vitro. *Eur J Cancer* 1976;12:1025-1026.
- Ganly I, Soutar DS, Kaye SB.** Current role of gene therapy in head and neck cancer. *Eur J Surg Oncology* 2000;26:338-343.
- Gleich LL, Zimmerman N, Wang YO, Gluckman JL.** Angiogenic inhibition for the treatment of head and neck cancer. *Anticancer Res* 1998;18:2607-2609.
- Gillison ML, Koch WM, Shah KV.** Human papillomavirus in head and neck squamous cell carcinoma: are some head and neck cancers a sexually transmitted disease? *Curr Opin Oncol* 1999;11:191-199.
- Glasser ST, Herrlin J, Pollock B.** Intra-arterial injection of penicillin for infections of the extremities. *JAMA* 1945;14:796-802.
- Gore ME, Riches P, MacLennan K, O'Brien M, Moore J, Dadian G, Lorentzos A, Garth R, Moskovic E, Archer D, Breach N, Henk M, Rhys-Evans P, King DM.** Phase I study of intra-arterial interleukin-2 in squamous cell carcinoma of the head and neck. *Br J Cancer* 1992;66:405-407.
- Gorski DH, Beckett MA, Jaskowiak NT, Calvin DP, Mauceri HJ, Salloum RM, Seetharam S, Koons A, Hari DM, Kufe DW, Weichselbaum RR.** Blockage of the vascular endothelial growth factor stress response increases the antitumor effects of ionizing radiation. *Cancer Res* 1999;59:3374-3378.
- Grant RT.** Observation on direct communications between arteries and veins in the rabbit's ear. *Heart* 1930;15:281.
- Greene HSN.** The heterologous transplantation of the V-2 rabbit carcinoma. *Cancer Res* 1953;13:610-612.
- Harima Y, Harima K, Hasegawa T, Shikata N, Tanaka Y.** Histopathological changes in rabbit uterus carcinoma after transcatheter arterial embolization using cisplatin. *Cancer Chemotherapy Pharmacology* 1996;38:317-322.
- Harker GJ, Stephens FO.** Comparison of intra-arterial versus intravenous 5-fluorouracil administration on epidermal squamous cell carcinoma in sheep. *European Journal of Cancer* 1992;28A:1437-1441.
- Hasenclever D, Loeffler M, Diehl V.** Rationale for dose escalation of first line conventional chemotherapy in advanced Hodgkin's disease. *Ann of Oncol* 1996;7:95-98.

## References

- Haughey BH, Gates GA, Arfken CL, Harvey J.** Meta-analysis of second malignant tumors in head and neck cancer: the case for an endoscopic screening protocol. *Ann Otol Rhinol Laryngol* 1992;101:105-112.
- Hawkins BL, Heniford BW, Ackermann DM, Leonberger M, Martinez SA, Hendler FJ.** 4NQO carcinogenesis: a mouse model of oral cavity squamous cell carcinoma. *Head Neck* 1994;16:424-432.
- Heddäus A.** Beiträge zur heilserumbehandlung des tetanus. *Münch Med Wochenschrift* 1914;61:2186-2189.
- Henriksson R, Widmark A, Bergh A, Damber JE.** Interleukin-2-induced growth inhibition of prostatic adenocarcinoma (Dunning R3327) in rats. *Urol Res* 1992;20:189-191.
- Hennink WE, Talsma H, Borchert JCH, De Smedt SC, Demeester J.** Controlled release of proteins from dextran hydrogels. *J Controlled Release* 1996;39:47-55.
- Herman PG, Kim CS, DeSousa MAB, Mellins HZ.** Microcirculation of the lymph node with metastases. *Am J Pathol* 1976;85:333-341.
- Heys SD, Franks CR, Eremin O.** Interleukin-2 therapy: current role in surgical oncological practice. *Br J Surg* 1993;80:155-162.
- Hong WK, Lippman SM, Itri LM et al.** Prevention of second primary tumours with isotretinoin in squamous cell carcinoma of the head and neck. *N Engl J Med* 1990; 323:1795-1801.
- Hora MS, Rana RK, Nunberg JH, Tice TR, Gilley RM, Hudson ME.** Controlled release of interleukin-2 from biodegradable microspheres. *Biotechnology* 1990;8:755-758.
- Hoshi S, Mao H, Takahashi T, Suzuki K, Bose M, Orikasa S.** Internal iliac arterial Infusion chemotherapy for rabbit invasive bladder cancer. *Int J Urol* 1997;4:493.
- Hsi RA, Rosenthal DI, Glatstein E.** Photodynamic therapy in the treatment of cancer. Current state of the art. *Drugs* 1999;57:725-734.
- Jain RK.** 1995 Whitaker Lecture: delivery of molecules, particles, and cells to solid tumors. *Ann Biomed Eng* 1996;24:457-473.
- Jeglum KA, Mangan C, Wheeler JE.** Enhanced antitumor effects with intralymphatic delivery using Bacillus Calmette-Guerin in animal models. *Cancer Drug Delivery* 1985;2:127-132.
- Johansson CJ.** Pharmacokinetic rationale for chemotherapeutic drugs combined with intra-arterial degradable starch microspheres (Spherex®). *Clin Pharmacokinet* 1996;31:231-240.
- Jovanovic A, Van der Tol IGH, Kostense PJ, Schulten EAJM, De Vries N, Snow GB, Van der Waal I.** Second respiratory and upper digestive tract cancer following oral squamous cell carcinoma. *Oral Oncol, Eur J Cancer* 1994;30B:225-229.

- Kappert A.** Zur behandlung mit intraarteriellen injektionen. *Helv Med Acta* 1948;15:25-41.
- Karanfilian RG, Rush F, Murphy T.** Regional vs systemic effect of cis-dichlorodiammine platinum (II) on squamous cell carcinoma in rats. *The American Surgeon* 1983;49:116-119.
- Kato T.** Microencapsulated mitomycin-c therapy in renal-cell carcinoma. *Lancet* 1979;2(8140):479-480.
- Kato T, Nemoto R, Mori H, Kumagai I.** Sustained-release properties of microencapsulated mitomycin-c with ethylcellulose infused into the renal artery of the dog. *Cancer* 1980;46:14-21.
- Kato T, Sato K, Sasaki R, Kakinuma H, Moriyama M.** Targeted cancer chemotherapy with arterial microcapsule chemoembolization: review of 1013 patients. *Cancer chemother Pharmacol* 1996;37:289-296.
- Kidd JG, Beard JW, Rous PJ.** Serological reactions with a virus causing rabbit papillomas which become cancerous. *J Exp Med* 1936;64:79.
- Kidd JG, Rous P.** A transplantable rabbit carcinoma originating in a virus induced papilloma and containing the virus in a masked or altered form. *Exp Med* 1940;71:813-837.
- Kim YS, La Fave JW, MacLean LD.** The use of radiating microspheres in the treatment of experimental and human malignancy. *Surgery* 1962;52:220-231.
- Kim WS, Im JG, Chung EC, Han MH, Han JK, Han MC, Ham EK:** Hematogeneous Pulmonary Metastasis. *Acta Radiol* 1993;34:581-585.
- Kovács AF, Turowski B, Ghahremani MT, Loitz M.** Intraarterial chemotherapy as neoadjuvant treatment of oral cancer. *J Cranio Maxillofac Surg* 1999;27:302-307.
- Kreidler JF, Siegers JR.** Combined treatment of maxillo facial carcinoma by intra arterial proliferation block and irradiating. In: *Recent Results in Cancer Research.* (Schwemmie K, Aigner K, eds.) Springer Verlag, Berlin, 1983:152-161.
- Kropveld A, Rozemuller EH, Leppers FG, Scheidel KC, de Weger RA, Koole R, Hordijk GJ, Slootweg PJ, Tilanus MG.** Sequencing analysis of RNA and DNA of exons 1 through 11 shows p53 gene alterations to be present in almost 100% of head and neck squamous cell cancers. *Lab Invest* 1999;79:347-53.
- Kuriakose MA, Chen FA, Egilmez NK, Jong YS, Mathiowitz E, DeLacure MD, Hicks WL, Loree TL, Bankert RB.** Interleukin-12 delivered by biodegradable microspheres promotes the antitumor activity of human peripheral blood lymphocytes in a human head and neck tumor xenograft/scid mouse model. *Head Neck* 2000;22:57-63.
- Lamont JP, Nemunaitis J, Kuhn JA, Landers SA, McCarty TM.** A prospective phase II trial of ONYX-015 adenovirus and chemotherapy in recurrent squamous

## References

cell carcinoma of the head and neck. *Ann Surg Oncol* 2000;7:588-592.

**Lang S, Whiteside TL, Lebeau A, Zeidler R, Mack B, Wollenberg B.** Impairment of T cell activation in head and neck cancer in situ and in vitro: strategies for an immune restoration. *Arch Otolaryngol Head Neck Surg* 1999;125:82-88.

**Latchaw RE, Gold LHA.** Polyvinyl foam embolization of vascular and neoplastic lesions of the head, neck, and spine. *Radiology* 1979;131:669-679.

**Layalle I, Flandroy P, Trotteur G, Dondelinger RF.** Arterial embolization of bone metastases: is it worthwhile? *J Belge Radiol* 1998;81:223-225.

**Li SL, Kim MS, Cherrick HM, Doniger J, Park NH.** Sequential combined tumorigenic effect of HPV-16 and chemical carcinogens. *Carcinogenesis* 1992;11:1981-1987.

**Lin WC, Yasumura S, Whiteside TL.** Transfer of interleukin-2 receptor genes into squamous cell carcinoma: modification of tumour cell growth. *Arch Otolaryngol Head Neck Surg* 1993;199:1229-1235.

**Lin MH, Hsieh SC, Li SY, Shih HC, Chiang T, McBride J, Todd R, Chou LSS, Chou MY, Wong DTW.** Sequential cytogenetic alterations in hamster oral keratinocytes during DMBA-induced oral carcinogenesis. *Oral Oncology, European Journal of Cancer* 1994;30B:252-264.

**Liu DL, Håkansson CH, Seifert J.** Immunotherapy in liver tumors: II. Intratumoural injection with activated tumor-infiltrating lymphocytes, intrasplenic administration of recombinant interleukin-2 and interferon- $\alpha$  causes tumor regression and lysis. *Cancer Letters* 1994;85:39-46.

**Liu DL, Yang MQ, Eberhardt J, Persson B.** Repeated immunotherapy using intratumoural injection with recombinant interleukin-2 and tumour-infiltrating lymphocytes inhibits growth of breast cancer and induces apoptosis of tumour cells. *Cancer Letters* 1996;103:131-136.

**Lorelius LE, Benedetto AR, Blumhardt R, Gaskill HV, Lancaster JL, Stridbeck H.** Enhanced drug retention in VX2 tumors by use of degradable starch microspheres. *Invest Radiol* 1984;19:212.

**Lygidakis NJ, Ziras N, Parissis J.** Resection versus resection combined with adjuvant pre- and post-operative Chemotherapy-immunotherapy for metastatic colorectal liver cancer. A new look at an old problem. *Hepato-Gastroenterol* 1995;45:155-161.

**Maas RA, Van Weering HJ, Dullens HFJ, Den Otter W.** Intratumoral low-dose interleukin-2 induces rejection of distant solid tumour. *Cancer Immunol Immunother* 1991;33:389-394.

**Mames RN, Snady-McCoy L, Guy J.** Central retinal and posterior ciliary artery occlusion after particle embolization of the external carotid artery system. *Ophthalmology* 1991;98:527-531.

**Manning PJ, Ringler DH, Newcomer CE.** The biology of the Laboratory Rabbit

(2nd ed). Academic Press, San Diego, 1994:57.

**Matsumoto K, Ninomiya Y, Inoue M, Tomioka T:** Intra-tumor injection of an angiogenesis inhibitor, TNP-470, in rabbits bearing Vx2 carcinoma of the tongue. *Int J Oral Maxillofac Surg* 1999;28:118-124.

**Matthijssen V, De Mulder PH, De Graeff A, Hupperets PS, Joosten F, Ruiter DJ, Bier H, Palmer PA, Van den Broek P.** Intratumoral PEG-interleukin-2 therapy in patients with locoregionally recurrent head and neck squamous-cell carcinoma. *Ann Oncol* 1994;5:957-960.

**McCarter DHA, Doughty JC, McArdle CS, Cooke TG, Reid AW.** Angiographic embolization of the distal internal mammary artery as an adjunct to regional chemotherapy in inoperable breast carcinoma. *J Vasc Intervent Radiol* 1995;6:249-251.

**Miguel RE, Villa LL, Cordeiro AC, Prado JC, Sobrinho JS, Kowalski LP.** Low prevalence of human papillomavirus in a geographic region with a high incidence of head and neck cancer. *Am J Surg* 1998;176:428-429.

**Miller DL, Haines GA, Juliano PJ.** Preoperative embolization of osseous metastases from hypervascular cancers. *J Surg Oncol* 1995;60:133-134.

**Million RR.** Natural history of squamous cell carcinoma. In: *Management of head and neck cancer* (Million RR and Cassisi NJ eds.) JB Lippincott Company, Philadelphia, 2nd ed. 1994:31-34.

**Morgan SJ, Darling DC.** Cryopreservation. In: *Animal cell culture, introduction to biotechniques*. Oxford: BIOS scientific publishers limited, 1993:73-77.

**Morris JC, Wildner O.** Therapy of head and neck squamous cell carcinoma with an oncolytic adenovirus expressing HSV-tk. *Mol Ther* 2000;1:56-62.

**Morrissey DD, Andersen PE, Nesbit GM, Barnwell SL, Everts EC, Cohen JL.** Endovascular management of hemorrhage in patients with head and neck cancer. *Arch Otolaryngol Head Neck Surg* 1997;123:15-19.

**Muckle DS, Dickson JA.** The selective inhibitory effect of hyperthermia on the metabolism and growth of malignant cells. *British Journal of Cancer* 1971;25:771-778.

**Müller JH.** Über die Verwendung von künstlichen radioaktiven Isotopen zur Erzielung von lokalisierten biologischen Strahlenwirkungen. *Experientia* II 1946;2:372-374.

**Müller JH, Rossier PH.** A new method for the treatment of cancer of the lungs by means of artificial radioactivity. *Acta radiol* 1951;35:449-468.

**Müller M, Gounari F, Prifti S, Hacker HJ, Schirmacher V, Khazaie K, Eblac Z.** Tumor dormancy in bone marrow and lymph nodes: Active control of proliferating tumor cells by CD8+ immune T cells. *Cancer Research* 1998;58:5439-5446.

**Mumper RJ, Yun U, Jay M.** Neutron-activated holmium-166-poly(L-lactic acid) microspheres: a potential agent for the internal radiation therapy of hepatic tumors.

## References

- Journal of Nuclear Medicine 1991;32:2139-2143.
- Nakashima T, Hudson JM, Clayman GL.** Antisense inhibition of vascular endothelial growth factor in human head and neck squamous cell carcinoma. *Head Neck* 2000;22:483-488.
- Nakhgevany KB, Spigos DG, Tan WS, Felix EL.** Intraarterial yttrium-90 in the treatment of carcinomas by local injections. *Cancer* 1988;61:931-940.
- Nauta JM, Roodenburg JLN, Nikkels PGJ, Witjes MJH, Vermey A.** Comparison of epithelial dysplasia - the 4NQO rat palate model versus human oral mucosa. *Int J Oral Maxillofac Surg* 1995;24:53-58.
- Nauta JM, Van Leengoed HLLM, Star WM, Roodenburg JLN, Witjes MJH, Vermey A.** Photodynamic therapy of oral cancer. A review of basic mechanisms and clinical applications. *Eur J Oral Sci* 1996;104:69-81.
- Nijhuis PH, Pras E, Sleijfer DT, Molenaar WM, Koops HS, Hoekstra HJ.** Long-term results of preoperative intra-arterial doxorubicin combined with neoadjuvant radiotherapy, followed by extensive surgical resection for locally advanced soft tissue sarcomas of the extremities. *Radiother Oncol* 1999;51:15-19.
- Nijssen JFW, Zonnenberg BA, Woittiez JRW, Rook DW, Swildens-Van Woudenberg IA, Van Rijk PP, Van het Schip AD.** Holmium-166 poly lactic acid microspheres applicable for intra-arterial radionuclide therapy of hepatic malignancies: effects of preparation and neutron activation techniques. *Eur J Nuc Med* 1999;26:699-704.
- Nishioka S, Fukushima K, Nishizaki K, Gunduz M, Tominaga S, Fukazawa M, Monden N, Watanabe S, Masuda Y, Ogura H.** Human papillomavirus as a risk factor for head and neck cancers, a case-control study. *Acta Otolaryngol Suppl* 1999;540:77-80.
- Noorman van der Dussen MF.** Combined therapy for non-resectable squamous cell carcinoma of the oral cavity. Thesis, University of Utrecht. Optimax, Wijk bij Duurstede, the Netherlands 1986.
- Novell JR, Hilson A, Hobbs KEF.** Therapeutic aspects of radio-isotopes in hepatobiliary malignancy. *Br J Surg* 1991;78:901-906.
- Novell JR, Hilson AJW.** Iodine-131-lipiodol for hepatocellular carcinoma: the benefits of targeting. *J Nuc Med* 1994;35:1318-1319.
- O'Brien CJ, Lee KK, Castle GK, Hughes C.** Comprehensive treatment strategy for oral and oropharyngeal cancer. *Am J Surg* 1992;164:582-586.
- Okamoto Y, Konno A, Togawa K, Kato T, Amano Y.** Microcapsule chemoembolization for head and neck cancer. *Archives of Otolaryngology* 1985;242:105-111.
- Osato T, Ito Y.** In vitro cultivation and immunofluorescent studies of transplantable carcinomas Vx2 and Vx7. *J Exp Med* 1967;126:881-886.
- Pahlplatz MMM, De Wilde PCM, Poddighe P, Van Dekken H, Vooijs GP,**

- Hanselaar AGJM.** A model for evaluation of in situ hybridization spot-count distributions in tissue sections. *Cytometry* 1995;20:193-202.
- Päuser S, Wagner S, Lippmann M, Pohlen U, Reszka R, Wolf KJ, Berger G.** Evaluation of efficient chemoembolization mixtures by magnetic resonance imaging therapy monitoring: an experimental study on the VX2 tumor in the rabbit liver. *Cancer Research* 1996;56:1863-1867.
- Perlin E.** Immunotherapy in patients with oral malignant disease. *Otolaryngologic Clinics of North America* 1979;12:195-199.
- Pillai KM, McKeever PE, Knutsen CA, Terrio PA, Prieskorn DM, Ensminger WD.** Microscopic analysis of arterial microsphere distribution in rabbit liver and hepatic VX2 tumor. *Selective Cancer Therapeutics* 1991;7:39.
- Podd TJ, Carton ATM, Barrie R, Dawes PKDJ, Robert JT, Tassen LFA, Henderson R, Macleod RL, Piggot TA.** Treatment of oral cancers using iridium-192 interstitial irradiation. *Br Oral Maxillofac Surg* 1994;32:207-213.
- Raoul JL, Heresbach D, Bretagne JF, Bentue Ferrer D, Duvaeferrier, Bourguet P, Messner M, Gosselin M.** Chemoembolization of hepatocellular carcinomas. A study of the biodistribution and pharmacokinetics of doxorubicin. *Cancer* 1992;70:585-590.
- Reichert TE, Kashii Y, Stanson J, Zeevi A, Whiteside TL.** The role of endogenous interleukin-2 in proliferation of human carcinoma cell lines. *Br J Cancer* 1999;81:822-831.
- Reichert TE, Nagashima S, Kashii Y, Stanson J, Gao G, Dou QP, Whiteside L.** Interleukin-2 expression in human carcinoma cell lines and its role in cell cycle progression. *Oncogene* 2000;19:514-525.
- Ribi EE, Meyer J, Azuma I, Zbar B.** Mycobacterial cell wall components in tumor suppression and regression. *Natl Cancer Inst Monogr* 1973;39:115-199.
- Ribi EE, Granger DL, Milner KC, Strain SM.** Tumor regression caused by endotoxins and mycobacterial fractions. *J Natl Cancer Inst* 1975;55:1253-1257.
- Robbins PD, Tahara H, Ghivizzani SC.** Viral vectors for gene therapy. *Trends Biotechnol* 1998;16:35-40.
- Robbins KT, Stormiolo AM, Kerber C, Vicario D, Seagren S, Shea M, Hanchett C, Los G, Howell SB.** Phase I study of highly selective supradose cisplatin infusions for advanced head and neck cancer. *J Clin Oncol* 1994;12:2113-2120.
- Robbins KT, Kumar P, Regine WF, Wong FS, Weir AB 3rd, Flick P, Kun LE, Palmer R, Murry T, Fontanesi J, Ferguson R, Thomas R, Hartsell W, Paig CU, Salazar G, Norfleet L, Hanchett CB, Harrington V, Niell HB.** Efficacy of targeted supradose cisplatin and concomitant radiation therapy for advanced head and neck cancer: the Memphis experience. *Int J Radiat Oncol Biol Phys* 1997;38:263-271.

## References

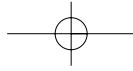
- Rocco JW, Li D, Liggett WH et al.** P161NK4A adenovirus mediated gene therapy for human head and neck squamous cell cancer. *Clin Cancer Res* 1998;4:1697-1704.
- Rosenthal RA, Glatstein E.** Photodynamic therapy in the treatment of cancer. Current State of the art. *Drugs* 1999;57:725-734.
- Rossenu S, Dewitte D, Vandekerekhove J, Ampe C.** A phage display technique for a fast, sensitive and systematic investigation of protein-protein interactions. *Journal of Protein Chemistry* 1997;16:499-503.
- Schlesinger VS, Pickartz H, Bier J.** Quantitative Verschiebung intra- und peritumoraler Zellpopulationen nach intratumoralen BCG-Zellwand-Therapie bei Plattenepithelkarzinomen der Mundhöhle. *Dtsch Zahnärztl Z* 1980;35:118-120.
- Schouwenburg PF, Van Putten LM, Snow GB.** External carotid artery infusion with single and multiple drug regimens in the rat. *Cancer* 1980;45:2258-2264.
- Schubinger PA, Beer HF, Geiger L, Rösler H, Zimmerman A, Triller J, Mettler D, Schilt W.** 90Y-resin particles-animal experiments on pigs with regard to the introduction of superselective embolization therapy. *Nucl Med Biol* 1991;18:305-311.
- Scully C.** Viruses and oral squamous carcinoma. *Oral Oncol, Eur J Cancer* 1992;28B:57-59.
- Shah SA, Dickson JA.** Effects of hyperthermia on the immunocompetence of VX2 tumor-bearing rabbits. *Cancer Res* 1978;38:3523-3531.
- Shah SA, Dickson JA.** Preservation of enzymatically prepared rabbit VX2 tumour cells in vitro. *Eur J Cancer* 1978b;14:447-448.
- Shklar G.** Experimental oral pathology in the Syrian hamster. *Program Experimental Tumor Research* 1972;16:518-538.
- Shope RE.** Infectious papillomatosis of rabbits. *J Exp Med* 1933;58:607.
- Sikora K.** Genes, dreams and cancer. *BMJ* 1994;308:1217-1220.
- Slootweg PJ, Hordijk GJ, Koole R.** Autopsy findings in patients with head and neck squamous cell cancer and their therapeutic relevance. *Oral Oncol, Eur J Cancer* 1996;32B:413-415.
- Spenlehauer G, Vert M, Benoît JP, Chabot F, Veillard M.** Biodegradable cisplatin microspheres prepared by the solvent evaporation method: morphology and release characteristics. *Journal of controlled Release* 1988;7:217-229.
- Steidler NE, Reade PC.** Experimental induction of oral squamous cell carcinomas in mice with 4-nitroquinoline-1-oxide. *Oral Surgery* 1984;57:524-531.
- Steinberg F, Kondering MA, Streffer C.** The vascular architecture of human xenotransplanted tumors: Histological, morphometrical, and ultrastructural studies. *J Cancer Res Clin Oncol* 1990;116:517-524.
- Stenekes RJH, Franssen O, van Bommel EMG, Crommelin DJA, Hennink WE.** The preparation of dextran microspheres in an all-aqueous system: effect of the for-

- mulation parameters on particle characteristics. *Pharm Res* 1998;15:557-561.
- Stewart HL, Snell KC, Dunham LJ, Schlyen SM.** V2 carcinoma, rabbit. In: Atlas of tumor pathology, transplantable and transmissible tumors of animals, section XII-fascicle 40. Washington D.C.: AFIP, 1959:38-42.
- Stribley KV, Gray BN, Chmiel RL, Heggie JCP, Bennett RC.** Internal Radiotherapy for hepatic metastases I: The homogeneity of hepatic arterial blood flow. *J Surg Res* 1983;34:17-24.
- Stupp R and Vokes EE.** Chemotherapy of head and neck tumours. In: Comprehensive Management of head and neck tumours (Thawley SE, Panje WR, Batsakis JG, Lindberg RD eds.) WB Saunders Company, Philadelphia, 2nd ed. 1999:141-156.
- Sullivan RD, Daly JF.** The treatment of head and neck cancer with the continuous arterial infusion of Methotrexate and the intermittent intramuscular administration of citrovorum factor. *Ann Otol Rhino Laryngol* 1961;70:428-443.
- Szabo G, Kreidler J, Hollmann K, Kovacs A, Nemeth G, Nemeth Z, Toth-Bagi Z, Barabas.** Intra-arterial preoperative cytostatic treatment versus preoperative irradiation: A prospective, randomized study of lingual and sublingual carcinomas. *Cancer* 1999;86:1381-1386.
- Szepezi T, Stadler B, Hohenberg G, Hollmann K, Kuhbock J, Mailath G.** Prognostische Faktoren bei der Behandlung inoperabler orofazialer Malignome mit simultaner Radio- und intraarterieller Chemotherapie. *Strahlentherapie* 1985;161:299-307.
- Taylor SG, Murthy AK, Griem KL, Recine DC, Kiel K, Blendowski C, Bull Hurst P, Showel JT, Hutchinson JC, Campanella RS, Chen S, Caldarelli DD.** Concomitant Cisplatin/5-FU infusion and radiotherapy in advanced head and neck cancer: 8-year analysis of results. *Head Neck* 1997;19:684-691.
- Tamargo RJ, Bok RA, Brem H:** Angiogenesis inhibition by minocycline. *Cancer Res* 1991;51:672-675.
- Thomas S, Wilson A.** A quantitative evaluation of the aetiological role of betel quid in oral carcinogenesis. *Oral Oncol, Eur J Cancer* 1993;29B:264-271.
- Tomura N, Kobayashi M, Hirano H, Watarai J, Okamoto Y, Togawa K, Kowada M, Murota H.** Chemoembolization of head and neck cancer with carboplatine microcapsules. *Acta Radiol* 1996;37: 52-56.
- Tomura N, Kato K, Hirano H, Hirano Y, Watarai J.** Chemoembolization of maxillary tumors via the superficial temporal artery using a coaxial catheter system. *Radiation Med* 1998;16:157-160.
- Tromberg BJ, Orenstein A, Kimel S, Barker SJ, Hyatt J, Nelson JS, Berns MW.** In vivo tumor oxygen tension measurements for the evaluation of the efficiency of

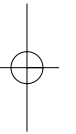
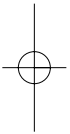
## References

- photodynamic therapy. *Photochemistry and Photobiology* 1990;52:375-85.
- Tubaro A, Velotti F, Stoppacciaro A, Santoni A, Vincentini C, Bossola PC, Galassi P, Pettinato A, Morrone S, Napolitano T, Frati L, Ruco L, Franks CR, Palmer PA, Poureau CN, Miano L.** Continuous Intra-arterial administration of recombinant Interleukin-2 in low-stage bladder cancer. *Cancer* 1991;68:56-61.
- Turner JH, Claringbold PG, Klemp PFB, Cameron PJ, Martindale AA, Glancy RJ, Norman PE, Hetherington EL, Najdovski L, Lambrecht RM.**  $^{166}\text{Ho}$ -microsphere liver radiotherapy: a preclinical SPECT dosimetry study in the pig. *Nucl Med Comm* 1994;15:545-553.
- Van Dijk-Wolthuis WNE, Kettenes-van den Bosch JJ, Van der Kerk-van Hoof A, Hennink WE.** Reaction of dextran with glycidyl methacrylate: an unexpected transesterification. *Macromolecules* 1997a;30:3411-3413.
- Van Dijk-Wolthuis WNE.** Biodegradable dextran hydrogels for pharmaceutical applications. Thesis, University of Utrecht, Ponsen & Looyen Ltd., Wageningen, the Netherlands 1997b.
- Van Es RJJ, Van Nieuw Amerongen N, Slootweg PJ, Egyedi P.** Resection Margin as a predictor of recurrence at the primary site for T1 and T2 oral cancers. *Arch Otolaryngol Head and Neck Surg* 1996;122:521-525.
- Van Es RJJ, Franssen O, Dullens HFJ, Bernsen MR, Bosman F, Hennink WE, Slootweg PJ.** The VX2 carcinoma in the rabbit auricle as an experimental model for intra-arterial embolization of head and neck squamous cell carcinoma with dextran hydrogel microspheres. *Lab Animals* 1999;33:175-184.
- Van Zandwijk N, Dalesio O, Pastorino U, De Vries N, Van Tinteren H.** EUROSCAN, a randomized trial of vitamin A and N-acetylcysteine in patients with head and neck cancer or lung cancer. *J Natl Cancer Inst* 2000; 92:977-986.
- Vasef MA, Ferlito A, Weiss LM.** Nasopharyngeal carcinoma with emphasis on its relationship to Epstein-Barrvirus. *Ann Otol Rhinol Laryngol* 1977;106:348-356.
- Visser O, Coebergh JWW, Otter R, Schouten LJ (eds.):** Head and neck tumours in the Netherlands 1989-1995. Association of comprehensive cancer centres: Utrecht, The Netherlands, 1998.
- Vlock DR, Snyderman CH, Johnson JT, Myers EN, Eibling DE, Rubin JS, Kirkwood JM, Dutcher JP, Adams GL.** Phase Ib trial of the effect of peritumoral and intranodal injections of interleukin-2 in patients with advanced squamous cell carcinoma of the head and neck: an Eastern cooperative oncology group trial. *J Immunother* 1994;15:134-139.
- Voelkel EF, Tashjian AH jr, Franklin R, Wasserman E, Levine L.** Hypercalcemia and tumor-prostaglandins: The VX2 carcinoma model in the rabbit. *Metabolism* 1975;24:973-986.

- Vokes EE, Weichselbaum RR, Lippman SM, Ki Hong W.** Head and neck cancer. *N Engl J Med* 1993;328:184-194.
- Wagner S.** Benign lymph node hyperplasia and lymph node metastasis in rabbits. Animal models for magnetic resonance lymphography. *Invest Radiol* 1994;29:364-371.
- Webber J, Herman M, Kessel D, Fromm D.** Current concepts in gastrointestinal photodynamic therapy. *Ann Surg* 1999;230:12-23.
- Wolf GT, Schmaltz S, Hudson J, Robson H, Stackhouse T, Peterson KA, Poore JA, McClatchey KD:** Alterations in T lymphocyte subpopulations in patients with head and neck squamous carcinoma. Correlations with prognosis. *Arch Otolaryngol Head Neck Surg* 1987;113:1200-1206.
- Woolgar JA, Rogers S, West CR, Errington RD, Brown JS, Vaughan ED.** Survival and patterns of recurrence in 200 oral cancer patients treated by radical surgery and neck dissection. *Oral Oncol, Eur J Cancer* 1999;35B:257-265.
- Wray A, McGuirt F.** Smokeless tobacco usage associated with oral carcinoma. Incidence, treatment, outcome. *Arch Otolaryngol Head Neck Surg* 1993;119:929-933.
- Yan Z-P, Lin G, Zhao H-Y, Dong Y-H.** An experimental study and clinical pilot trials on yttrium-90 glass microspheres through the hepatic artery for treatment of primary liver cancer. *Cancer* 1993;72:3210-3215.
- Yang J, Ma X, Zou Z, Wei S-L.** Experimental maxillofacial arterial chemoembolization with encased cisplatin ethylcellulose microspheres. *AJNR* 1995;16:1037.
- Yang J, Ma X, Zou Z-J, Wu Q-G, Wei S-L.** Percutaneous internal maxillary arterial embolisation with ethylcellulose microspheres. *Invest Radiol* 1995b;30:354-358
- Yoneda T, Kitamura M, Ogawa T, Aya S, Sakuda M.** Control of VX2 carcinoma cell growth in culture by calcium, calmodulin and prostaglandins. *Cancer Res* 1985;45:398-405.
- Yoshikawa T, Kokura S, Oyamada H, Iinuma S, Nishimura S, Kaneko T, Naito Y, Kondo M.** Antitumor effect of ischemia-reperfusion injury induced by transient embolization. *Cancer Res* 1994; 54:5033-5035.
- Zimmermann A, Schubinger PA, Mettler D, Geiger L, Triller J, Rösler.** Renal pathology after arterial yttrium-90 microsphere administration in pigs. A model for superselective radioembolization therapy. *Invest Radiol* 1995;30:716-723.



Dankwoord





## 2.1 Dankwoord

Vele personen hebben bijgedragen aan de verschillende onderzoeken en de uiteindelijke totstandkoming van dit proefschrift. Aan allen die mij hebben geholpen en gesteund, ben ik veel dank verschuldigd. Zonder anderen tekort te doen, wil ik enkelen met name noemen.

Hooggeleerde promotor, beste Ron, dank voor mijn vorming als kaakchirurg en de hulp bij het afronden van dit project. Maar ook voor het feit dat je hoofd van onze afdeling wil zijn in deze zo lastige tijd van 'moeten (durven) kiezen'.

Hooggeleerde promotor, beste Piet, dank enerzijds voor de voortvarende hulp in het creëren van de rode draad in dit onderzoek en anderzijds voor de inspirerende wijze waarop je de mond- en kaak-pathologie uitdraagt.

Hooggeleerde Egyedi, geachte professor, het was een voorrecht U nog als opleider te hebben gehad (en samen nog een voorhoofdslap te snijden). U bent voor mij een inspirerend voorbeeld geweest, als clinicus, als inventief onderzoeker maar vooral als mens.

Hooggeleerde den Otter, dank voor de leerzame bijeenkomsten betreffende IL-2 onderzoek, het beschikbaar stellen van laboratorium-faciliteiten en voor het vertrouwen in mijn kwaliteit als bus-chauffeur.

Zeergeleerde co-promotor, beste Hub, dank voor al je praktische hulp bij de proeven en bij het verweken en beoordelen van het histologisch materiaal.

Zeergeleerde i.s.n. Frank Nijsen, dank voor de goede samenwerking. Als jij aan de beurt bent delen we samen nog eens een bruine boterham met kaas.

Dank ook aan alle anderen van de afdeling Nucleaire Geneeskunde die bijgedragen hebben aan de proeven.

Bedankt Okke Franssen en Jenny Cadée, van de faculteit Farmacie, voor de vervaardiging van de dextraan hydrogel microbolletjes.

Medewerkers van het Gemeenschappelijk Dieren Laboratorium, dank voor de hulp bij de uitvoering van de dierproeven en de goede verzorging van mijn konijnen.





---

**Dankwoord**

Veel dank aan alle medewerk(st)ers van de afdeling Mondziekten en Kaakchirurgie van het UMCU: De verpleegkundigen, de dokters/tandarts-assistentes, de secretaresses (Jaqueline, het is klaar!) en de assistenten in opleiding.

Amici, maten Ron, Albert, Toine en Gert, dank voor alle fysieke en morele steun, vooral in de -in meerde opzichten- 'sombere maanden voor kerst'. Zonder dat jullie mij vrij hielden was dit boekje niet gedrukt. Fijn ook dat jullie, Toine en Gert, mijn paranymphen willen zijn. Ik wens nog een lange collegiale samenwerking.

Mijn ouders, dank voor het mij in de gelegenheid stellen van het volgen van de studies van mijn keuze en jullie warme belangstelling voor mijn werk en onderzoek. Pa, ik ben blij dat je dit nog mee kunt maken.

Mijn gezin, lieve klein aap, Celine, Laurian en Elenoor, de dank voor jullie steun is niet in woorden uit te drukken, een kus en knuffel derhalve.



 Curriculum Vitae

Robert Jelle Johan van Es werd geboren op 8 november 1962, te Amersfoort. Hij behaalde in 1980 zijn VWO- $\beta$  diploma aan het Johan van Oldenbarnevelt Gymnasium te Amersfoort en in 1985 en 1990 respectievelijk zijn tandarts- en arts-examen aan de Rijks Universiteit te Utrecht. Tijdens militaire dienst was hij in 1991 arts-assistent op de afdeling KNO-heelkunde van het Militair Hospitaal 'dr. A. Mathijssen'. Na een AGNIO-schap Kaakchirurgie in het St. Radboud te Nijmegen in 1992 (hoofd: prof.dr. H.P.M. Freihofer) werd hij in het Academisch Ziekenhuis Utrecht tot kaakchirurg opgeleid (opleiders: prof.dr. P. Egyedi en prof.dr. R. Koole). Sinds inschrijving in het specialisten register in 1996, is hij werkzaam als stafid op de afdeling Mondziekten, Kaak- en Aangezichts-chirurgie van het UMC te Utrecht. In november 1995 ontving hij via de Nederlandse Vereniging voor Mondziekten en Kaakchirurgie een 'Rhône-Poulenc-Rorer Research Grant' voor de studieopzet die de basis vormde voor deze dissertatie. Wegens speciale interesse op het gebied van de kaakchirurgische oncologie was hij in 1998 tijdelijk werkzaam in het Mt. Vernon Hospital te Londen, waar hij klinische ervaring opdeed in de microchirurgie. Hij is gehuwd met J.I. de Mik en heeft drie dochters.



Dis die blond,  
dis die blou:  
dis die veld,  
dis die lug;  
en 'n voël draai bowe in eensame vlug -  
dis al.

J.F.E. Celliers

